

NEWCASTLE UNIVERSITY

Virtual Sub-zero Life: An agent based approach to modelling cryopreservation of biological tissues

Jack Lee Jennings

Supervised by:
Dr. Roman Bauer,
Prof. Marcus Kaiser,
Dr. Paolo Zuliani
Dr. Harold Fellermann

Thesis submitted in partial requirement for the degree Doctor of Philosophy at Newcastle University.

September 12, 2024

Abstract

The long-term storage of organs and tissue at low temperatures has become a popular area of study for biomedical science and biophysics over the past century. The applications of cryobiology extend to multiple fields including organ transplantation, pharmaceutical research, in vitro fertilisation, food preservation and others.

Currently, however, cryopreservation of cells and tissue above the 1-3mm length scale is challenging. This is due to different cell and tissue types requiring specific combinations of cooling rates, cryoprotective agent concentrations and thawing trajectories. The wide variation in the responses of cells to cryopreservation therefore requires extensive trial and error wet lab work, a highly wasteful approach to the optimisation of cryopreservation protocols.

The aim of this PhD project is to investigate the use of a computational framework that accounts for key physical differences between cell types during cryopreservation with suitable extensibility for future improvements to include predictions for cryopreserved tissue. The ultimate goal of this work being the optimisation of experimental cryopreservation through computational methods from first principles.

Our models take into account multiple factors of the cryopreservation process. These include cellular membrane and osmotic properties, statistics for intracellular ice formation, chemical diffusion and heat transfer in 3D space and finally intercellular forces. The response of cells to these factors is then simulated and our models can make post-thaw survival predictions for cells based on their individual responses to local environmental variables.

Based on our computational approaches, we have successfully made post-thaw survival predictions for three cell types: (1) Jurkat T lymphocyte cells, (2) HeLa cells and (3) Human induced pluripotent stem cells. Our modelling shows excellent agreement with experimental literature for the post-thaw survival, cooling rate and cryoprotectant concentrations for all three cell types.

In addition, we also have also utilised our model to investigate the effect of nonstandard cooling profiles upon the post-thaw survival of cells in suspension. Our results show that cell death post-thaw can be reduced by more than one order of magnitude via the utilisation of multi-step cooling profiles during the freezing process. This outcome was first predicted through our computational software and we later validated these findings from our modelling process experimentally.

Our research has demonstrated that the use of *in silico* models in combination with experimental work represents a powerful method for reducing the wastage of cells for optimising cryopreservation procedures. The ability of our computational models to accurately predict the post-thaw survival of multiple cell types in 3D space, such as Jurkat cells, means we can better quantify and optimise the post-thaw viability

of cells in suspension. In addition, the findings from our work that utilisation of a multi-step cooling profile can significantly improve cellular post-thaw viability represents an additional strength of computational assistance. This is a key example where physical optimisation would not be practical or feasible. The final design of our work constitutes a foundational framework for the optimisation of cells undergoing cryopreservation with high extensibility for future work investigating tissues and organs.

Dedication

To my Grandma,

For it was her who set me on the journey of climbing this mountain.

My own Kilimanjaro.

Acknowledgements

I first wish to thank my wife for her unconditional and constant support throughout the long course of this work. Her endless patience, belief and cups of tea provided in trying times has been a consistent boon.

I also wish to thank my supervisors Dr. Roman Bauer, Prof. Marcus Kaiser, Dr. Paolo Zuliani and Dr Harold Fellermann. In addition, I also wish to thank Newcastle University's school of computing for giving me the opportunity to conduct my PhD research through a doctoral studentship.

I would like to thank Sanja and Alex for assisting me in the laboratory throughout my studentship. Being patient and taking the time to discuss and teach me experimental procedures. In addition to taking on extra work to help with the completion of vital experiments. Without their help the experimental side of this work would have been considerably more difficult.

To all the members of the BioDynaMo collaboration I also wish to give a big thank you for allowing me to work as part of such an active and knowledgeable team. I especially wish to thank Jean, Lukas, Ahmad, Nicolo and Tobias who provided thought provoking and interesting conversations in regards to how best to conduct our simulations and improve our work.

To all my friends at ICOS I also extended a special thank you for providing me with unforgettable memories and experiences.

I finally wish to thank my parents and family. The support, belief and comfort provided throughout these past years has been a constant wellspring from which to draw. Especially during difficult times.

Contents

1	Introduction		9			
	1.1	Motivation for study and Problem statement	9			
	1.2	Aims and Objectives				
	1.3	Thesis Structure	12			
	1.4	List of publications	13			
2	Bac	kground and history of cryopreservation	14			
	2.1	Early cryopreservation	14			
	2.2	Cryopreservation cycle	16			
		2.2.1 CPAs and equilibriation with cells	16			
		2.2.2 Cooling and Injury	18			
		2.2.3 Warming	21			
3	Bac	kground of cryopreservation modelling	26			
	3.1	Cryopreservation Modelling	26			
		3.1.1 Modelling transport of water and CPAs	26			
		3.1.2 Intracellular ice formation	30			
		3.1.3 Predicting cell death	33			
	3.2	Jurkat cell post-thaw survival	41			
		3.2.1 Experimental procedures	41			
		3.2.2 Results	42			
		3.2.3 Discussion	43			
	3.3	Multi-cell type post-thaw survival prediction	43			
		3.3.1 Modelling approach	44			
		3.3.2 Results	45			
		3.3.3 Discussion	47			
		3.3.4 Limitations	48			
	3.4	Conclusions and Outlook	48			
4	Bio	DynaMo - A mechanistic modelling approach	49			
	4.1	General work within BioDynaMo	50			
		4.1.1 High Performance Computing	50			
		4.1.2 Cell cycle demo	51			
		4.1.3 2D growing mono-layer demo	53			
	4.2	Chemical diffusion	55			
	4.3	Runge-Kutta solution	57			
	4.4	BioDynaMo modelling of cell water				
	4.5	Thermodynamic Simulations	62			

5	Jurkat cell cryopreservation using multi-step cooling profiles				
	5.1	Introd	luction	66	
	5.2	lling and Methods	67		
		5.2.1	Experimental procedures	69	
		5.2.2	Multi-step cooling profiles	69	
		5.2.3	Double cooling profiles	69	
	5.3	ssion	78		
		5.3.1	Simulate multi-step cooling profiles of Jurkat cells	78	
		5.3.2	Experimental validation of multi-stepped cooling predictions .	78	
	5.4	Limit	ations	80	
	5.5	Concl	usions	81	
6	Cor	nclusio	ns and Future Work	82	

List of Figures

2.1 2.2 2.3	Freezing cycle of cellular cryopreservation storage and retrieval Freezing outcomes of cellular cooling	
3.1 3.2	Cellular osmotic responses	29
3.3	(Yellow) rescuable and (Green) safe	$\frac{36}{38}$
3.4	Experimental vs survival curves	42
3.5	Chart showing modelling approach	45
3.6	Chart showing modelling approach	46
3.7	Triple survival curves	47
4.1	Percentage time required for computing BioDynaMos cell growth and division on an HPC based on number of cores used compared against a 4 core system	50
4.2	Graph structure for the flow cytometry separated cell cycle for a cells which have 4 distinct phases G0/G1, S, G2 and M which divide upon returning from the M to G0/G1 state. The default phase is marked	
4.3	"start"	52
1.0	equivalent simulation time of 48 hours	53
4.4	Comparison between experimental and simulated growth of a tissue	
	2D mono-layer over a 12 day period	54
4.5	One-dimensional finite difference	56
4.6	3D grid for finite difference	57
4.7	Simulated water loss from mouse zygotes undergoing cooling at 0.5	
	$^{\circ}$ C min^{-1} , 2.0 $^{\circ}$ C min^{-1} , 4.0 $^{\circ}$ C min^{-1} , 8.0 $^{\circ}$ C min^{-1} and 20 $^{\circ}$ C	
	min^{-1} . Eq here represents the max water loss from mouse zygotes	
	during cooling at the lowest possible cooling rate	60
4.8	Simulated loss of intracellular water from a cooling mouse zygote into	0.5
4.0	extracellular space	61
4.9	Simulated loss of intracellular water from thousands of cells into ex-	62
4.10	tracellular space during cooling	63
4. TU		UU

Computational modelling and optimisation for cryopreservation of cells and tissues.

4.11	Cryovials in Asmptote freezer	64
4.12	Simulated vs Real Freezer Recordings	65
5.1	Jurkat simulated double cooling survival with -25°C switch	70
	Jurkat simulated double cooling survival with -35°C switch	
5.3	Error corrected Jurkat survival rates	73
5.4	Jurkat simulated double cooling survival with -25°C switch	74
5.5	Two-stepped cooling predictions	75
5.6	Multi-stepped vs Standard cooling	76
5.7	Simulated three stepped cooling time of Jurkat cells with survival rates	77

Chapter 1

Introduction

1.1 Motivation for study and Problem statement

The long-term storage of organs and tissue at low temperatures has become a popular area of study for biomedical science and biophysics over the past century. Significant renewed interest appearing due to significant technological advancements allowing for a greater understanding through research. Special interest being placed on its possible benefits for medical applications. For example, if one had the ability to indefinitely store or extend the window for which donor organs and tissues are viable it may be possible to reduce the number of patients on waiting lists. This would be especially beneficial if tissues or organs could be stored indefinitely in "cryo banks" until a suitable recipient is in need. Reducing wait times and ensuring that organs or tissue could have more thorough profiling for best fits to patients. In a best-case scenario full erasure of such waiting lists may be possible and be able to be transported not only cross country but cross continent as needed.

Currently for donor heart and lungs the maximum storage time from donor to transplantation, with the organ in question remaining viable, is between 4-6 hours. For other organs such as the kidneys or liver, this preservation time increases to between 24 – 36 hours [1]. This lack of suitable short term storage options has caused up to half of possibly viable organs to be wasted, as they perish before being received by a suitable recipient. Thus, improvements to short term storage would drastically reduce such organ waste [2].

The utility of cryopreservation is not only limited to organ and tissue banking for transplantation however; successfully cryopreserving tissues and cells can assist in many areas of general research. Stem cells, for example, have great potential for research and utility due to their ability to be differentiated into a wide variety of cells and tissue but cannot be stored in a standard manner for sufficient time lengths with consistent quality and quantity [3]. The banking of such cells would allow for a ready supply of tissue for use in pharmaceutical research rather than requiring fresh sample equivalents [4]. Toxicology testing of newly designed drugs being a prime example of a pharmaceutical process requiring a readily available source of tissue analogues [5]. Additionally, the availability of suitable biological material for testing would reduce the need for animal based counterparts. The storage of cells used for in vitro fertilisation represents another key area of interest for improved preservation protocols [6]. Outside of the obvious human need, the preservation of genetic material of endangered species will be of key importance in the future for

use in preservation efforts [7]. However, the differential storage techniques required for each individual species cells makes this difficult, with some species reproductive cells still unable to be preserved reliably.

The reasons it is difficult to cryopreserve living cells is due to the fact that once biological samples are taken to sub-zero temperatures they begin to encounter lethal damage due to several factors. Firstly, intracellular ice formation (IIF) [8] caused by cooling rates being too high results in water still remaining within intracellular space leading to organelle or cellular membranes being damaged. Secondly, the solution effect, whereby cells are exposed to high concentration of CPA or solutes for extended periods of time [9]. The solution effect occurring when the sample is being cooled too slowly. Thirdly, irreparable damage to the cell membrane can be caused due to critical volume changes which can lead to the osmotic rupture of cells or compromised cellular membrane integrity. This causes the cellular membrane to become permeable to electrolytes [10, 11, 12] leading to cell death upon thawing. The mitigation of these risk factors to cells are incredibly important to post-thaw survival. As one must consider that cells need traverse the hazardous sub-zero 0 to -40°C temperature region twice, once for cooling and then again for thawing. It is thus the understanding of this hazardous region and the osmotic response of cells that is of key importance to determining cell and tissue viability post thaw for cryopreservation, finding optimum cooling and thawing trajectories is of keen interest as it will greatly improve post that viability of cells and tissue.

If a standardised model could be developed across multiple cell or tissue types, one could readily predict the response of cells to given cryopreservation protocols. Allowing for a better understanding and development of optimal protocols for storage and retrieval. This is a difficult process, as the cellular response and chemical composition varies between different cell types due to size and morphology. These differences even applying between the same cell type for different species. For example, some forms of fish spermatozoa still cannot not be cryopreserved reliably due to specific cellular dependencies [13]. Despite it being possible in other species even with significant research [13]. In the case of tissue, this is made more complex due to bulk cell-cell constructs having different thermodynamic and fluid dynamic properties compared to single cell counterparts. As unlike single cells suspended in a medium, within tissue cells inhibit each other's movement in response to ice growth. Due to the extracellular medium being limited to canals between cells determined by cytoskeletal formations [14]. Tissues are also more difficult to uniformly distribute CPA throughout as their structure limits the movement of chemical concentrations through extracellular space. This has made it difficult to cryopreserve large biological tissues above the 1-3mm being difficult to cryopreserve. These problems are further exacerbated for tissues which have a low surface area to volume ratio. Thus, tissues cannot release heat at a fast enough rate to mitigate re-crystallization occurring during the thawing process. If one could create a model that can account for such physical differences in tissues and cells this would allow for predictive modelling of cellular responses to cryopreservation. Additionally, this may allow for such models to be applied across multiple cell and tissue types. Such a model would allow for phenomenal progress to be made in the understanding of cryopreservation and the possibility of long term complex tissue storage may become possible. For these reasons, the creation of an in-depth computational model seems perfectly suited for use in predicting cellular or tissue responses to cryopreservation procedures. Especially if one could utilise hybrid computing to reduce the run time of massive biological simulations. The majority of the work in this thesis outlines the use of agent based modelling for simulating cryopreserved cells in suspension with a future outlook on expanding to tissue style systems. An overall excellent fit for a PhD project in computational biology at Newcastle University due to both its complexity and possible level of impact.

1.2 Aims and Objectives

The greater objective of this thesis was the development of a novel computational model which utilises agent based (AB) simulation tools, CryoDynaMo. Expanding upon the equations of Peter Mazur in combination with other cryopreservation and cellular biophysics equations such as those of Toner *et al* to make post thaw viability predictions for cryopreserved cell samples based on:

- Cellular membrane parameters and cooling rate.
- The dynamics of CPAs, solute and solvents within the extracellular space and approximations for intracellular space.
- Probability of cell death due to IIF and lethal solute concentration.

CryoDynaMo simulations are validated via comparison with analogous cell cryopreservation data. CryoDynaMo was developed from and simulated utilising the BioDynaMo project's existing computational framework [15]. A collaborative platform for the simulation of biological tissues developed between Newcastle University, CERN openlab and many other institutes. BioDynaMo has already been shown to capable of modelling vast AB modelling systems for millions of cells and their interactions, accurately reflecting real world biological counterparts [16]. Additionally BioDynaMo his highly modular and focused on speed up through parallelism making it superbly fitted to our modelling approach.

The major questions being addressed throughout this doctoral project are outlined below:

- 1. Can an AB simulation model the response of cells to osmotic changes during cryopreservation?
- 2. Can an AB model be used to predict the formation and impact of intracellular ice on cells during cryopreservation?
- 3. Can an AB model be used to predict post that viability of cells?
- 4. Can an AB model be used to effectively optimise cryopreservation protocols to improve post that viability?

A major advantage of such a computational model will be the direct visualisation of the solute and solvent concentrations as they move through the extracellular space and thermodynamic calculations allowing for an accurate prediction of cellular temperature within a 3D space. In addition, the ease of parallelisation will allow us to run large scale predictions for cryopreservation protocols.

1.3 Thesis Structure

This thesis is organised into six chapters, including this one. The introduction and problem statement behind this work; general background of cryopreservation and the modelling process; discussion around the BioDynaMo modelling framework and its implications for an agent based approach to this work; making predictions for post-thaw survival of multiple cell types undergoing cryopreservation; two chapters containing our overall contributions to cryopreservation research; conclusions and possible future work and limitations.

Chapter 2, History and background of cryopreservation Introduces the core concepts of cryopreservation and quantitative methods used in modelling the cryopreservation process. Giving an initial outline on the biological process of cryopreservation with a overview on relevant literature to date. In addition, this chapter outlines some of the foundational concepts behind our computational modelling approach.

Chapter 3, Cryopreservation modelling Within this chapter we describe the history and development behind cryopreservation modelling from initial to more recent works. Including the modelling of water and CPA transport, intracellular ice formation prediction, cell death predictors such as solution toxicity and intracellular. Finally outlining works relating to modelling of cryopreserved tissue. Additionally, Here we present CryoDynaMo's first use case. Assisting in the optimisation of in vitro cell cryopreservation via the modelling of a cells osmotic response to cooling and thawing, with predictions for intracellular ice formation and toxic solute exposure. Our main contribution here is displaying the ability for a computational model to take cell specific osmotic parameters to estimate optimal cryopreservation protocols. Presenting comparisons between CryoDynaMo's predictions to results from literature for three cell types: (1) Jurkat cell's; (2) Human induced pluripotent stem cells (HiPSCs) and (3) HeLa cells. CryoDynaMo's predictions showing good agreement in all cases. Overall, presenting the basis for computational predictions as a useful technique for quickly determining optimal parameters for storage that could be used in vitro.

Chapter 4, Mechanistic modelling - BioDynaMo Describes modelling of cells, thermodynamics and chemical diffusion within 3D space based on a hybrid agent based and finite difference grid method. In addition, we describe other work which has been conducted through the course of this work for the BioDynaMo modelling platform. Finally we present computationally modelled freezer cooling profiles with comparisons to in lab measurements.

Chapter 5, Multi-step cooling of cells in suspension In this chapter we present the improvement in post thaw survival of cryopreserved cells in suspension by utilising multi-step cooling rates. Here we present two major findings towards the field of computational cryopreservation: (1) Utilising a two-step cooling rates between 0 to -40°C predicts better post thaw survival than utilising a single cooling rate for the entire temperature drop; (2) Further to 1, the utilisation of an accelerating three cooling rate predicts for even greater post thaw survival than previous cooling with the ultimate implication that an accelerated cooling protocol predicts better for post thaw survival of cells ins suspension than a singular constant cooling rate. These results are compared against our own novel experimental work for Jurkat cells using single and multi-step cooling profiles.

Chapter 7, Future Work and Limitations The ultimate chapter of the thesis, discussing the overall conclusions to this work with an outlook on possible future work. Additionally, we also discuss the limitations behind this work and possible methods for improvement.

1.4 List of publications

Research outputs:

1, BioDynaMo: a general platform for scalable agent-based simulation 10.1101/2020.06.08.139949 (Accepted by Plos Computational Biology, Co-author)

Additional outputs:

1. D3.5. Second PerMed technology observatory release and benchmark report Version 3.0, HPC/Exascale Centre of Excellence in Personalised Medicine. 2. Investigating the power of eyes open resting state EEG for assisting in dementia diagnosis. Published in Alzheimers research and therapy. Primary author.

Chapter 2

Background and history of cryopreservation

2.1 Early cryopreservation

The impact of low temperatures on biological bodies was first explored in the 17th century by physicist Sir Robert Boyle. In his work Boyle investigated the impact of "touching cold" on bodies and how this impacted their function [17]. Much of Boyle's work focused on investigating the ability of ice to preserve human bodies and animals. Boyle being regarded as the first to discover that certain species of frogs and fish could survive while encased entirely within ice in addition to some initial first investigations into the cryopresrvation of spermatozoa [18]. However, for the most part Boyle's work often focused on speculation of the impact of such preservation, as limited equipment and understanding prevented significant further analysis. Many consider the research of Italian priest Lazzaro Spallanzani in the late 18th century to be the first early steps in experimental Cryobiology at a cellular level. Spallanzani investigated the impact of sub-zero temperatures on the motility of spermatozoa from: horses, salamanders, humans, dogs, frogs and bulls [19]. Being the first work of its kind to investigate the impact of subzero temperatures on live animal cells with post-thaw viability assessment via cellular function. Spallanzani observed in their work that cryopreserved spermatozoa had a significant decrease in motility and fertility. Additionally, Spallazani found that even seemingly "healthy" spermatozoa used for artificial insemination often lead to to embryonic death [20]. Spallanzani being the first person to successfully utilise AI to lead to the natural birth of live young [21]. Spallanzani's work was heavily linked to his interest in artificial insemination (AI) representing an important milestone for both cryopreservation and AI. Regarded by many as one of the key starting points for both areas of research. This has lead to a long running connection between the research of cryopreservation and AI with major interest for both economic and preservation purposes.

Many scientists followed in the steps of Spallanzani throughout the 1800's investigating the effects of extreme cold on living cells. The majority of such early cryopreservation work on different types of spermatozoa and red blood cells. However, a significant roadblock for such research at the time was the relatively poor viability results due to cellular damage at low temperatures. Leading to the understanding in the field that the exposure of cells to low temperatures led to cell death

through some mechanism induced by the cold. However, the overall reason behind this was unknown. It was not until the 1900's when the cryopreservation of bull spermatozoa became a key area of interest for the dairy industry that significant work could be carried out to study the mechanisms behind cryopreservation induced cell death [22]. During this period it was discovered that cryopreserved cells would often lyse upon being retrieved from low temperatures. This further promoted research into approaches to avoid scuh damage to cell. In the 1950's two labs independently showed that the chance of haemolysis in blood cells upon retrieval could be significantly reduced through the addition of sugars to the cell suspension medium, specifically glycerol [23, 24]. This built on previous work from Polge et al in the 1940's that the addition of glycerol to frozen rabbit spermatozoa significantly increased post-thaw cellular motility [25]. This led to the understanding that the mechanisms that damaged cells during cryopreservation could be prevented to some degree but not entirely prevent it. The usefulness of these preserving agents was validated shortly after in Polge et al's 1952 follow up work, leading to the first successful case of insemination from frozen bull spermatozoa [26] and later the first case of successful pregnancies and live birth in humans [27]. In modern cryobiology these solutes are referred to as cryo-protective agents (CPAs). James Lovelock soon after showed that cryopreserved samples of red blood cells which had glycerol added precooling showed a significantly reduced rate of ice crystal formation around cells and a proportional reduction in haemolysis post-thaw relative to the level of such reduced extracellular ice formation [28]. Being the first research of its kind to develop an understanding for the role of CPAs in cryopreservation and the first indication that ice crystals formation during cryopreservation may be directly linked to cell death. Further research within the 1950's led to the discovery of several other solutes with similar cryoprotective capabilities [29]. This included: sucrose, glucose, acetamide, methanol and dimethyl sulfoxide. Investigations into the difference in capabilities of these solutes revealed that dimethyl sulfoxide (DMSO or Me2SO) significantly reduced cell death during cryopreservation compared to other previous CPA's such as glycerol [30]. To this day DMSO is still one of the most ubiquitous CPAs used across modern cryobiology research due to its well understood characteristics. The discovery of CPA's led to a renewed interest in low temperature biology as a possible avenue for storing biological material. The additional protection against ice formation that CPAs provide allowed for the successful cryopreservation of tissues for the first time within the next decade, including human corneal tissue [31] and skin [32]. However, CPAs are not a magic catch all fix. This is due to all CPAs with high enough concentrations being toxic to cells [33] leading to cell death regardless of minimised ice formation. The fact that optimal methods for CPA addition [34] and toxicology is cell dependent further complicates this matter. More recent research has also discovered that high concentrations of some CPAs such as DMSO may also damage cellular processes and chromosome function within human cells [35]. The work within the 1950s and 1960s laid the ground work for modern cryobiology research with many of the developed practices and techniques still used to this day. The majority of investigative work now revolves around the mitigation of cryopreservation induced cell death for cells in suspension within the 0 to -40°C sub-zero region where cells are at greatest risks due to both CPA toxicity and ice formation.

2.2 Cryopreservation cycle

Cryobiology has now grown into a fully fledged field of research with significant applications to many areas of science, including: stem cell research [36, 37, 38, 39], medical storage systems [6] and storage of reproductive cells for both animals [7, 40, 41] and humans [42, 43, 44], in addition to many other cell types [18].

The cryopreservation of cells in suspension now follows a well-structured process for storage and retrieval. The process can be broken down into several distinct phases. (1) Cell sample acquisition; (2) Dehydration of cells by introduction of cryo-protective agents (CPAs), solutes and solvents; (3) Cells are then cooled using one of two techniques: (3.1) The first technique is most often referred to as the "slow cooling" approach. Cells are cooled from some initial temperature (most commonly between 0-4°C) down to -40°C utilising a single cooling rate ranging between -0.1 to -10° C min^{-1} .(3.2) The second technique used for cooling is vitrification. For vitrification cells first need to be suspended within much higher concentrations of CPAs before being rapidly cooled to the liquid nitrogen plunge phase. Often at cooling rates well above -200° C min^{-1} . The differences between these techniques is discussed in more detail later in this chapter; (4) Cells are plunged to -193°C utilising liquid nitrogen and are maintained at this temperature for the remainder of storage; (5) Cells are then rapidly warmed from subzero temperatures to 0°C and above, unlike cooling this is always performed rapidly to avoid ice re-crystallization; (6) CPAs are removed from cells upon reaching supra-zero temperatures via washing; (7) Viability assays are performed upon the retrieved cells via determination of apoptosis, necrosis and other mechanisms such as cellular function. The next phase in the process will depend upon the results of step 7. (8) If the viability assay determines that cells are not suitable for their intended purpose, testing of cell storage will need to continue with modified cryopreservation procedures. However, if the results of the viability assay are determined to be acceptable then cells will be utilised for the output of interest. Once an acceptable storage procedure is determined it can be utilised for bulk storage of the desired cell type for future needs. This process is summarised in Figure 2.1.

2.2.1 CPAs and equilibriation with cells

The discovery of CPAs in the 20th century [26] was a major break through for cryopreservation as it allowed for the consistent freezing and retrieval of viable cells for the first time. As mentioned previously, many break through were later made by other identifying further suitable cryoprotective solutes [23, 24, 29, 30].

Further work into the effects of CPAs showed that they fall into one of two distinct categories, penetrating or non-penetrating. Some CPAs are incapable of permeating cells, such as many sugars, while others can permeate into the cellular interior through equilibriation [45], such as DMSO. To date most popular CPAs used in cryoprotectant tend to be permeating variants such as DMSO, glycerol, ethelyne glycol or propylene glycol [46]. All sharing two key properties for their use in cryopreservation: high water solubility at low temperatures and the ability to easily cross cellular membranes. Additionally, all CPAs are required to be relatively non-toxic to the cells they are used for with this interaction being highly cell dependant. Non-penetrating CPAs are often much larger molecules and thus are unable to pass

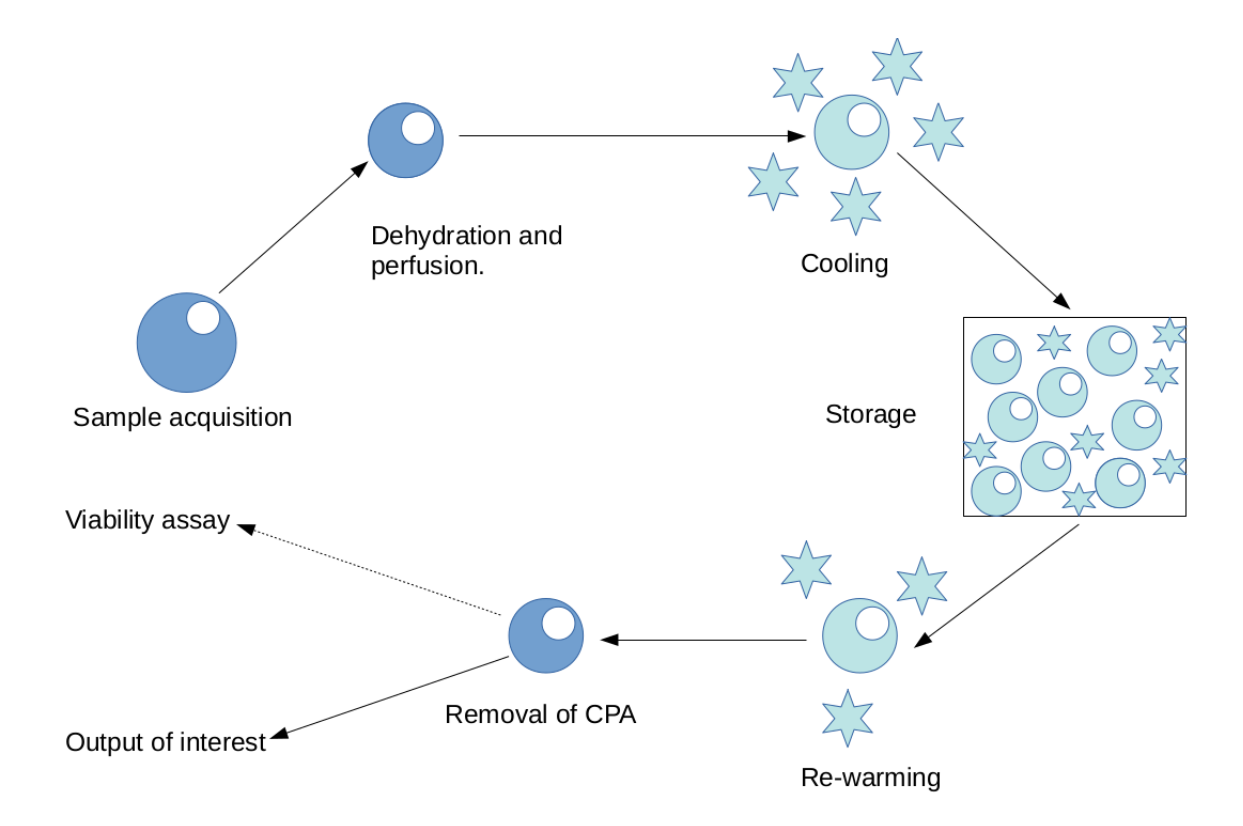


Figure 2.1: Freezing cycle of cellular cryopreservation storage and retrieval

through cellular membranes. Non-permeating CPAs are most often utilised in mixtures alongside permeating CPAs to assist in the suppression of extracellular ice. As this reduces the need for larger quantities of permeating CPAs, as non-permeating solutes size physically increases the distance between available nucleation sites for ice thus reducing extracellular ice formation.

Overall, penetrating and non-permeating CPAs both reduce the risk of intracellular ice formation during freezing. However, the effects by which the two types of CPAs achieve this is not the same. As discussed in the work of Mandumpal et al [47], recent research has shown that penetrating CPAs reduce ice formation through two processes: inhibiting water molecules ability to coalesce and reducing the freezing temperature of water. Both of these effects are achieved through the affinity of these CPAs to bind to water molecules through hydrogen bonding. When penetrating CPAs bind to water molecules this leads to a reduction in the freezing temperature of that water molecule reducing its affinity to nucleate with non-cpa bound water molecules. Additionally, water molecules bound to CPA molecules have fewer binding sites for other water molecules to attach to. This makes it difficult or even impossible for those molecules to reach the critical nuclei size required for ice formation to occur. This binding however is not a physical bond, instead this interaction is caused due to the hydrogen bonding strength between some CPAs and water, such as DMSO [48], being stronger than that between water molecules. Nonpenetrating CPA's instead act as a ice formation inhibitor through the dehydration of freezing cells. As such CPAs will cause internal cellular water to be transported through osmotic into the surrounding medium. Additionally, non-permeating CPAs have also been shown to been shown to inhibit both the glass transition temperature and freezing temperature of water due to a combination of their high molecular

17

weight [49] and high viscosity at subzero temperatures [50]. Non-permeating CPAs are most often used in vitrification process over slow cooling due to their ability to promote glass formation [51]. Recent research showing that mixtures of permeating and non-permeating CPAs can significantly increase the post thaw viability of vitrified tissues such as ovarian tissue over non-mixed equivalents [52]. Permeating CPAs have allowed for the successful cryopreservation of many smaller mammalian tissues including: embryos, reproductive tissue, cartilage, bones and kidney [53]. Permeating CPAs are however must less frequently used in slow cooling rate cryobiology research as the overall slower approach to the glass transition temperature of samples.

Despite their protective, CPAs are not a catch all solution to the issue of ice formation. As CPAs at high enough concentrations (permeating or non-permeating) can become toxic to cells, leading to the toxic shock of cells and cell death. Additionally, the toxicity of CPA concentration can not simply be tested on cells at temperatures close to zero, e.g 4 - 0 °C. This is due to the effect of ice crystal formation and the properties of the bound water molecules contained within. Once ice nucleation occurs at low temperatures other liquid phase water molecules will bind to the forming crystal. These bound water molecules will push away other solutes, leading to an effective increase in local concentrations. As ice formation progresses the solute concentrations will continually increase as ice crystals grow larger and force solutes to aggregate further. This effectively leads to an increase in the concentration of CPA agents which are forced away from growing ice crystals. Thus, causing CPAs which are initially at safe concentrations to reach a level at which they are toxic due to osmotic effects and cellular membrane damage. Additionally, many permeating CPAs such as DMSO are toxic to cells at temperatures close to 37°C. This means that CPAs must be added at or close to sub-zero temperatures to prevent toxic shock and to ensure the equal distribution of the CPA throughout the media.

2.2.2 Cooling and Injury

Cells being taken to sub-zero temperature utilising slow cooling are most often cooled using a single linear cooling rate to cross the 0 to -40 °C range before being plunged to liquid nitrogen storage temperatures. The two best-established methods for the cooling of cells during cryopreservation are vitrification and slow-cooling. Vitrification is a relatively new method which uses high cooling rates. Due to the need for such high cooling rates this necessitates the use of liquid nitrogen based freezing to reach suitable cooling profiles. However, vitrification also requires high concentrations of cryoprotective agents (CPAs) to inhibit intracellular and extracellular ice formation (IIF and EIF). Vitrification can result in excellent post-thaw survival rates (80 - 95.6%) [54, 55]. However, vitrification is problematic with regard to medical applications due to lack of scalability, due to necessary high CPA concentration and the possibility of sample contamination through direct contact with liquid nitrogen [56, 57, 58]. Slow-cooling cryopreservation protocols avoid IIF through the use of tailored combinations of cooling rates and CPA concentrations. Notably, recent work shows that slow-cooling can provide comparable post-thaw survival results for ovarian tissue and other cryopreserved biological materials to that of vitrification and state of the art methods [59, 60].

In addition to the standard slow cooling and vitrification methodologies for cryopreservation several alternative methods have also been shown to give promising post-thaw survival results. First, isochoric cryorpreservation is a method of cryopreserving cells, tissue and organs in a sealed rigid container. During cooling of samples sealed in such rigid volumes water is unable to spontaneously freeze into ice. This is due to increasing pressure suppressing the ability of water to transition to the solid ice phase due to the required expansion in volume to form ice crystals from liquid water. This effectively leads to indirect compression of the water molecules within the sample. Several studies have already shown that isochoric cryopreservation can achieve excellent results for tissue and organ cryopreservation compared to other methods [61, 62, 63]. In some cases this has even been achieved without the need for osmotic CPA addition [64]. Second, hyperbaric cryopreservation works similarly to isochoric cryopreservation but instead directly applies high pressure to the freezing medium as to suppress ice crystal formation. Showing promise in the preservation of cells and animal organs [65, 66]. However, there is still a need to research the damage which can occur in such high pressure environments to cells, tissues and organs [67].

It is during the 0 to -40 °C temperature range that cells are most at risk to factors which will result in cell death upon warming to physiological temperatures. Despite the fact that cells can appear viable upon warming upon initially reaching supra-zero temperatures post-thaw, the cells fate is often already determined during the sub-zero temperatures before reaching warming. This is often referred to as cryopreservation induced onset cell death. The cause of cell death and some possible explanations towards the mechanisms behind it were first discussed by Mazur et al in 1972 with experimental reasoning behind the effects [68]. Ultimately, this can be seen as a combination of two main risk factors. Damage through exposure to high concentrations at slow cooling rates, such as the solution effect, and damage due to the formation of ice in intra- and intercellular space during cooling and rewarming leading to damaging of cellular structures. These effects are summarised for a hypothetical cell undergoing cooling in Figure 2.2. The mitigation of these risk factors to cells are incredibly important to post-thaw survival. As one must consider that cells need traverse the hazardous sub-zero 0 to -40°C temperature region twice, once for cooling and then again for thawing. One must also consider that ice crystal growth will still progress during warming as long as water remains below its freezing temperature. Thus, crystals that previously were non-lethal during cooling may reach large enough sizes to induce either concentration dependant toxic effects or physically damage cells. It is thus the understanding of this hazardous region and the osmotic response of cells that is of key importance to determining cell viability post that for cryopreservation.

2.2.2.1 The solution effect

Once cryopreserved samples cross into the sub-zero temperature region, ice crystals begin to nucleate in extracellular and intracellular space. These crystals effectively reduce the osmotic water content of extracellular space as liquid water turns into solid ice. This in turn results in other extracellular solutes and CPAs reaching greater overall concentrations through a reduction in dilution. Due to this, water is then drawn passively from intracellular to extracellular space. As to keep the cell in equilibrium with its surrounding medium. In turn this causes the overall

concentration of intracellular solutes to increase. As cooling continues this water is then moved through osmosis towards ice crystals. Thus, further water is lost from cells until homogeneous ice formation occurs out a sample, ceasing such transport. If cells are cooled too slowly, this leads to build up of solutes in the extracellular space surrounding cells and within intracellular space leading to cell death. This is commonly known as the "Solution Effect". It must also be noted that this effect occurs in both the presence and absence of CPAs. As other extracellular solutes can still build up to toxic levels around cell surfaces. The exact cause of this toxic shock effect is not exactly understood but it is theorised that such cell death is linked to irreparable damage to the cellular membrane. Theorised, causes for such membrane damage are that of critical volume changes which can lead to the osmotic rupture of cells/ auto-lysis or the compromising of cellular membrane integrity. Leading to the cellular membrane of affected cells to become permeable to electrolytes [10, 11, 12] leading to cell death upon thawing due to the disruption of biological pathways.

2.2.2.2 Intracellular ice formation

During cryopreservation if cells are cooled too quickly they are unable to fully dehydrate, leaving a significant amount of within the freezing cell. This allows for sufficiently large ice nuclei to form within intracellular space leading to ice crystal formation through nucleation [8]. These ice crystals forming within intracellular space are extremely detrimental to cellular post-thaw survival and are often fatal above very small sizes. This is due to ice crystals continuing to grow during the cooling process until the homogeneous ice nucleation temperature is reached. If these ice crystals reach a large enough size within intracellular space they can damage cells in multiple ways. Firs, large ice crystals in contact with cells membrane can cause irreparable cellular membrane or if large enough cause complete cellular rupture via physically breaking through the cellular membrane [34]. Second, ice crystals can damage internal cellular structures [34] such as organelles or the cellular nuclei meaning upon rewarming that cells will autolyse due to non-viability or a breakdown in cellular pathways. The exact cause of such crystallisation is still not completely understood. However, there are currently three majorly accepted causes for the seeding of intracellular ice:

- 1. Ice crystals spontaneously seeds on the inner surface of a cells plasma membrane once it becomes suitable as a catalysing surface with the presence of extracellular ice. Referred to as surface catalysed nucleation (SCN). Leading to ice continuing to grow from the first point of nucleation on the membrane.
- 2. Ice crystals spontaneously seed within the cytoplasm volume, catalysed by internal particles within the cytoplasm. Particulates become suitable for seeding at a significantly lower temperature than the cellular membrane. Refereed to as volume catalysed nucleation (VCN)
- 3. Due to channels within the cellular membrane, ice crystals can transfer from extracellular space to intracellular space causing nucleation to occur near the cellular membrane. This is theorised to happen due to specific protein channels within the cells plasma membrane allowing for the transport of suitably small nuclei. This effect is theorised to be caused by the presence of extracellular

ice outside of cellular membranes close enough to such protein channels. Here we refer to as transport catalysed nucleation (TCN).

Within current literature it is not known whether TCN and SCN are the same or distinctly different forms of ice nucleation [69]. However, it is well enough understood that during freezing both SCN and VCN can occur. However, VCN has been found to occur at temperatures significantly below that of SCN.

Ice formation itself within intracellular space is not inherently a death sentence for cells. As research has shown that some cells that have intracellular ice during freezing can be saved during re-warming [70]. However, for this to be successfully the intracellular ice nuclei must be suitably small that damage has not been caused during either cooling or warming.

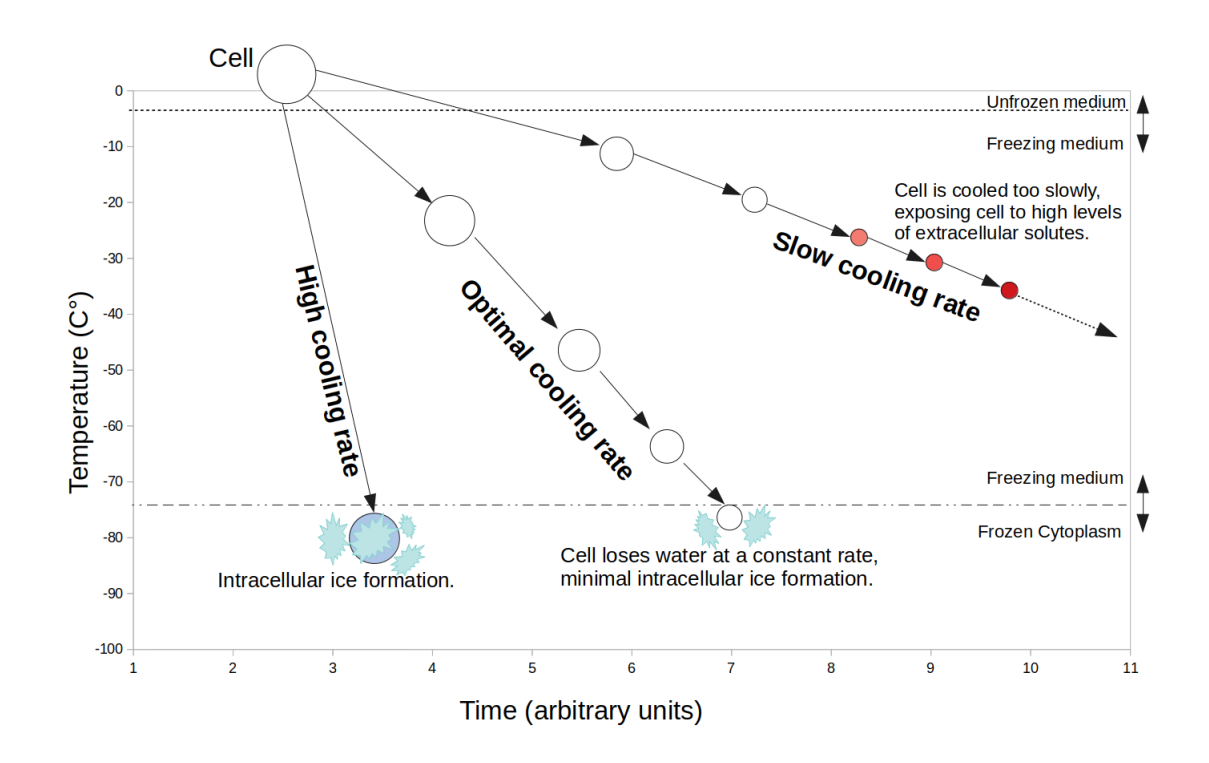


Figure 2.2: Freezing outcomes of cellular cooling

2.2.3 Warming

The freezing process for cryopreservation is paralleled in importance by that of the warming process. As previously mentioned the cells do not simply have to avoid damage during the cooling stage. Upon re-warming cells are still in critical danger for those processes which can damage them during cooling. Mainly, ice formation. As samples are re-heated to supra-zero temperatures. Ice crystals can still continue to grow a cause potentially lethal damage to cells. There is a major consensus however that rapidly warming samples avoids most of this possible damage, several studies across multiple cell types including bovine embryos [71], oocytes [72], T-cells [73] and many others. Similar to other problems faced in cryopreservation considerations for individual cell types still need to be taken. As warming a sample to rapidly can

lead to cell death through rupturing. As extracellular ice melts leading to a rapid influx of water into intracellular space. Leading to cell rupture through stresses being induced via rapid volume expansion.

The most common form of sample re-warming in use currently and considered the gold standard is water bath re-warming [74]. Due to its ease of use and relative success in re-warming of cell in suspension samples. However, new methods are still being developed due to some inherent drawbacks of water baths. First, water baths have some issues with sterility which could possibly compromise samples being warmed [74]. Second, water baths do not always provide consistent heating across the entire samples [74]. This is especially problematic for larger samples above the 2mL cryovial size as warming rates will not be consistent throughout the entire sample. Thus allowing for possible damage to sections of samples. For complex systems such as tissues this can lead to cracking across samples due to uneven heating rates generating stresses through the overall tissue structure [75, 76, 77]. Thus, alternative warming techniques such as magnetic resonance nano-particle heating [78, 79] and laser re-warming [80]. Both have shown promise in rewarming single cells, especially in the case of vitrified samples. Nano-particle re-warming has even been able to improve the post-thaw survival of animal organs such as rat hearts [81] and rabbit kidneys [77]. To date though water baths are still the most used method due to their ease of access, relative cost, well understood nature and lack of need to introduce further foreign matter to samples such as nano-particles. Identifying suitable methods for re-warming dates back very far in cryopreservation research itself. As J.E Lovelock et al investigated alternative methods as early as the 1950s [82] utilising magnetrons, constituting an early microwave.

2.2.3.1 The "Inverted-U" Curve

One must also consider that the issues presented by intracellular ice formation and the solution effect for slow cooling cryopreservation is not a binary issue. Instead we can more accurately represent these factors by two intercepting sigmoid curves, as displayed in Figure 2.3. The likelihood of death due to either the solution effect or IIF becoming more likely as cooling becomes slower or more rapid respectively. If one maps these curves onto one another for any individual cell type, the point of intersection would represent the optimal cooling rate for cell survival.

The shape shown in Figure 2.3 is often referred to as the "Inverted-U" survival curve. This shape has thus far been seen in some variation for the survival rate of all cell types undergoing standard single rate slow cooling with examples of multiple cell types post-thaw survival displayed in other work [83]. A single peak at some optimal cooling rate B_{opt} with diminishing survival returns at lower and higher cooling rates. Thus, it is this cell survival peak that survival optimisation work must find.

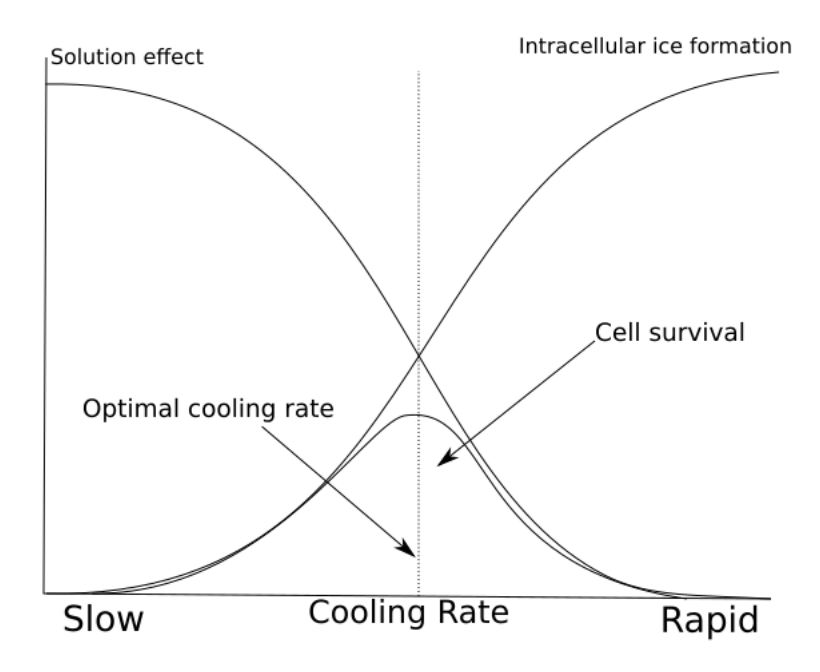


Figure 2.3: "Inverted U" plot for the survival rate curve of a hypothetical cell undergoing cryopreservation based on the intersection of intracellular ice formation and solution effect sigmoid curves. Optimal cooling rate for this cell is indicated by the dashed central line.

2.2.3.2 Cryopreservation of tissue

Despite the well understood nature and success in preserving most cells at sub-zero temperatures, the preservation of tissues at similar temperatures represents a much greater challenge. The end goal of cryopreservation has long been the expansion to more complete structures such as tissues or organs. However, considerable complexity is added when moving from free floating cells in suspension to more confined and restricted structures such as tissues [84, 85]. This ultimately comes down to several key features of tissue which do not need to be considered for freely moving cells. The main push for such preservation is often medically founded. As the true preservation of human tissues and organs would allow for significant reduction in transplant waiting lists through the ability to essentially "bank" critical organs and tissues.

First, unlike suspensions, tissues are most often not of a single homogeneous cell type. This already represents a significant issue as even in the case of only a two cell type tissue a single optimised regime for a single cell does not likely apply. Instead one could view this as the combination of two distinct "inverted U" curves for both samples being combined. Thus resulting in a new and more complex landscape. This may not be a significant issue if both cells optimal cooling independently falls at similar values. As one may only expect minor reductions in overall survival. However, if these two supposed cell types had an optimal cooling of 1 and 10 °C min^{-1} one can already imagine the challenge in finding a suitable optimal cooling. Especially when one must consider that this would be the most simple possible case for tissue cryopreservation while not considering other tissue properties. More complex tissues of multiple cell types being even more difficult to optimally cool if an abundance of distinct cell types are present.

Second, tissues are made from cells which are bound together in distinct structures with critical cell-cell interactions [86]. Thus, during cryopreservation these super-structures are at distinct risk of being disrupted and damaged by ice formation in extracellular space. As ice will expand through extracellular space within the tissues intercellular matrix. As this ice grows it forces cells out of the way and grows rapidly withing the confined space. This presents multiple significant risks to both the overall tissue super structure and cells themselves. As cells are not able to be "pushed" away from ice as freely as they would be in suspension they can be compressed and or damaged by ice as crystals expand. Additionally, ice is more likely to come in direct contact with cells leading to membrane rupture cell death.

As ice crystals form they "press" on cells forming the surrounding tissue super structure. This results in stress being applied across that region of the tissue. If such stresses become high enough the tissue can essentially fracture to relieve stress. Leading to large cracks in the frozen state that will become tears upon rewarming.

One must also consider that when thawing occurs. Ice melts essentially leaving "void" space. This is due to the fact that ice has an overall lower density than water but a greater volume due to strong hydrogen bonding and organisation. Thus, rewarmed regions recede rapidly and if surrounding cells cannot reform into their original structure additional void space is left between cells leading to the weakening of tissue.

Despite this there has been some recent advances in cryopreservation allowing for several whole organs to be successfully cryopreserved. This includes rat kidneys [87], hearts [88] and whole porcine ovary cryopreservation [89]. Thus indicating that cryopreservation is advancing to the point at which whole animal organs can be cryopreserved. However, as of time of writing this thesis no human organs have yet been successfully cryopreserved then retrieved and transplanted into recipients.

For the work within this thesis we have chosen to focus on slow cooling cryopreservation over other methodologies. In the case of vitrification this is due to several main factors. Firstly, the substantial amount of cryo-protective agents required for vitrification can present issues due to toxic effects to cells that the high concentrations can cause [90]. This would add extra difficulty to our optimisation approach. Second, the ability to evenly per-fuse high concentrations of CPAs without damaging cells through toxic shock pre-storage is made significantly more difficult with increasing structure complexity (For example going from cells in suspension to tissue). Therefore we believe that the slow rate approach is better for possible future expansions to the work within this thesis. Finally, for similar reasons to perfusion, the removal of high CPA concentrations can also cause damage to cells which would lead to further optimisation issues. In the case of isochoric and hyperbaric cryopreservation, despite the promise of post-thaw survival results, the ability to test and optimise such setups experimentally was outside the scope of this work. This initial outline of a cells response to cooling already outlines the main body of work to be investigated within this thesis. Post-thaw survival of cryopreserved cells is an optimisation problem of two major factors:

- 1. Optimisation of CPA concentrations through sufficiently fast cooling that the diffusion of internal water from a cell into extracellular space can mitigate the toxic effects of extracellular concentrations (Solution effect).
- 2. Inhibition of intracellular ice formation through sufficiently slow cooling to

avoid cellular membrane and internal structure damage due to ice nucleation.

This clearly presents an optimisation issue for the cryopreservation of cells and tissues. The combinations of cellular osmotic response, CPA toxicity and ice formation with the shared dependence on temperature presents a significantly complex problem which is highly suited for computational modelling and optimisation.

Chapter 3

Background of cryopreservation modelling

3.1 Cryopreservation Modelling

Biological research and in silico research have been strongly connected since the early 50s. One of the first examples of computational modelling of biological problems was that of tissue morphogenesis [91] by Alan Turing in 1952. Widely regarded as the genesis of computational biology with a rich history of advancement during the 50s and 60s. Cryopreservation similarly has had ties to modelling as early as the the 1960s, when Peter Mazur first developed the model for cellular damage during cryopreservation due to high cooling rates [92]. This paper represented the first mathematical model for cells undergoing cryopreservation and is regarded as the foundation of modern cryobiology modelling research. A model which Mazur later expanded on in the 1970s to introduce detrimental effects to cells subjected to cooling rates which where too low [68]. To this day the some variation of Mazur's 1972 model is still one of the most widely used across cryobiology modelling research.

3.1.1 Modelling transport of water and CPAs

In his 1972 paper, Mazur proposed that the osmotic response of a cell could be represented by a ratio of intracellular and extracellular vapour pressures. As cells which are taken to sub-zero temperatures have water transported in and out of their membrane purely by osmotic forces due to the pausing of biological functions. Mazur's model proposed the rate of change of cellular water volume in time as the difference between those intracellular and extracellular pressures as follows:

$$\frac{dV}{dt} = \frac{\left(L_p ART ln(\frac{p_e}{p_i})\right)}{v_1^0} \tag{3.1}$$

Here V is cellular water volume (um^3) , t is time (minutes), Lp is the hydraulic permeability of the cellular membrane $(ummin^-1atm^-1)$, A is the effective surface area of the cell (um^2) , R is the universal gas constant, T is the temperature (K), p is the vapour pressure for the intracellular (I) and extracellular (e) environment respectively and the molar volume of water v_1^0 . This can be seen as water moving in and out of cells based on interior and exterior osmotic pressures. It is also noted that due to biological processes in cells essentially "pausing" at sufficiently low

temperatures, during cryopreservation water is entirely transported through these means. Within this model such transport is purely passive and relies on the fact that cell membranes are relatively "thin" compared to overall diffusion length scales. It must also be noted that this model relies on a few fundamental assumptions. First, no-biological functions are active below sub-zero temperatures. Second, cells act as point sources within there environment and do not inhibit heat transfer. This is for one major reason, such that the temperature across a cell is even and that any change in temperature across the cell will be instantaneous. Finally, within this model and most other models cells are essentially assumed to be a sphere with a thin barrier containing only some fraction of solutes/solvents and water. As the model itself does not account for more complex cellular structures or components. Thus, it is likely that this form of modelling may not accurately capture the response of cells with more complex structures and/or shapes. Such as plant cells which have surrounding walls. For the purpose of most cells however this modelling approach has already shown to be relatively accurate. This includes ram spermatozoa [93], human spermatozoa [94] and many others [95, ?, 68, 96, 97, 98, 83].

As mentioned in Mazur's work, one must consider that not all water contained within cells is able to be osmotic-ally influenced. This is due to a significant proportion of cellular water being bound within proteins, solutes, lipids, organelles and other cellular structures. Thus, the intracellular water content of cells (V_c) must be broken down into two components. An osmotic-ally interacting volume (V) which can freely move in and out of the cell and non-osmotic-ally interacting volume (V_b) . This is summarised in Equation 3.2. Doing this allows one to calculate the rate of change of a cells volume in time purely as that of the osmotic-ally interacting water component. Here it is also assumed that all water that is bound within the osmotic-ally non-interacting state remains so with no unbinding due to effects such as protein degradation. However, this is likely to be true as all biological functions will have ceased within the cell.

$$V_c = V + V_b \tag{3.2}$$

It is also important to understand that many of the parameters relating to the membrane of a cell are not constant. Instead they have been shown to change based on temperature. For example, the hydraulic permeability (L_p) of cells has been shown to be a non-constant and temperature dependant variable. It has been well documented that the membrane permeability of cells to water likely follows an assumed Arrhenius relation to temperature [99, 100, 101]. This temperature dependence is well expected, as permeability parameters for cells to any solute/solvent are based on a simple diffusion based model. Thus, as temperature decreases membranes will become more permeable. However, some other more complexes changes in cellular structure such as phase change in the lipid layer of the membrane could also play a role. A simplified version of this relationship is given given by:

$$L_p = L_{pg} exp \frac{-E_a}{R} \left[\frac{1}{T} - \frac{1}{T_a} \right]$$
 (3.3)

Here Lpg is the hydraulic permeability at a reference temperature Tg and Ea is the cellular membrane activation energy. This Arrhenius relationship of membrane permeability modelling also relies upon a linear cooling rate. Thus, either a single linear cooling rate must be utilised or multiple distinct linear cooling rates. As the utilisation of a more complex non-linear cooling profile, such as an exponential rate, could break this relationship.

Equation 3.1 is more often seen in cryopreservation work relative to temperature rather than time. This can be done via a simple conversion from a time derivative to a temperature derivative by introducing a rate of change of temperature per until time (B = dT/dt) as follows:

$$\frac{dV}{dT} = \frac{1}{B} \frac{dV}{dt} \tag{3.4}$$

$$\frac{dV}{dT} = \frac{(L_p ART ln(\frac{p_e}{p_i}))}{Bv_1^0} \tag{3.5}$$

This variant of the equation is more commonly seen for cells undergoing cryopreservation as a direct relationship can be made between the change in cellular
volume and temperature. The variable B is most often referred to as the "cooling
rate" and in most models is assumed to be at the same rate which a freezer would
be cooling the sample space. Alternative versions of Peter Mazur's equation have
been derived over several decades. Such a the simplified version of Equation 3.1
derived by G. M Fahy (1981) [102]. Fahy instead related the change in volume of
a cell to several more easily identifiable and measurable variables such as the glass
transition temperature of water.

$$\frac{dV}{dT} = \frac{L_p ART}{Bv_1^0} \left[\frac{\Delta H_f}{R} \left(\frac{1}{T_g} - \frac{1}{T} \right) - \ln \left(\frac{V}{V + n_s v_1^0} \right) \right]$$
(3.6)

Here V_w is the partial molar volume of water, Δ Hf is the latent heat of fusion of water and n_s is moles of solute inside the cell. Taking Equation 3.6 and simplifying it two sided problem, left hand side (LHS) and right hand side (RHS), we can see that cells have three possible responses for their volume change during cryopreservation:

- 1. RHS of equation gives a positive value. Indicates an increasing cellular volume due to an intake of extra-cellular water.
- 2. RHS equates to zero, intracellular and extracellular osmotic forces are in equilibrium leading to no change in volume or the cell has no remaining osmotically active internal water.
- 3. RHS equation gives a negative value. Indicating decreasing cellular volume due to the expulsion of water from the cell.

These results can be applied for both cooling and thawing as water transport from the cell remains passive until biological activity restarts at near 0 or supra-zero temperatures. A visible representation of these responses can be found in Figure 3.1.

In addition to water transport, cells undergoing cryopreservaiton also experience a change in volume due to the passive diffusion of permeating CPAs and solutes. The flux equation derived by Whittingham *et al* (1972) [103] was one of the first models to include such non-water transport and was later simplified in 1981 by Fahy *et al* [102]. Ultimately, following a similar form to that of water transport:

$$\frac{dn_e}{dT} = \frac{P_s A n_e \times 10^{15}}{B} \left(\frac{1}{V_{eq}} - \frac{1}{V} \right) \tag{3.7}$$

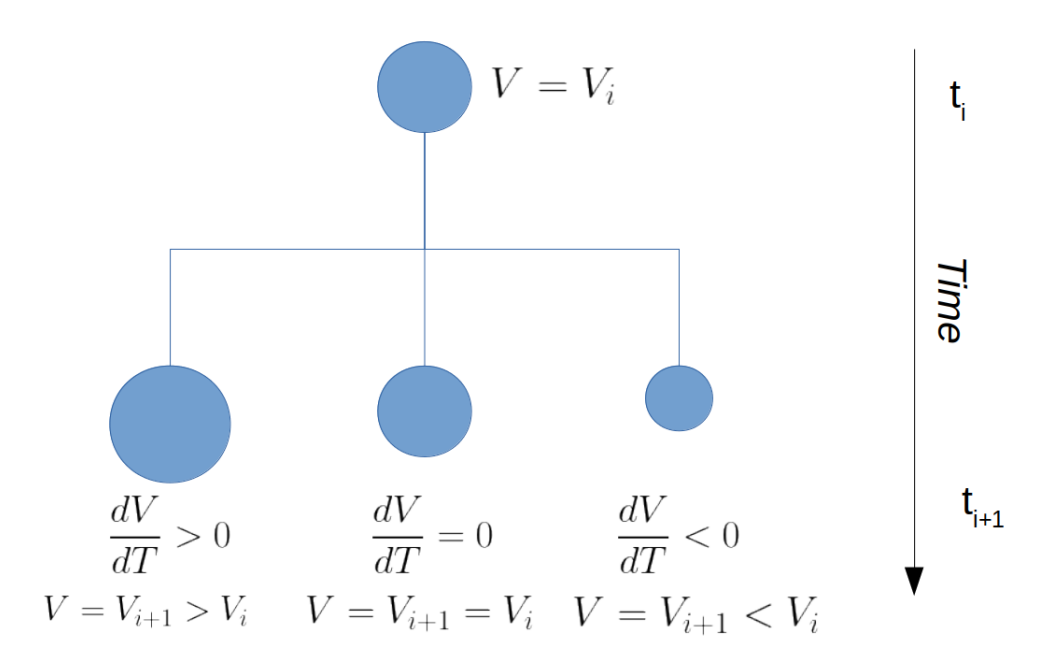


Figure 3.1: Cellular osmotic responses

Here n is moles of solute, P_s is the cell membrane permeability coefficient to the given CPA and V_{eq} is the equilibrium volume of the cell. P_s like L_p is also temperature dependant and varies as follows:

$$P_s = P_{s_0} exp \frac{-E_a s}{R} \left[\frac{1}{T} - \frac{1}{T_q} \right]$$

$$\tag{3.8}$$

 P_s follows similar assumptions to that of L_p , having an Arrehnius relationship with temperature during linear cooling. However, some arguments have been made that due to the solutes having varying mobility based on temperature that this equation may not fully encapsulate the Arrhenius relationship of P_s below 0°C [104, 105]. Instead it was proposed by Katov that P_s should instead follow a relation ship of $P_s = \omega RT$, where ω is the mobility of the solute in question. It has also been further proposed that the P_s is not actually a single variable but instead a "lumped" variable of multiple temperature dependant variables such as diffusivity and solute mobility [105]. This is further complicated by the fact that many solvents and solutes go through density and volume changes at sub-zero temperatures. Thus, as temperature decreases the overall concentration of a given solute/solvent can change without a necessary loss in the overall available amount. Combining all these factors together means that overall P_s is a very difficult variable to accurately predict but current models seem to be sufficient for the purposes of modelling for most CPAs. In the absence of permeating CPAs this equation can effectively be set to 0. Additionally, it is also key to point out that at sub-zero temperatures that ion channels on cellular membranes will be inactive during cryopreservation. Thus large extra cellular solutes such as salts will be unable to pass in or out of cells. Thus, such molecules are not accounted for similar to non-permeating CPAs.

Finally, one must also consider that a cell may contain some non-permeating CPA's or solute within their intracellular space. This is due to a specific phase transition experienced by membranes as it enters sub-zero temperatures. As cells are cooled below 0°C their lipid membrane surrounding becomes "leaky" as they transitions to the context of the

sition from a crystalline liquid phase to a gel phase [99, 106]. This phase transition leads to brief leakiness in cellular membrane integrity allowing for the entrance of non-permeating extracellular solutes, solvents and salts. After re-organisation of the membranes lipid tails into a more "solid" form, cells will then regain previous impermeability to some CPAs. Thus at any given time a cells total volume can assumed to be given by a combination of its osmotic-ally interacting water volume V_b , non-osmotic-ally interacting water V_b , permeating CPA content V_p and non-penetrating components $V_n p$.

One issue with current models for estimating the change in volume of cells during cryopreservation, as outlined above, is the requirement for multiple cell dependent variables. This often requires in depth experimental work and can even be dependant on cell type as to which method can be used. As mentioned in other works [105], measuring the initial volume of cells and ascertaining membrane parameters of cells often takes one of three approaches: impedance testing, optical measurements and more recently fluorescence measurements. For impedance testing cells are passed through a small aperture of variable size and the "impedance" caused by the proceeding cell can be utilised to calculate cellular volume. Despite the fact that only a single cell can pass through an aperture at a time it is a relatively fast process and thousands of cells per-minuted can pass through the system. Additionally, impedance testing is a direct measurement of cellular volume allowing for a relatively accurate prediction of the average cell volume throughout the sample. One drawback to this method however is its necessity for a large sample of cells to be tested. Optical measurements are more commonly used in the case of cells for which mass samples cannot be ed. Be this due to the relative size of cells or difficulty of acquisition. Optical measurements instead directly recording the in volume of a cell as extracellular media is changed. This allows for the direct measurement of a cells volume and membrane properties at specific temperature. However, compared to impedance testing, optical measurements are much more involved requiring the measurement of individual samples and utilising image analysis techniques to asses aforementioned variables. Thus, this is not a high-throughput experiment and is incredibly time intensive. Finally, some limited use of fluorescence has been used to asses cellular water volume. However, this method does not test directly measure cellular volume itself and must be used in combination with other techniques.

From Equations 3.2, 3.3, 3.6,3.7 and 3.8 an initial basis for modelling and simulating the osmotic response of cells to various cryopreservation procedures can already be developed. Overall, laying out the foundation for our modelling approach for cells within this work. This already allows for several key predictions for cells undergoing cryopreservation. First, using the outlined equations one can already begin to predict the kinematic water loss of cells during cryopreservation [97, 68]. Including cells responses to multiple cooling rates in various different forms of CPAs.

3.1.2 Intracellular ice formation

Arguably the most key part of modelling cryopreservation is predicting ice formation in cells undergoing cooling and thawing. Especially when one considers that the majority of cell death during cryopreservation at slow cooling rates will be down to some combination of either extracellular or intracellular ice formation. As even the solution effect at low cooling rates is primarily driven by extracellular ice formation.

The quantification of intracellular ice formation for biological cells was first explored by Peter Mazur [92] in 1963. Based on observations experimentally that intracellualr ice formation had a significantly higher likelihood when intracellular solutions were suitably super cooled. In later models developed by R.E Pitt et al (1989) and M. Toner et al (1989) the first example of estimating intracellular ice formation was made [107, 108]. These models were later improved upon by J.O.M Karlson (1994) [109] based on diffusion limited ice growth. Karlsson further improved his modelling approach and made predictions for several cell types including bull spermatozoa. In 2014 G. Yu et al [97] further improved on this form of modelling including newer implications for the formation and growth of ice crystals in freezing cells. Predicting the likely hood of intracellular ice formation within any given cell as a density distribution of nucleation rates based on a cells volume and area. Here we outline the methodology and how it is integrated into our computational framework. Importantly. Yu et al's model was validated against experimental data showing a better fit to the in vitro freezing of cells. Only requiring a slight modification compared to that of classical models.

As mentioned previously in Chapter 2, Ice formation currently is believed to occur by three major avenues. Catalysation of ice crystals on the inner surface of cell membranes (SCN), via ice nuclei travelling through membrane water channels (TCN) and nuclei catalysing within the cytoplasmic volume of cells (VCN). The probability of IIF occurring within any cell can therefore be expressed as a combination of these factors. As their is no clear understanding if SCN and TCN are distinctly different these are also often group into the same category for modelling. Thus, predicting ice nucleation inside of cells is often expressed as follows:

$$P_{IIF} = P_{IIF}^{SCN} + \left(1 - P_{IIF}^{SCN}\right) P_{IIF}^{VCN} \tag{3.9}$$

Here P_{IIF} is the total probability of IIF occurring within a cell, P_{IIF}^{SCN} and P_{IIF}^{VCN} being the probability of surface and volume catalysed nucleation occurring respectively. The overall value ranging between 0 (zero ice formation chance) to 1 (100% chance of ice formation within the specified cell).

The individual forms of each type of IIF occurring has been defined in many works in a variety of ways. We have chosen to utilise the probability of each IIF type occurring as derived in Yu *et al*'s model. As it is the most modern variation of the intracellular ice formation model with proven accuracy over alternative methods. Within their work ice formation of each type is defined by following equation:

$$P_{IIF}^{XCN} = 1 - exp^{\left[-\frac{1}{B} \int_{T_0}^T Z I_{XCN} dT\right]}$$
 (3.10)

Here XCN represents SCN or VCN. For SCN Z is the effective surface area of the cell A. Effective surface area meaning the maximum amount of effective contact a cell can have with its extracellular environment. As this will change for cells based on morphology, structure e.t.c.. For VCN Z is the cellular volume V. I_{XCN} is the nucleation rate of ice as described in the work of Yi.G et al (2014) [98]. Here, the entire volume of a cell is assumed to contribute to VCN ice formation. However, arguments could be made that certain areas of the cell should not be included within this total. Such as those which are much more difficult to freeze like the cell nucleus or other structures with high non-osmotic water content. The combination of ZI_{XCN} can be taken as the probability density of XCN type ice formation and is defined via an integral over. This integral can take one of two forms:

$$-\frac{1}{B} \int_{T_0}^T Z I_{XCN} \, dT = -\int_0^t Z I_{XCN} \, dt \tag{3.11}$$

Additionally, one must also apply conditional probabilities to a cell freezing during cryopreservaiton. This is to account for critical variables being reached such as: available osmotic-ally interacting water and meeting the requirements for water to freeze withing cellular space. This can be summarised as follows:

$$P_{IIF} = \begin{cases} 0 & \text{if } V = V_b \\ P_{IIF}^{SCN} + (1 - P_{IIF}^{SCN}) P_{IIF}^{VCN} & \text{if } V = V_b \text{ and } T \le T_f \\ 0, & \text{if } T \le T_f \end{cases}$$
(3.12)

We can setup these equations within code via if statements, the following example is given in sudo code:

```
 \begin{aligned} &\text{if } (\ V > V_b and and T \leq T_f) \ \{ \\ \ // &\text{Evaluate equations for PIIF} \\ \dots \\ &\text{SetPIF}(\mathbf{x}); \ // &\text{Here } \mathbf{x} \text{ is calculated from calculations of nucleation rate and probability density.} \\ &\text{} \\ &\text{} \\ &\text{SetPIF}(0); \ // &\text{Cell object is outside of a boundary condition thus preventing IIF.} \\ &\text{} \\ \end{aligned}
```

This puts two conditions upon predictions for ice formation. Firstly, V_b is the non-osmotically interacting volume of our cell. This is represented as a condition above due to the inability for ice to form within a cell if it has no more water available for forming ice. Secondly, T_f represents the equilibrium freezing temperature of cytoplasm, thus preventing ice nucleation if this temperature is not yet reached. Thus, at any given time point one can predict if a cell is likely to undergo intracellular ice formation.

Many variations of this form of ice formation have been shown to successfully predict intracellular ice formation across multiple cell types. Including hepatocytes [110], mouse oocytes [109, 111], stem cells [56, 112, 95], HeLa cells [97] and many others [72, 113, 114]. These models have even proved useful in small embyos such as that of the Drosophila [115, 116]. Most of these works utilise a variation of the Karlsson model and have overall been shown very capable of predicting expected quantities of ice formation and percentage of frozen cells. However, as this modelling approach essentially follows on from that of Mazur and similar work they essentially act as "saline bag" models. In which the only two distinct aspects of the cell are a membrane surrounding an internal volume of intracellular material. Overall, having no distinction for cellular structures or exact sites of nucleation. In most cases this is not an issue for most cell types. However, this model may not fully capture more complex interactions for cells with distinct cellular structures or non-uniform volumes. For example, spermatozoa or neuron like cells. Some more complex modelling approaches have been utilised for approaching these problems such as "network" based systems [117]. This model differentiates cells into 3 major regions: membrane, cytoplasm and nucleus. Nodes are then laid out across these region in a pattern accounting for edge and inner space with independent parameters for each region. This type of model allows for more in depth computational investigation on the effect of ice nucleation conditions based on specified nucleation sites. Something that is not possible with a simple "sack of saline" style modelling that is utilised in classic cryopreservation modelling. Additionally, such form of modelling would allow for investigating more in-depth how possible imbalances in water and cpa concentrations across a cell may lead to differential ice nucleation. Furthermore, such a model could be further expanded to incorporate even more complex cellular structures through the node based layout. However, compared to classic modelling approaches, this type of modelling is much more computationally intensive also within the scope of the current work we do not believe this level of detail is yet required. However, this modelling approach could prove useful for future avenues of research into more complex cell types.

One current issue of debate in cryopreservation modelling is that these forms of models may also have issue with cells that have high levels of adhesion when within media [118]. This is due to the main crux of these models revolving around the possible "entrance" of ice into cells through either direct contact with ice crystals or transport through water channels. Thus, an overall reduction in the effective contact area of the cells with the extracellular environment may lead to inaccuracies in the estimation of ice formation. More importantly, this could lead to compounded inaccuracies in predicting IIF within tissues. As cells will have considerably less direct interface with the extracellular media. Some research has already been done in this regard. Introducing the probability of IIF essentially being "passed" between connected cells [119]. However, thus far these models have only been utilised in 2D computer simulations. The lack of a 3rd dimension and the difficulty to validate such models easily still leaving this overall an unsolved problem. Some pre-publication work does exist for more complex agent based systems in 3D space [120]. However, this work is as of writing this thesis not not published but overall exemplifies the need for a movement towards agent based modelling system for solving these problem in cryobiology.

3.1.3 Predicting cell death

The main crux of modern cryobiology modelling revolves around predicting and improving the post-thaw survival of biological materials undergoing freezing. Thus, a considerable amount of recent research has endeavoured to predict cell death during cryopreservaiton based on models outlined in previous chapters. This problem can be seen as a rough three part system. Cell death due to exposure of cells to sufficiently high concentrations of solutes for extended period of times (The solution effect). Cell death due to osmotic-ally induced lysis on re-warming (flux induced damage). Intracellular ice formation induced cell death due to ice crystal formation within intracellular space.

3.1.3.1 Chemical toxicity

The modelling of cell death due to toxicity is often considered to be a combination of two main factors. First, chemical concentrations within intracellular and extracellular space are a direct cause of cell death. Second, as cells are to be maintained at low temperatures for extended periods of time, one must also consider that cell death due to toxicity must also be time dependant. Benson first define this idea mathematically for a "cost-functional" in their 2006 work [121]. Later going on to describe the function more fully in their 2012 work as time dependant power law [122] as follows:

$$J(m^e) = \int_0^{tf} f(m^i(t), t)dt = \int_0^{tf} (m_s^i(t))^{\alpha} dt$$
 (3.13)

Here m^i and m^e represent intracellular and extracellular molalities respectively, t^f if the timepoint at which a cell reaches a desired intracellular state. α is a constant proposed by Benson in their 2008 work and is based on cited existing studies for support [121]. Here J is described as "The accumulated damage to the cell as a function of equilibriation or time.

In, addition to these, Benson also made two additional possible cost functions. First, the toxic cost function may also require the introduction of non-permeating solute molality. This expands the above equation to become:

$$J(m^e) = \int_0^{tf} ((m_s^i(t))^{\alpha} + \epsilon (m_n^i(t))^{\beta}) dt$$
 (3.14)

However, this is still ongoing work and the fully functional form of such a relationship is not yet clear. As such a toxicity model could have much further complexity with "instantaneous" damage [105]. Bensons original toxicity model was aimed at CPA equilibriation experiments. However, the toxicity model can also be used as a measure of damage during cryopreservation. Anderson *et al* used a variation of Equation 3.14 in their 2019 work to define a solution based injury to cell based on this principle in combination with an ice formation model. Anderson's version of the solution cost function which is a modification of Benson's is as follows [123]:

$$J(m^e) = \int_0^t ((m_s^i(t))^{\alpha_s} + \epsilon(m_n^i(t))^{\alpha_n}) ds$$
 (3.15)

Here α_s and α_n are positive constants. This equation is based also temperature dependant based on solute motility. One can already begin to generate an effective argument that a cells tolerance to solutions would be based on that of its cellular water content and overall cellular volume. Or that a cell could "tolerate" a certain level of solute molality with increase beyond that leading to cell damage and thus cell death. This is summarised in other work [122] for Equation 3.15 as follows:

$$\left| m_s^i(t^f) - m_s^{des} \right| \le tol \tag{3.16}$$

Where tol is some acceptable tolerable amount and m_s^{des} is the desired volume/time points molality. Utilising such a cost function one can already begin to generate the lower cooling rate half of the "inverted U" curve. As shown in recent works, utilising data of a mouse embryonic stem cell during cooling generates the expected "solution-effect" damage to cells at low cooling rates [105].

As previously any such integral equation can be changed to terms of temperature instead of time through the application of Equation:

$$\frac{dt}{dT} \times dT = dt \tag{3.17}$$

Converting this to:

$$\frac{1}{B} \times dT = dt \tag{3.18}$$

Here B representing the cooling rate. Equation 3.14 becomes:

$$J(m^e) = \frac{1}{B} \int_{T_i}^{T_f} ((m_s^i(t))^{\alpha} + \epsilon (m_n^i(t))^{\beta}) dT$$
 (3.19)

 T^f here representing the desired temperature or in most cases the end temperature of -40°C before plunge freezing.

Converting Equation 3.19 into a probability we get the following equation:

$$P_{sol} = 1 - exp^{\left[\frac{1}{B} \int_0^{Tf} ((m_s^i(t))^{\alpha} + \epsilon (m_n^i(t))^{\beta}) dT\right]}$$
(3.20)

When accounting for the solution effect one must also consider that the intracellular water content of a cell is highly important for the dilution of intracellular solutes. As with a reduced intracellular water content a cell will effectively experience a comparatively higher concentration permeating CPA's or salt for example. G.Fahy (1981) [102] first quantified a possible mechansim for tracking such cellular damage through water flux during cooling and warming.

$$J_{com} = CR \frac{\Delta V}{\Delta T} \times \frac{1}{V_0} \times \frac{1}{A}$$
 (3.21)

This lead to the effective death of cells through a build of extracellular and intracellular concentration relative to the effective surface area of a cell and its intracellular water content compared to its initial water volume.

Combining Equations 3.20 and 3.21 we can get a an overall "solution effect" based chance of cell in suspension undergoing cryopreservation.

Utilising these Equations one can therefore begin to generate the first picture for cell death within the lower cooling rate region of the the "inverted-U" curve. As described in other works the utilisation of these equations can already generate useful data for optimising the lower region of cellular cryopreservation leading towards the locating of an optimal cooling rate [102, 105].

In the absence of extracellular or permeating CPA's these equations are still capable of explaining cell death through compliance injury. As cells grow too large compared to their initial water content and *in vitro* would lyse through osmotic rupturing. Second these equations still account for other non-cpa related toxicity effects as cell will still experience an effective toxic build up of other extracellular and intracellular solutes. Example of similar but modified equations seen in other works for estimating cell death of human induced pluripotent stem cell cryopreservation [?, 95].

3.1.3.2 Ice formation induced cell death

Utilising previous equations for predicting ice formation and employing a random variable distribution we can predict if a cell undergoes lethal intracellular ice formation. However we must set up one more boundary conditions for lethal intracellular ice formation. To gain an initial quantifiable boundary condition for the likelihood of IIF causing damage to cell we must further break down ice formation into "Survivable" and "Not-Survivable". As discussed by both Mazur et al and Fahy et al [124] a cell requires a minimum amount of osmotically interacting water for "lethal IIF" to take place. As if their is not enough free water molecules to bind within a cell to form a sufficiently large ice crystal then it will not be lethal to a cell. It is estimated that this quantity is around 15% of a cells initially available osmotically

interacting water. Below this value a cell is considered to be "Rescuable" or to have a "Low lethal IIF chance". A cell which is rescuable is one which is considered to have a low chance of death due to IIF with sufficiently fast re-warming. An example of these three possible responses in terms of relative volume of cell water for mouse oocytes undergoing multiple cooling profiles is displayed in Figure 3.2. The figure itself is a modified version of the graph presented by Mazur in other work [125].

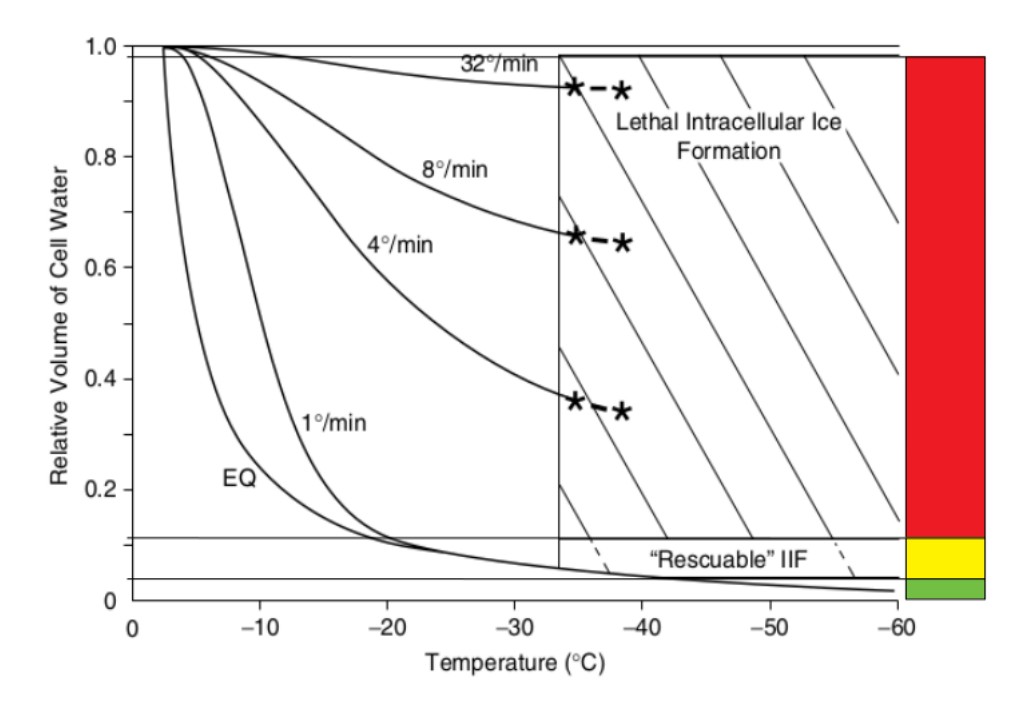


Figure 3.2: Relative volume of cell water against temperature for mouse oocytes with outlines for IIF type based on remaining volume. (Red) lethal, (Yellow) rescuable and (Green) safe.

Now we can define a "Survivable" and "Non-Survivable" state due to IIF for any given cell within our simulations undergoing cryopreservation. This can be developed into a simple boundary condition problem for each cell as shown in Equation 3.22.

$$P_{IIF}^{Lethal} = \begin{cases} 0 & \text{if } V < 0.15V_i \\ P_{IIF}, & \text{if } V \ge 0.15V_i \end{cases}$$
 (3.22)

It is to be noted however that the maximum "Rescuable" region can fluctuate from 0.1 to $0.2~V_i$ [92, 124]. Thus our value of 0.15 could lead to either over or under estimation of cell death due to intracellular ice formation based on different cell types. Thus, in the case of specific cells it may require further optimisation to accuratly capture the chance for that given cell to undergo lethal IIF. These boundary conditions can be represented in sudo code in the following form:

```
if (V > 0.15 \times V_i) {
    if (V > V_b and and T \le T_f) {
        // Evaluate equations for PIIF
        ...
        SetPIF(x); // Here x is calculated from calculations of nucleation rate and probability density.
    } else {
        // Evaluate equations for PIIF
        ...
        SetPIF(y); // Here y can be 0 for no cell below this threshold allowing for IFF or instead calculate // recoverable IIF.
    } else {
        SetPIF(0); // Cell object is outside of a boundary condition thus preventing IIF.
    }
```

As our framework is an agent based system each individual cell will have an independent probability density distribution based on internal characteristics and local environment variables. An example of such a distribution is shown in Figure 3.3 for a hypothetical simulated cell. The probability of intracellular ice forming can then be estimated via integrating over the distribution from some initial temperature T_0 to temperature T as outlined in Equation 2.9. T_0 is often the minimal temperature required for IIF to take place during the given freezing scenario. Giving an individual cells chance of undergoing IIF during cryopreservation at any given time point in a simulation.

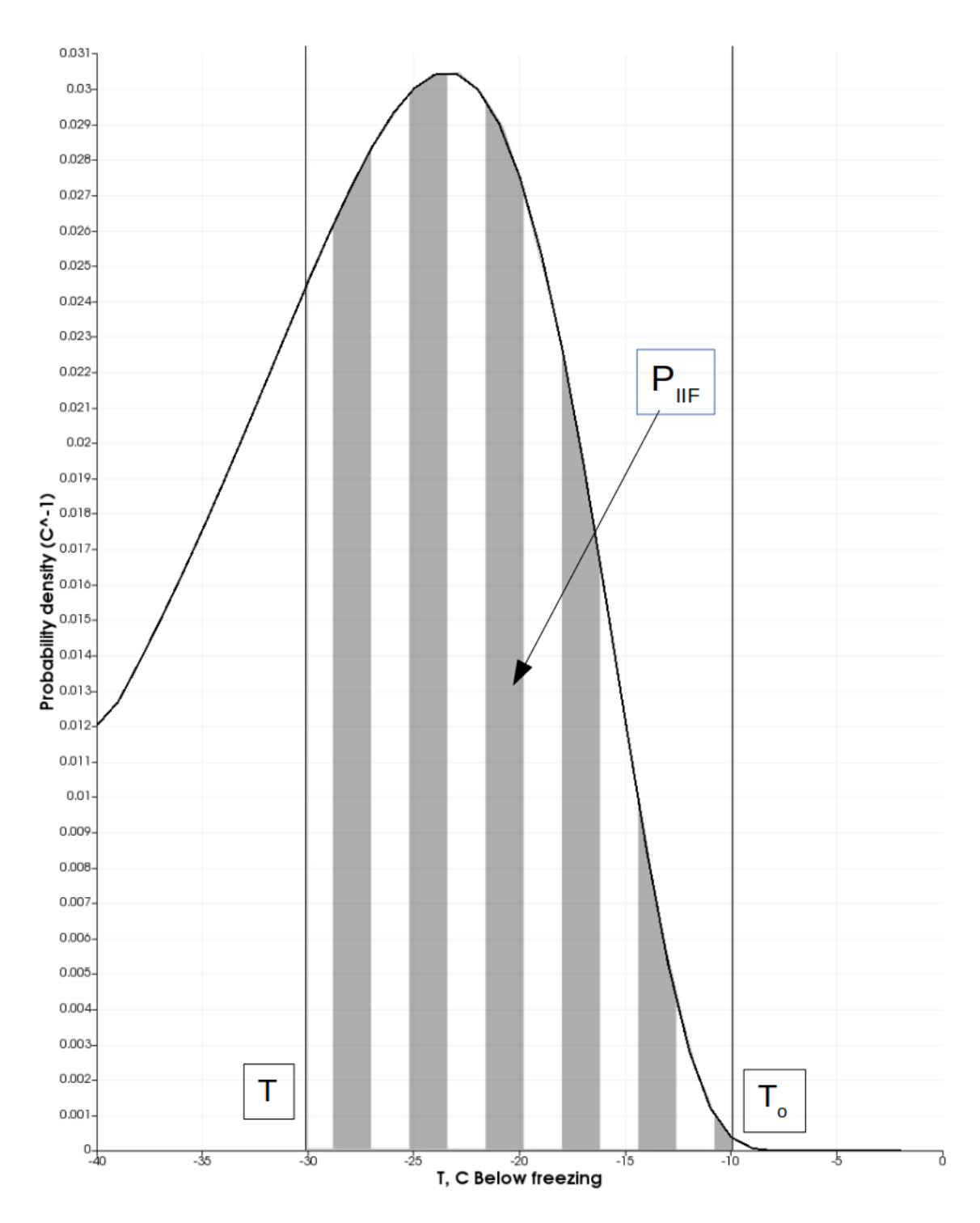


Figure 3.3: Example probability density of ice formation in a cell during cooling.

Utilising a simple integration across the current simulation time one can then make predictions for each individual cell and assign a likelihood of cell death based on current intracellular water volume and if IIF has occurred. Then one can assign cells one of three labels: Safe, Rescuable or Dead. Safe cells are those which undergo IIF with a intracellular water content of less than 10% of their initial water content. Rescuable cells are those which undergo IIF with an intracellular water content ¿10% but ;15% of their initial water content. Dead cells in the current iteration are any cell which undergoes intracellular ice formation with a water content ¿15% of their initial water content and are assumed un-recoverable. The rescuable cell fraction is that which will be altered based on specific cell type. As if cells can undergo IIF with up to 20% of their initial water content freezing post-thaw survival results may seew towards lower cooling rates. Where as if a cell is less tolerable to inracellular ice this may lead to a skewing of the optimal survival towards the faster cooling rates.

This form of modelling is already sufficient for most cells to give a general idea of lethal ice formation ranges above that of the optimum. As higher cooling rates utilising slow stepped cooling will always be lethal. This could possibly lead to a slight skewing of the optimal peak to slightly higher cooling rates but is already sufficiently accurate enough to massively reduce the need for wet lab experimentation.

3.1.3.3 Recreating the "inverted U"

From the models outlined in sections above one can begin to create an overall probability function for the likelihood of cells undergoing cryopreservaiton induced cell death. This can be defined as:

$$P_{SUR} = 1 - (P_{SOL} + (1 - P_{SOL}) P_{IIF})$$
(3.23)

Similar forms of this model have already been shown capable of predicting the chance of cell death in mouse embryonic stem cells and human induced pluripotent stem cells [105, ?]. Outlining the basis of a predictive model for the post-thaw survival of cells in suspension undergoing cryopresertvation. Thus, utilising this model in an agent based simulation makes a great deal of sense. As cells could have their individual "cost" of cooling based on independent local concentrations, temperature, water volume and IIF. However, this model would likely not be sufficient in its current form to make predictions for cells in tissue. Due to the increased complexity of cell fate in more complex structured systems. As the model will likely also need to include some form of cost based on physical tolerance due to stresses created on cells during cryopreservation. This would present a starting point for such works though. As the foundation of a predictive cryopreservation model for cells in suspension could later be expanded upon to include more complex cellular geometries based on finite element or volume. Argument could be made that a vertex based simulation could be useful for epithelial tissue analysis as this is already a widely used modelling approach in many areas of research. However, vertex models are not easily adapted to 3D space and are considerably more computationally expensive. A continuation of an agent based modelling approach seems better suited for several reasons. Firstly, our initial modelling approach for cells in suspension will take an agent based modelling approach and is likely easy to expand upon through the introduction of cellular interactions, adhesion and forces. Second, agent based models are already widely utilised for the simulation of tissue in several works, including: cancer research [126, 127], tissue patterning and mechanics [128, 129, 130, 131], wound healing [132], long scale tissue signaling and forces [133, 134, 135] and many other applications. For this reason I believe agent based modelling is perfectly suited to this work due to its application across multi-scales, individual cell modelling and interactions and its pre-existing use for modelling single cells, tissues and possible expansion to organs.

Through a combination of this Chapter and Chapter 2, one can already begin to create a suitable model for predicting the post-thaw survival of cells during cryopreservation. With some success already show in other works. Additionally, the models outlined above are highly suited to an agent based modelling approach due to the ability for each cell agent to have individual properties connected to a matrix of the extracellular environment. However some limitations still exist. As previously mentioned these models are suitable to "cell in suspension" modelling but may miss key factors of tissue or organ based cryopreservation. Similarly such modelling does not account for cellular structures due to its "bag of saline" nature. Thus, it is unlikely if such models would be suitable for cells which have more non-uniform shapes or complex intracellular structures. These forms of models are also dependant on multiple cell specific variables. Thus, cellular variables must still be acquired from pre-existing works or new experimental work. However, this is not unexpected and will likely allow for a significant reduction for repeat in vitro work if successfully applied. These forms of models also require the definition of an extracellular space such that extracellular concentrations can be directly tracked and reflect changes in cellular water and CPA contents through osmotic effects. This however will be discussed within a later section of this work.

The two best-established methods for cryopreservation are vitrification and slow-cooling. Vitrification is a relatively new method where high cooling rates are employed. To this end, usually liquid nitrogen is used. However, vitrification requires high concentrations of cryoprotective agents (CPAs) to inhibit intracellular and extracellular ice formation (IIF and EIF). Vitrification can result in excellent post-thaw survival rates (80 - 95.6%) [54, 55]. However, vitrification is problematic with regard to medical applications due to lack of scalability, high CPA concentration requirements and possibility of sample contamination through direct contact with liquid nitrogen [56, 57, 58].

The second technique uses a stochastic Differential Evolution algorithm (DEA), as defined by Storn and Price [136]. This method combines computational modelling with iterative experimental feedback to optimise cooling rates and CPA concentrations through an evolving algorithm. DEAs have shown success in the work of Tsutsui et al and Pollocket al for predicting and optimising the post-thaw survival of multiple cell types [137, 138]. However, a major issue with the DEA method is its need for repeat experimental feedback in an iterative cycle between experimental and computational data. Thus, it reduces one of the major benefits of optimising protocols computationally, i.e. the significant reduction in costs related to repeated experimental data acquisition.

Thus, we used a computational model for simulating the cryopreservation of cells in suspension with a focus on applying our model across multiple cell types and validating our work experimentally *in silico*. Necessary parameters for cell properties are taken from relevant literature with comparisons made against pre-

existing experimental data. Ultimately, we have utilised our model to investigate two major questions: (1) Can an agent based model for cryopreservation predict the post-thaw survival of cells in suspension? (2) Can such models be used to make predictions for multiple cell types?

3.2 Jurkat cell post-thaw survival

To test our model as outlined in the equations above we chose to investigate simulating the post-thaw survival of Jurkat cells. Jurkat cell were chosen due to several major regions. First, at the time of conducting this work Jurkat cells were the easiet cells to aqquire and maintain based on limited availability to access and work in the laboratory. Second, Jurkat cells have a wide range of well established literature in and out of cryopreservation. Finally, Jurkat cells are widley used in many areas of biomedical and pharmecutical research. Within these simulations we matched our simulation parameters to those of G Yu et al [139]. In addition to conducting our own cooling of Jurkat cells in vitro to compare against both our simulated results and the results from literature. In our simulations Jurkat cells utilised the following parameters from experimental literature; membrane water and experimental parameter values were taken from the work of Yang et al [140].

3.2.1 Experimental procedures

Experimental protocols where carried out by Dr Sanja Bojic for this section. Jack Jennings took part in initial freezing protocols, assisted in designing experimental protocols and post-thaw cell counting.

3.2.1.1 Cell cultures

For our wet-lab experiments, we used human T lymphoblasts - Jurkat cells (Clone E6-1; TIB-1522; American Type Culture Collection, Manassas, VA). Jurkat cells were cultured in a complete growth medium containing RPMI 1640 Medium (A1049101; Thermofisher Scientific, Massachusetts, US), 10% fetal bovine serum (10270106; Thermofisher Scientific, Massachusetts, US), and 1% penicillin-streptomycin (15140122; Thermofisher Scientific, Massachusetts, US) in a tissue culture incubator at 37°C with a humidified atmosphere containing 5% CO2. Cells were grown in suspension in T75 tissue culture flasks and maintained at a concentration between 1×10^5 and 1×10^6 cells $\rm mL^{-1}$, as recommended by the supplier.

3.2.1.2 Freezing and thawing

For cryopreservation experiments, Jurkat cells were dispensed into cryovials at $3.0x10^6$ cells mL⁻¹, in a complete medium with the addition of 10% DMSO (102952; Merck, Darmstadt, Germany) as a cryoprotective agent. Cells were cryopreserved using a Kryo 360 controlled rate freezer (Planer, Middlesex, UK). Cells were cryopreserved using three cooling rate profiles at 0.5, 3 and 10° C min^{-1} . All the experimental conditions were tested as both technical and biological triplicates. Before freezing the Kryo 360 controlled rate freezer was cooled down to 4° C, which was used as a starting temperature for all experiments. After reaching -50°C, cells were kept

41

frozen for one additional hour. Afterward, vials were quickly thawed in a 37°C water bath.

3.2.1.3 Staining and cell counting

As soon as an experimental vial content was thawed, the cell suspension was transferred to a centrifuge tube containing 9 mL complete medium and centrifuged at 1000 rpm for 5 minutes. After spinning cells down, the supernatant was removed, and the remaining cell pellet was re-suspended in the complete medium, dispensed into a 75 cm² tissue culture flask, and incubated in a tissue culture incubator at 37°C with a humidified atmosphere containing 5% CO2. The living cells were counted using a trypan blue exclusion test, 1 hour and 24 hours after thawing, with at least 200 total cells counted for each experimental condition tested.

3.2.2 Results

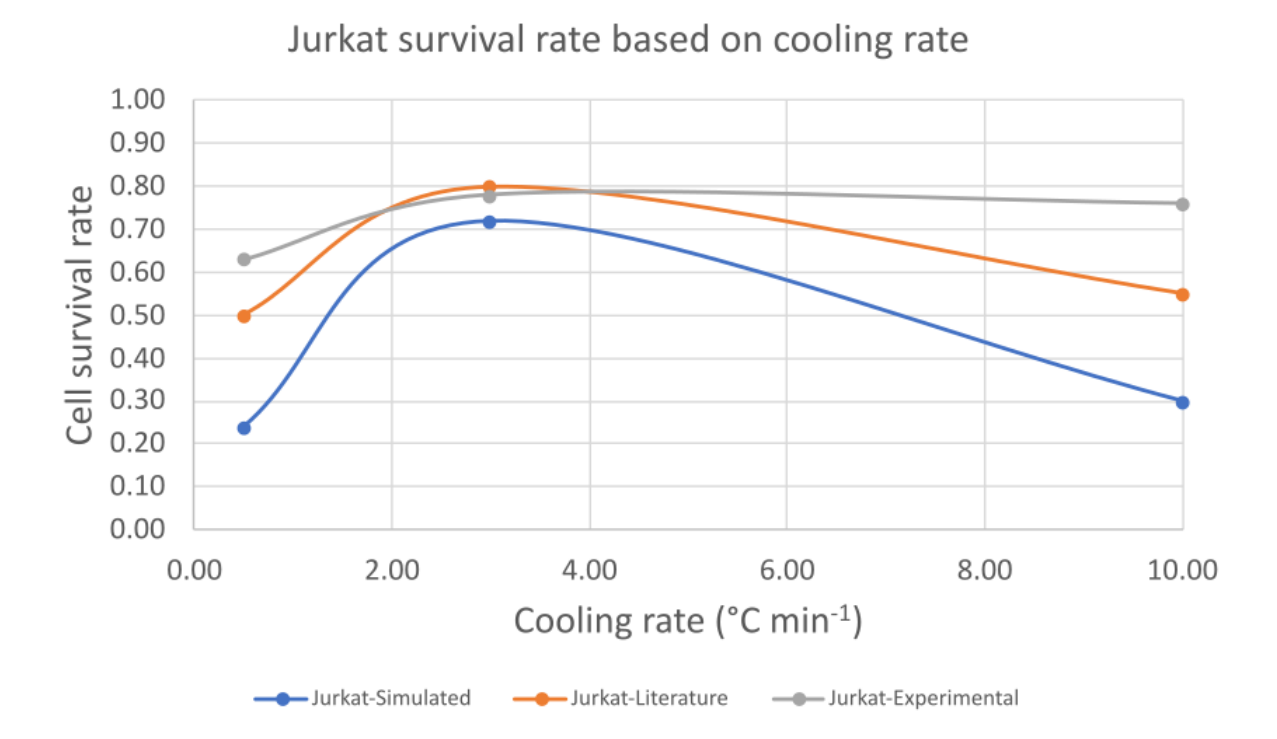


Figure 3.4: Post-thaw survival rate curves for Jurkat cells for Simulated (Blue), Experimental (Grey) and Literature (Orange). Utilising cooling rates of 0.5, 3 and 10 °C min^{-1} .

Overall our experimental results and simulated results both had a well matched shape of their Inverted U curves to that in the work of G Yu et~al, as show in Figure 3.4. Achieving an optimal post-thaw recovery around 3 °C min^{-1} with an overall lower estimated survival at 0.5 and 10 °C min^{-1} . Our experimental results have the closest match to the work of Yu et~al at 0.5 °C min^{-1} and 3 °C min^{-1} achieving similar results with a post-thaw survival of 0.64 and 0.79 for 0.5 and 3.0 °C min^{-1} respectively. However, at 10 °C min^{-1} our experimental work achieved a significantly greater post-thaw survival than that of Yu et~al's work,

achieving a viable recovery of 0.76. Only slightly below the optimal retrieval rate. Simulated results on the other hand predicted a significantly reduced post-thaw survival. Simulations predicting a post-thaw survival of 0.24 and 0.30 at 0.5 and 10° C min^{-1} respectively. For simulated cells this reduction in survival was lessened at the optimum predicting a post-thaw survival of 0.71, not significantly below that of our own or Yu et~al's experimental results.

3.2.3 Discussion

Our simulated and experimental results achieved similar results to those in the work of Yu et al. Predicting optimal survival at 3°C min⁻¹ out of the three selected cooling rates with diminishing returns in survival either side of the optima. With both experimental and simulated works re-creating the classical "Inverted U" curve described in the works of Mazur. Our simulated results had well matched predictions to those of both our experimental work and the results of Yuet al at 3° C min^{-1} . achieving a maximum post that survival of 0.72 compared to our in vitro result of 0.79 and Yu et al's result of 0.8. At 0.5 and 10 °C min^{-1} , our simulated cells had the expected reduction in post-thaw survival due to the solution effect and lethal IIF respectively. However, our simulated cells had an overall significantly reduced retrieval rate compared to that of either our experimental work or that of Yu et al. For higher cooling rates this is likely due to our relatively strict recoverable IIF level at 15% culling any simulated cells that may have been recoverable in vitro. However, without performing complicated cryo-microscopy experiments it would likely be difficult to define an acceptable tolerance outside of a slight increase in tolerable frozen water content. Future work in this regard could revolve around exploring how the tolerance to predicted IIF levels at certain cellular water volume contents could impact overall survival curve shapes. Similarly, such future work could also include a tolerance based on diminishing returns rather than a direct cut off. With survival chances above a certain water volume fraction causing a rapid reduction in post-thaw survival chance. This is likely also the reason that simulated Jurkat cells display a significantly lower survival chance at low cooling rates with an overly aggressive prediction of a cell tolerance to extracellular concentration build ups. Thus it may be wise in future work to perform a parameter sweep for likely suitable levels of tolerance to both IIF and extracellular concentration build ups. However, this form of future work will need more thorough planning to avoid the possibility of essentially biasing the predicted survival curve towards that of experimental results. For example, such a parameter search could be used to possibly predict the likelihood of a cells response to a change in CPA concentration to verify the accuracy of the framework used within this thesis.

Overall, this outlines our models capability to make predictions for cellular postthaw survival based on experimental parameters with overall well matched results to those of both *in vitro* work and experimental literature.

3.3 Multi-cell type post-thaw survival prediction

The utilisation of a general cryobiology computational modelling will allow for easy modification and optimisation of many cells experimental protocols. If suitable variables are readily available in literature, can be gained through experimentation or can be inferred from pre-existing experimental data. However, one limitation is the ability for computational models to be applied more generally across multiple cell types.

Two techniques have been shown to yield satisfactory results for the simulation of cellular responses cells during cooling. The first is a hybrid mathematical model used for simulating the cellular response to cryopreservation using physical cellular properties, temperature conditions, ice formation and chemical diffusion. This form of method is outlined within Chapter 3. Variations of this model have already been used to simulate mass and heat transfer in cryopreserved cells [141] and ice formation within cells [142, 97]. This type of model was recently expanded upon and used by Hayashi et al to predict the post-thaw survival of cryopreserved human induced pluripotent stem cells (hIPSCs) [56]. However, currently variant of these model still have some drawbacks. Firstly, they do not compare the ability of their model for predicting the post-than survival of cells against multiple cell types. Second, none of these model types predictions have yet been experimentally tested for in regards to optimal cooling rates. Hayashi et al's work, for example, despite predicting an optimal cooling procedure does not validate the cooling profile experimentally. However some of Hayashi's other work have been used in the optimisation of cryo protocols through computational modelling of thermodynamics with promising results of up to 0.90 survival rate [143]. Additionally, a hybrid modelling approach has yet to be used to predict the post-than survival of multiple cell types.

The second technique uses a stochastic Differential Evolution algorithm (DEA), as defined by Storn and Price [136]. This method combines computational modelling with iterative experimental feedback to optimise cooling rates and CPA concentrations through an evolving algorithm. DEAs have shown success in the work of Tsutsui et al and Pollocket al for predicting and optimising the post-thaw survival of multiple cell types [137, 138]. However, a major issue with the DEA method is its need for repeat experimental feedback in an iterative cycle between experimental and computational data. Thus, it reduces one of the major benefits of optimising protocols computationally, i.e. the significant reduction in costs related to repeated experimental data acquisition.

Within this section we chose to explore the utilisation of our computational modelling approach across three distinct cell types: Jurkat cells, Human Induced Pluripotent Stem Cells and HeLa cells. Presenting the usability of a hybrid modelling approach towards as a general platform for cryopreservation computational modelling

3.3.1 Modelling approach

We utilise a multi-factor hybrid mechanistic model for predicting the post-thaw survival of cells in suspension undergoing cryopreservation. This framework is based on the extended equations of P.Mazur [8] as outlined above in addition to the works of G.Fahy [102] and Benson [83]. Our modelling for the response of cells in suspension to various cryopreservation procedures takes a hybrid approach to predicting cellular post-thaw survival. An outline of how our algorithm works can be found in Figure 3.6.

A hybrid modelling approach allows for several major benefits. Firstly, a hybrid model is highly modular. Allowing for the easy addition of other building blocks of

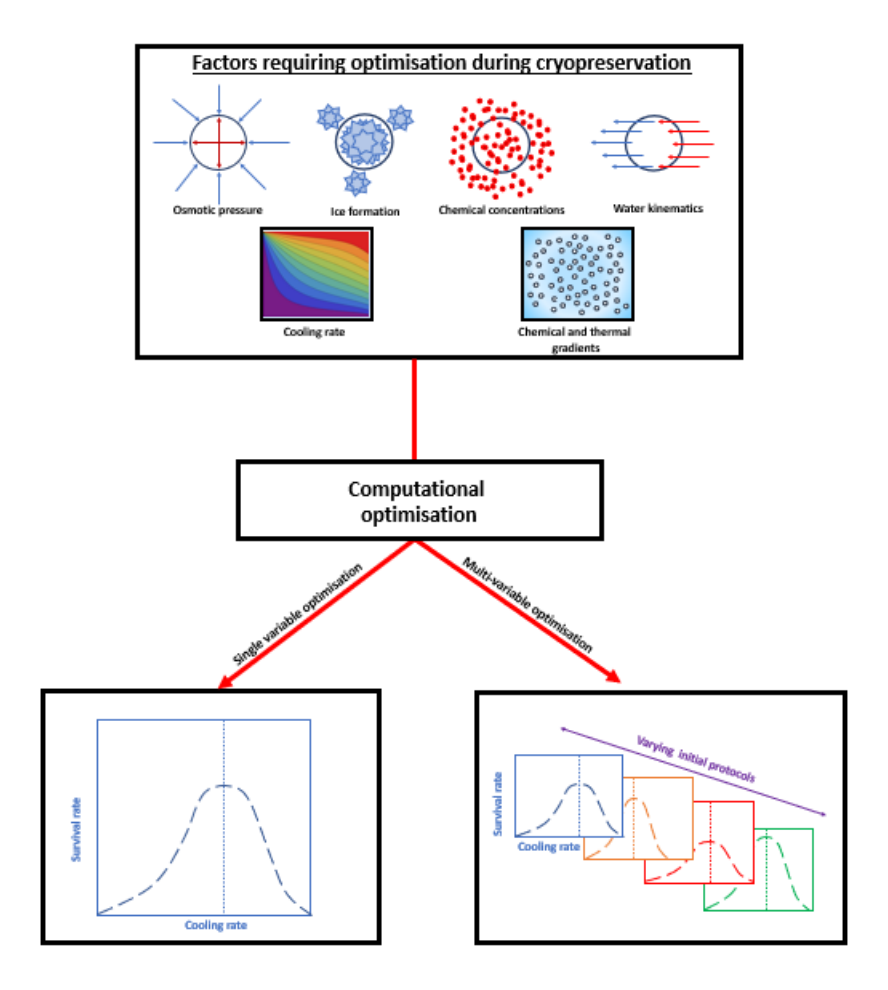


Figure 3.5: Our computational framework utilises a hybrid model for simulating and optimising the response of cells to various cryopreservation protocols. The framework uses initial cellular and environmental variables to simulate the cryopreservation of cells and then predict post-thaw survival chance for each individual cell in the suspension. The results from our algorithm can be used to optimise cryopreservation based on changing a single variable or multiple.

cryopreservation modelling. E.g more complex fluid behaviours such as in the work of Hayashi $et\ al\ [143]$. In addition to the possibility of future adaptation of more complex thermodynamic approaches such as convection or complex fluid dynamics for extracellular matrices. In addition, such modularity also allows for us to possibly expand our future work to include more in-depth cell-cell or cell-matrix interaction, such as those expected in tissue simulations.

3.3.2 Results

Here we present the outputs from our computational framework for predicting the post-thaw outcomes of multiple cells in suspension to various cryopreservation protocols. Our computational framework uses a mechanistic approach for simulating cellular response, intracellular ice formation and extracellular solutes. Predictions made using these variables are compared to available experimental literature and our own experimental work. An outline of computational framework can be found in Figure 3.6.

45

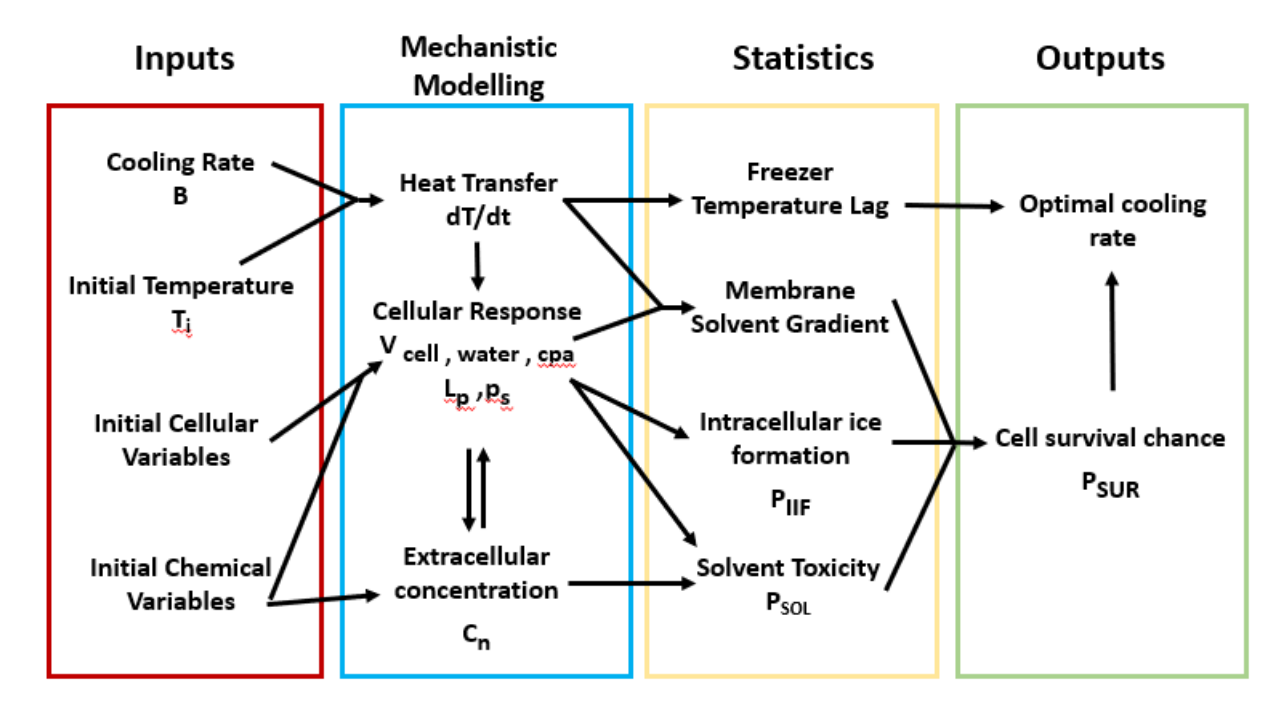


Figure 3.6: An overview of the hybrid modelling approach taken by our computational framework with four major sections which are handled during simulation. Inputs are all initial variables which are required for modelling such as: cell type, CPA, extracellular concentrations etc. Mechanistic modelling handles all of the advancing simulation parameters such as heat transfer, mass transfer and cellular responses. Statistics includes any calculations for probabilities and similar events. Finally, outputs are the final variables calculated during simulation and output at the final step.

Using standard linear cooling, we predict the post-thaw survival of three cell types: Jurkat, HeLa and human induced pluripotent stem cells (HiPCs). These results are then compared against the experimental results of Yu et al [139] for Jurkat cells, Hayashi et al [56] for stem cells, and McGrath et al for HeLa cells [144]. Simulations for the cryopreservation of each cell type followed the same protocols as stated in their respective works. Jurkat simulations were performed with cooling rates from 0.1 to 10 °C min^{-1} utilising the same experimentally determined parameters as used previously in this chapter. HeLa simulations were performed with cooling rates from 1 to 120 °C min^{-1} with all experimentally determined parameters taken from the work of Yi et al [97]. Finally, HiPSCs were simulated with cooling rates from 0.1 to 10 °C min^{-1} utilising the experimentally determined parameters values from the work of Hayashi et al [?]. The predictions for the post-thaw survival of cells undergoing standard freeze/thaw procedures compared against experimental literature are displayed in Figure 3.7. Maximum post-thaw survival for simulated and experimental results are highlighted by black arrows.

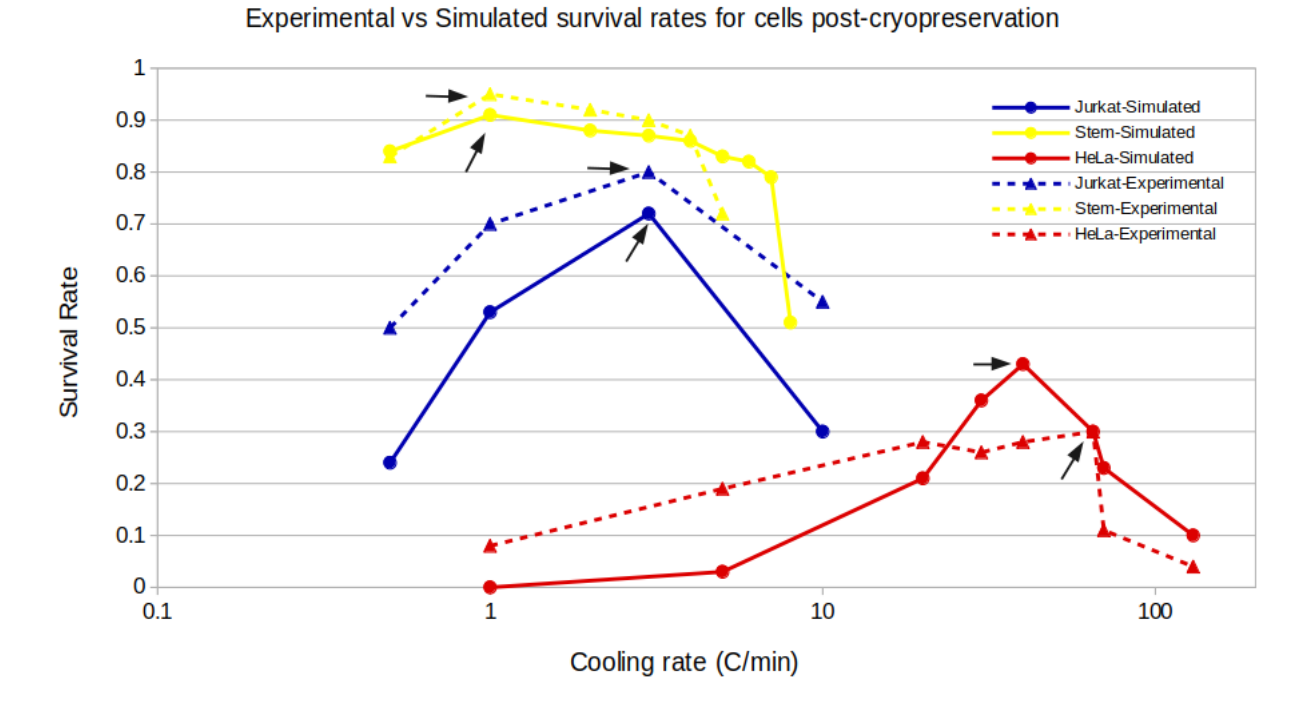


Figure 3.7: Post-thaw survival rate curves for Jurkat (Blue), HeLa (Red) and Human induced pluripotent stem cells (Yellow). Experimental (dashed) and simulated (solid) lines. Arrows indicate optimum cooling rates for post-thaw survival of cells.

3.3.3 Discussion

Using standard cooling procedures, we have investigated our computational frameworks capability to predict the post-thaw survival of cells undergoing cryopreservation. From our simulations, it was observed that cells cooled slower than the optimum experienced a greater risk of cell death due to an inability to dilute surrounding solutes, leading to a toxic build up of chemicals at the membrane. Furthermore, cells cooled at rates higher than the optimum experienced a decrease in post thaw survival due to an increasing likelihood of IIF. Overall, our results for standard cooling profiles are well matched to the "Inverted-U" survival curve defined by the two-factor hypothesis of Mazur et al and others [103, 8, 96].

The results for post-thaw survival results of our computational model are compared against experimental data from multiple sources [139, 56, 144] yielding excellent agreement (Figure 3.7).

Our computational model for hiPSCs predicted that a maximum post-thaw survival of 0.91 ± 0.2 could be achieved using a cooling rate of 1 °C min^{-1} . This is well matched to Hayashi et~al who achieved a maximum survival of 0.96 ± 0.03 using the same cooling rate [56]. Notably, our simulation also displayed a similar decrease in cellular post-thaw survival at cooling rates higher than 7°C min^{-1} as found in Hayshi et~al's work. This rapid reduction in post-thaw survival of hiPSCs is discussed in other work as being due to the cell type having greater vulnerability to IIF at higher cooling rates [145]. This accordance shows that our computational framework may also be predicting cellular responses outside of the optimum. For HeLa cells, our framework predicted a maximum post-thaw survival of 0.43 ± 0.05 when cooled at 40°C min^{-1} . This is slightly higher than the 0.3 achieved by McGrath et

47

al using a cooling rate of 65°C min^{-1} [146]. Finally, our framework predicts that a maximum post-thaw survival of 0.71 \pm 0.02 can be achieved for Jurkat cells using a 3 °C min^{-1} cooling rate. This prediction is well-matched to the experimentally observed optimum of 0.8 \pm 0.03 at the same cooling rate in G. Yu et al's work [139].

Overall, the predicted post-thaw cell survival outcomes from our computational framework are well matched to those achieved experimentally. The ability of computational simulations to achieve such results displays the possible power *in silico* simulations could have in assisting wet-lab cryo work of multiple cell types. Especially when one considers the capability of such models to have well matched results outside of the optimum. Indicating that relatively few variables are required to encapsulated specific cellular responses.

3.3.4 Limitations

The work presented in this section has considerable reliance on exact experimental protocols. Thus, our computational framework only predicts the response of the specified cell type with regards to a given CPA, salt and extracellular medium concentrations. Thus, if any change is made to an initial experimental setup; all simulations must be ran again to accurately predict a cells response to other parameters. Thus, in future we will expand our model to be more flexible with predictions that are made from initial conditions.

3.4 Conclusions and Outlook

In this chapter we have presented our algorithms ability to make accurate *in silico* predictions for the response of multiple cell types to differential cryopreservation protocols utilising standard cooling procedure. One major benefit of our algorithm is its ability to make these survival predictions for cells across a large range of cooling rates from a small number of initial variables. In addition, we have also compared our predicted results for Jurkat cells against both available literature and our own experimental results. Overall, our work presents a strong foundation for the optimisation of cells undergoing cryopreservation with our models being suitably extensible to tissues for future work.

Chapter 4

BioDynaMo - A mechanistic modelling approach

During the early stages of my work I was given the opportunity to join the BioDynaMo development team. BioDynaMo is a collaboratively developed high-performance computational framework for simulating cells and biological tissues (BioDynaMo v1.01.115-e1088d4a)[147]. The collaboration consists of many institutes including Newcastle University, Surrey University, CERN openlab, The University of Geneva and multiple others. BioDynaMo focuses on delivering high-performance, easily programmable agent-based simulations from single cell to large scale tissues. The core base of BioDynaMo is developed within the C++ programming language and can be easily developed with a limited understanding of the programming style. As part of the BioDynaMo development team I worked on implementing, testing and improving several aspects of the core framework. This included chemical diffusion, creating demos and exporting BioDynaMo to high performance computing systems (HPCs). BioDynaMo has already been shown to be capable of modelling vast AB modelling systems for millions of cells and their interactions, which both correctly reflect real world biological counterparts and utilises computational power in an efficient manner. Successful applications include: simulating radiation induced lung fibrosis [148], optimising biological dynamics [16] and cancerous tumour growth [149]. Thus, presenting BioDynaMo as the perfect foundation for our cryopreservation computational framework CryoDynaMo. Our initial focus for this work is on the simulation of cells in suspension. However, the pre-existing features of BioDynaMo make it an excellent fit for possible future expansion to tissue or organ based simulations.

BioDynaMo is licensed under the open-source Apache License, Version 2.0 and the source code for the project can be found at https://github.com/BioDynaMo/biodynamo.

Section 4.1.2 and 4.1.3 were completed in part for work in collaboration with the Barcelona super computing institute to compare the use of multiple modelling platforms on high performance computing systems. I worked as a 3 man group as part of the BioDynaMo team to develop, test and execute multiple types of simulations on the state of the art Barcelona super computing cluster. I took part in development of all tests and use cases for the project. This work will be published at a later date as part of the PerMedCoe project (https://permedcoe.eu/). As of the writing of this work is as yet un-published. This work was developed to assist in the collaboration and open communication between major cell based modelling

platforms.

4.1 General work within BioDynaMo

4.1.1 High Performance Computing

As biological simulations can require million-billions of cells to correctly encapsulate necessary dynamics it was decided on that our framework needed to be made compatible with high performance computing systems (HPCs). This was not only applicable to BioDynaMo but also possible future work involving our cryobiology framework. As the expansion from cells in suspension to tissues or organs would lead to significantly higher computational costs. Such as the inclusion of complex finite volume calculations, ODE solvers for extra and intracellular space or tracking stresses applied across tissues. Therefore it was decided that BioDynaMo would need to be made compatible with HPC systems which often run external software through docker or singularity based systems. I assisted in the development, exporting and testing of BioDynaMo utilising singularity and the relative speedup of tests on HPC based systems. Primarily through benchmark testing on HPC systems in line with the current BioDynaMo testing style. Here, I briefly present a comparison of relative speedup based on number of cores used for varying simulation scales. The same simulation was utilised in each speed test. A number of dividing cells freely moving around through random motion with a cell cycle based division rule. Results for the relative speed of each simulation are displayed in Figure 4.1. Three simulation lengths were ran of 500,650 and 750 steps. Across multiple core configurations : 4, 8, 16, 32, 64 or 96.

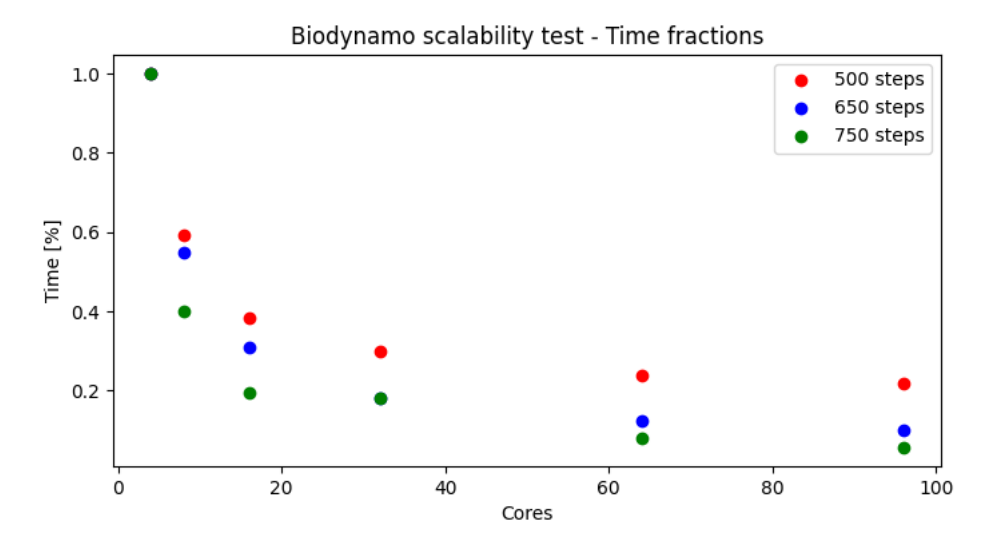


Figure 4.1: Percentage time required for computing BioDynaMos cell growth and division on an HPC based on number of cores used compared against a 4 core system.

The relative speed up achieved based on number of cores used displayed an exponential decrease as number of cores increased when compared to the same simulation length. Simulations with the largest number of time steps displaying the largest relative speedup when compared against the 4 core base. For example, at 96 available cores a 750 step simulation had a 10 times speedup compared to base

while a 500 step simulation only achieved a 5 times speedup. Overall, this indicates that the use of BioDynaMo on a HPC system can lead to significant speedup for more complex simulations, in this case represented by increasing number of agents in simulation. Due to hardware availability I was unable to test for systems with a larger number of available cores. However, It is likely that after 96 cores the system would reach a computational bottleneck based on the relative speed of the language regardless of the number of additional cores or time-steps. As BioDynaMo is already a fully parallelised framework this is likely the maximum speedup that is currently achievable, at roughly 5% runtime compared to a 4 core system when ran on a 96 core setup for a 750 step simulation. Further possible speedup may only be achievable through GPU implementations or other similar hardware exploitation to prevent bottle-necking or possible future improvements to physical hardware such as silicone chips.

The ability to achieve such speed ups when utilising HPC system architecture is key to possible future applications of BioDynaMo as well as our work. As complex simulations with multiple interacting independent factors being modelled over long length and time scales, such as tissue, will require considerably greater computational power to run. Another major benefit of being able to deploy BioDynaMo on HPC systems is the ability to exploit their much greater computational hardware. Allowing for the simulation of complex biological systems that might not be practical or feasible on more traditional systems. This is especially pertinent when one considers that future expansions of our cryobiology framework will need to include tissue scale forces and ode solvers to account for stresses and strains on tissues. Requiring a significant amount of computational power to expand to length scales that would be appropriate to tissues in 3D space.

4.1.2 Cell cycle demo

As a use case for BioDynaMo we created a simulation for cells with a fixed cell cycle model with each phase having distinct timings and a division event upon the end of the cycle if a critical volume is reached. In total a cell could exist in one of 4 possible states: G0/G1, S, G2 and M. Cells advanced through these stages in a single direction as, shown in Figure 4.3. Each stage of the cell cycle had a fixed duration of 7, 6, 3 and 2 hours for the G0/G1, S, G2 and M stages respectively. Totaling a time of 18 hours for one entire cycle. Within these simulation cell were modelled to grow with a constant rate until reaching a target volume of double their initial size. This was implemented as follows:

$$V_{t+1} = V_t \times \frac{V_{max} - V_t}{V_{max}} \tag{4.1}$$

In addition, if a cell was within the M state and had at least 195% of its initial cell volume they would divide to form two new daughter cells. Running a simulation with an equivalent 48 hour time scale we can generate the dynamics of changes in volume over time for a specified cell system. As shown in Figure 4.3.

The ability to use and run such cell cycle simulations are of great utility in the understanding of biological systems and can provide system-level properties that can be key to further understanding complex biological processes [150, 151, 152]. In addition, such systems also have the ability to assist in the modelling of other

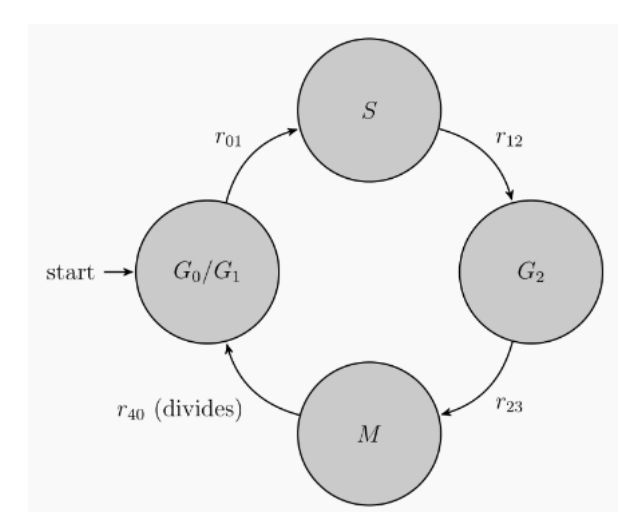


Figure 4.2: Graph structure for the flow cytometry separated cell cycle for a cells which have 4 distinct phases G0/G1, S, G2 and M which divide upon returning from the M to G0/G1 state. The default phase is marked "start".

systems, such as the oscillations present in circadian rhythms [153] or biochemical networks [154].

Overall, the test performed well and gave the expected repeated circadian rhythm style of the cell population. As this is a fixed state cell cycle model all cells will divide at the same time. Due to a lack of randomness in either initial starting cell volume or noise in terms of cell growth.

An additional test was also developed for a random cell cycle model with stochastic cell growth, noisey initial volume and probability of cell division.

Fixed duration cell cycle model.

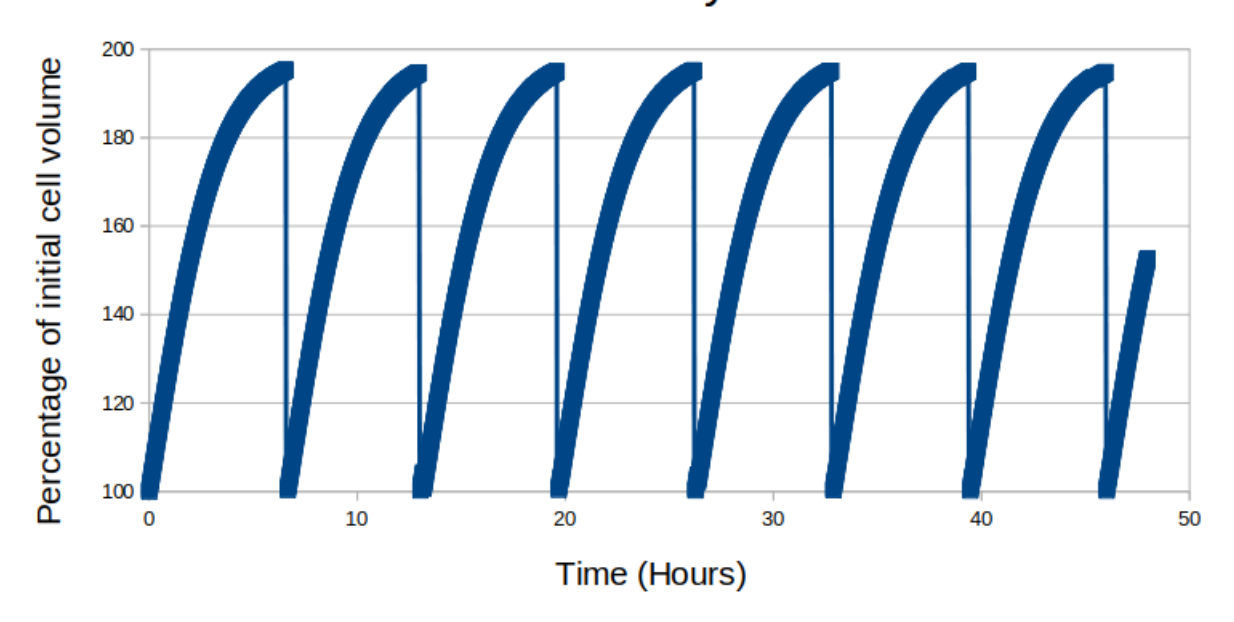


Figure 4.3: Relative volume of cells in a fixed length cell cycle model across an equivalent simulation time of 48 hours.

4.1.3 2D growing mono-layer demo

Another relevant demo case that was developed by us for BioDynaMo is that of a growing cellular 2D mono-layer. Here we utilise several of BioDynaMos core utilities including cellular growth, migration and cell-cell interactions. Here we aimed to simulate a one-cell thick tissue growing on a flat surface with a fixed cell cycle model. For this demo we measured our results against the work Bru et al (1998) [155]. Tissue was simulated over a 12 day equivalent with comparisons made between tissue diameter in silico and experimental data. Overall, we achieve well matched results to the experimental data as shown in Figure 4.4 through only utilising a simple cell cycle growth model. Both experimental and simulated data following a general linear growth phase. It must be noted however that for this demo we specifically simulated the linear growth portion of tissue growth. As in Bru et al's work it can be seen that tissue first initially goes through an exponential increase in tissue diameter before reaching a linear growth phased. This demo has direct applications in several aspects of biological research including the modelling of cancerous tissue [156], pharmaceutical testing [157] and growth of bacterial colonies [158]. In addition, BioDynaMos previous success in simulating cancerous tissue growth outlines that such models can be easily expanded from 2D to 3D space [149]. This demo also has direct implications on possible future work involving the cryopreservation of tissues and possibly organs. As on could combine concepts for cryopreservation modelling outlined in Chapter 2 with several features such as cellular interacting forces for simulating possible damage and tears in tissue layers due to tissue dynamics during freezing and thawing. This work is also a direct stepping off point for the creation of tissue based cryopreservation models. Likely with initial applications to less complex epithelial tissues which would grown in similar 2D plains with possible expansion to 3D tissues. However this is only an

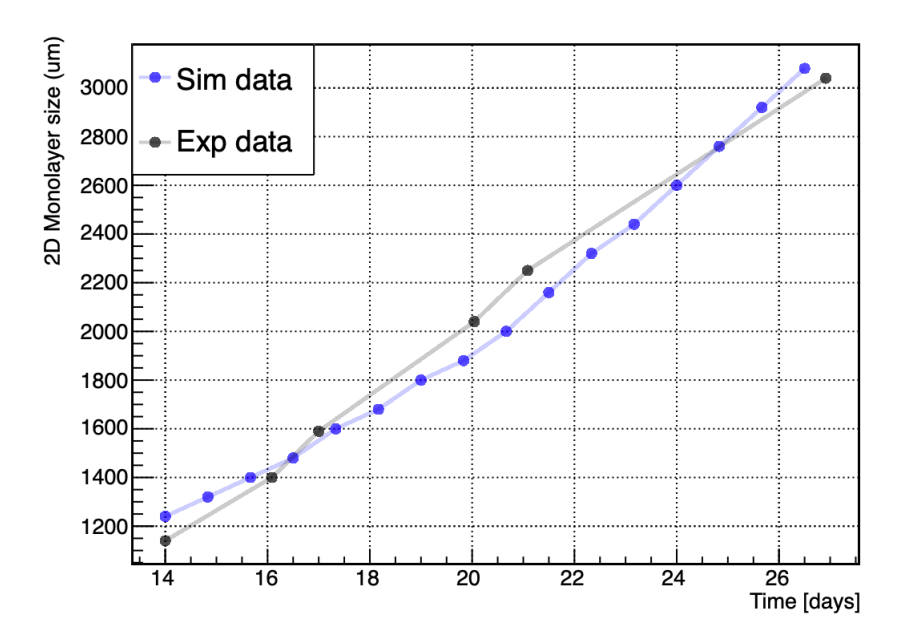


Figure 4.4: Comparison between experimental and simulated growth of a tissue 2D mono-layer over a 12 day period.

initial touching point for utilising BioDynaMo as a tool for simulating tissues.

4.2 Chemical diffusion

In addition to modelling cells, the ability to model extracellular substances and heat transfer is key to making predictions for cellular dynamics during cryopreservation. Especially for future possible expansions to large scale volumes of cells in suspension, tissue or organs. This is key when one considers that even for only cells in suspension the effects of cryopreservation are container shape specific. As several studies have shown that the size and shape of the container for cryopreservation can have significant impact on concentration and temperature dynamics in addition to extracellular ice formation seeding temperature [159, 160]. Most current predictive models rely on continuum-type abstraction for cell density, concentration values and temperature dependence. Our aim, with this cryogenics modelling framework, is to simulate full scale 3D diffusion of chemical concentrations and heat in parallel with the simulation of thousands to millions of cells in suspension undergoing cryopreservation. Allowing for cells to interact independently with their local environments exchanging water and solute contents with a larger macro scale diffusion.

For this purpose, we chose to utilise a finite difference-based extraction for modelling 3D space as utilised in the BioDynaMo modelling framework. Finite difference was decided upon for its ability to simulate multi-scale models with controllable resolution and high computational speed when executed in parallel. As this will also allow for easier future improvements to the model to easily be integrated for tissue scale cryopreservation. Using this 3D space we can incorporate intra-, inter and extracellular processes within a high-resolution environment for our computational framework.

Finite difference is a method of approximating derivatives in the form of partial differential equations (PDEs) and ordinary differential equations (ODEs) via a Taylor series discretization formula of derivatives. Being widely used already in multiple areas of biological computational modelling including epithelial tissues, organs and many others.

4.2.0.1 One-dimensional

The most basic form of a finite difference modelling method is in 1-dimensional space in the form of a substance (u) diffusing in the x co-ordinate space based on some diffusion parameter. Taking the following form in 1D space:

$$\frac{\delta u}{\delta t} = \alpha \frac{\delta^2 u}{\delta x^2} \tag{4.2}$$

Here u represents chemical concentration, t is time, α is the diffusion coefficient (or heat capacity) and x is the spatial parameter. We can convert the right hand side (RHS) of Equation 4.2 as follows to map our diffusion onto a 1D grid moving through time:

$$\left(\frac{\delta u}{\delta t}\right)^n \approx \frac{u_i^{n+1} - u_i^n}{\Delta t} \tag{4.3}$$

Similarly, the left hand side (LHS) can be converted also:

$$u_i^{n+1} = u_i^n + A \left(u_{i+1}^n - 2u_i^n + u_{i-1}^n \right)$$
(4.4)

Thus equation 4.2 becomes:

$$\left(\frac{\delta^2 u}{\delta x^2}\right)_i^n \approx A \frac{u_{i+1}^n - 2u_i^n + u_{i-1}^n}{\Delta x^2} \tag{4.5}$$

Here $A = \frac{\alpha \Delta t}{\Delta x^2}$. Due to the 1D heat equation not being unconditionally stable we must also impose a stability criterion as follows.

$$|A| < \frac{1}{2} \quad or \quad \frac{\alpha \Delta t}{\Delta x^2} < \frac{1}{2} \tag{4.6}$$

This provides us with an initial set of conditions and methods for calculating diffusion in 1D through a combination of Equation 3.4 and Equation 3.6. Figure 3.1 displays how the 1D spatial space is set up in time for simulation with time as our y axis and spatial position as our x axis.

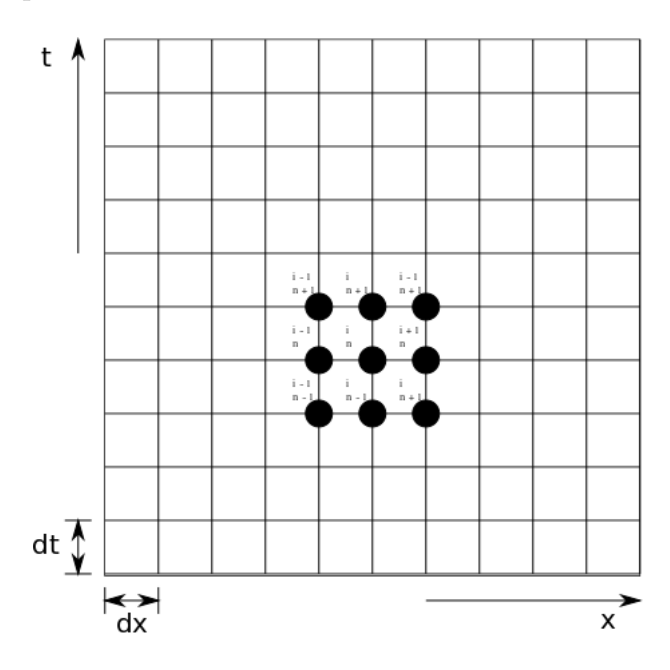


Figure 4.5: One-dimensional finite difference

4.2.0.2 Three-dimensional

Further expansion of our grid can be made to change our one dimensional space as shown in Figure 4.5 into a three dimensional environment. Our new space being a box of length L which is broken down into voxels of a side lengths Δx , Δy and Δz . The 3D space created via this change is displayed in Figure 3.2.

Assuming our space is made of voxels with equal side lengths, we get an altered 3D variation of equation 3.4 as follows:

$$\Delta x^2 = \Delta y^2 = \Delta z^2 \tag{4.7}$$

$$u_{i,j,k}^{n+1} = u_{i,j,k}^{n} + A((u_{i+1,j,k}^{n} - 2u_{i,j,k}^{n} + u_{i-1,j,k}^{n}) + (u_{i,j+1,k}^{n} - 2u_{i,j,k}^{n} + u_{i,j-1,k}^{n}) + (u_{i,j,k+1}^{n} - 2u_{i,j,k}^{n} + u_{i,j,k-1}^{n}))$$

$$(4.8)$$

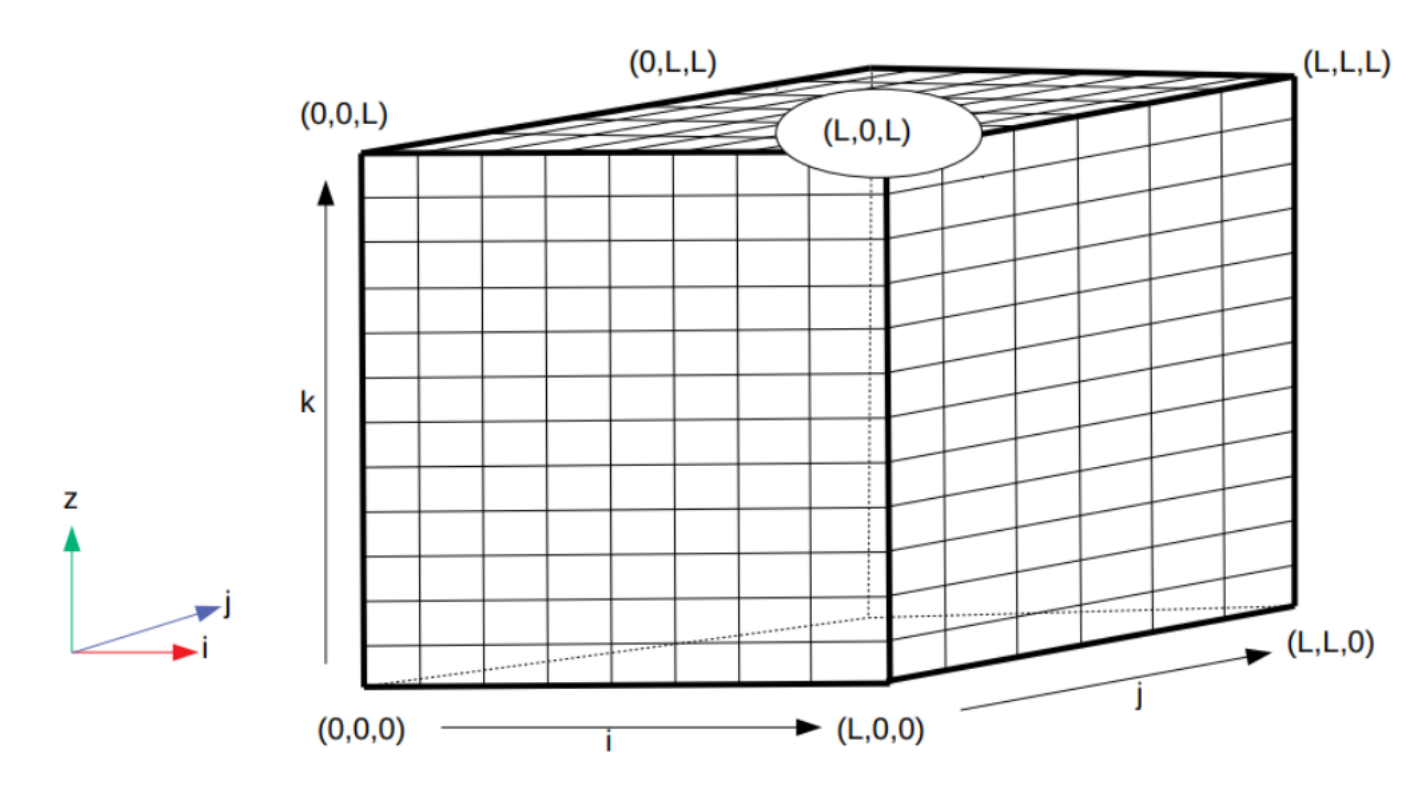


Figure 4.6: 3D grid for finite difference

Here i,j and k represent spatial positions for x,y and z respectively. For our work we have chosen to utilise cube based voxels such that all side lengths are equal for simplicity and computational speed. However future improvements may necessitate more complex geometries.

The 3D variant of the diffusion equation additionally has an updated stability constraint:

$$|A| < \frac{1}{6} \quad or \quad \frac{\alpha \Delta t}{\Delta x^2} < \frac{1}{6} \tag{4.9}$$

This variant of the diffusion equation is often refereed to as the Euler method. Being widely used in biological computational modelling for its simplicity and ease of implementation. Even this simple version of finite difference is already suitable for basic simulations of extracellular diffusion and heat transfer. However, the instability of the Euler variation of finite difference does have underlying issues with accuracy due to necessitating having either larger voxel side lengths or a considerably smaller time-step leading to higher computational demand. This can rapidly lead to computational resource overload as one must consider the spatial domain is to the power of two with time at base one. Thus, we chose to additionally employ a slightly more robust improvement to the Euler finite difference method allowing for greater resolution of our grid.

4.3 Runge-Kutta solution

The Euler diffusion equation for finite difference is one of the simplest forms of solving techniques for partial differential or ode equation systems. Its relatively ease of

implementation and minimal computational load is highly suited for simplified modelling of 2D and 3D space. However, the inherit instability of the system and limited accuracy due to greater step estimation can lead to inaccuracies for systems with a large number of dependent individual agents. Thus, we chose to employ a slightly more complex and robust ODE-solver, the Runga-Kutta method. Runge-Kutta finite difference modelling is a more robust iterative method for solving ODE's, both implicitly and explicitly. Additionally, having the benefit of being a multi-order systems. With higher order systems leading to greater accuracy through increased estimation steps for a single time point.

Runge-Kutta finite difference modelling is a more robust iterative method for solving ODE's, both implicitly and explicitly. Runge-Kutta is a multi order method for solving ODE's. Meaning that it can be altered based on individual need for increased accuracy of diffusion estimations. However, utilising a Runge-Kutta method on an order greater than three is complicated due to requiring more accurate estimation of individual steps and rapidly increasing computational costs when employed in silico. Higher order Runge-Kutta systems lead to greater accuracy due to making a larger number of estimations between each individual time step. At the first order, the Runge-Kutta system simplifies down to reproduce the heat Euler equation. Above the first order, Runge-Kutta systems become inherently stable. Already providing a significant benefit over the Euler method. As one can investigate much greater resolution diffusion grids without the need for rapidly increasing time steps.

Due to the inherent benefit of employing a Runge-Kutta based system over the simpler Euler diffusion equation we chose to employ the use of the Runge-Kutta approach within our cryobiology framework.

Unlike the Euler method, which estimates the next time step based on the rate of change of the defined ODE at the current point, the Runge-Kutta method is a family of schemes. These schemes utilise slope estimations between the current and next time step with increasing accuracy based on the number of slope estimates taken. The number of slopes estimated being proportional to the order of the Runge-Kutta method being utilised.

The Runge-Kutta method has been integrated into CryoDynaMo using the following form:

$$\frac{dy}{dt} = f(y(t), t) \tag{4.10}$$

This equation is solved explicitly through the following steps. First, we estimate our derivative at a time $t = t_0$.

$$k_1 = f(y'(t_0), t_0) (4.11)$$

We then make an intermediate estimation of our function at $t = t_0 + \frac{h}{2}$.

$$y_1(t_0 + \frac{h}{2}) = y'(t_0) + k_1 \frac{h}{2}$$
(4.12)

Another estimate is then taken of the slope at $t = t_0 + \frac{h}{2}$.

$$k_2 = f(y_1(t_0 + \frac{h}{2}), t_0 + \frac{h}{2})$$
 (4.13)

A final estimation is then taken for y at time $t = t_0 + h$.

$$y'(t_0 + h) = y'(t_0) + k_2 h (4.14)$$

Here k_1 and k_2 are the slope value taken at the midpoint of the interval and h determines the interval being solved for.

Some consideration must be made when deciding to either simulate using the Euler or Runge-Kutta method. This is due to the increased computational work required for the Runge-Kutta method compared to the Euler. Thus, if the increased time of simulation and required computational power is not required one can instead employ the more simplistic Euler method. In addition, as one increases the order of the Runge-Kutta method you must also employ further intermediate steps; again increasing computational workload.

4.4 BioDynaMo modelling of cell water

Our first use case and test for BioDynaMo was to investigate the most widely used applications for cryobiology modelling. The modelling of water kinematics of cells during freezing across multiple cooling rate regimes. To do this we implemented Equations 3.6 and 3.8 as outlined in Chapter 2. It was decided that we would utilise mouse zygotes as our initial target cell. As data is readily available for this cell type from many other experimental works. Primarily focusing on reproducing the work Bo Jin (et al) 2016 [161].

Within our model cells were simulated as individual agents with applied cooling rates of 0.5, 2, 4, 8 and 20 °Cmin⁻¹. Cellular parameters were taken from other works as follows: Osmolality of cytoplasm: $M_i = 1.34$ Osmolal, Cytoplasm freezing point: $T_f = 270.6$ K , Initial volume of cell water (T = T_f): $V_i = 1.88 \times 10^5 \ m^3$, Osmolal solute in cell: $N_2 = 2.52 \times 10^{-10}$, Hydraulic conductivity: $L_p = 0.43$ (At 22° C) $mmin^{-1}atm^{-1}$, Activation energy of L_p : $E_a = 13.5$ kcal mol^{-1} , Area of cell: A = $1.84 \times 10^4 \ m^2$, Gas constant: R = $82.057 \times 10^{12} \ m^3 atmcal^{-1} mol^{-1} K^{-1}$, Molar volume of water: $V_w = 18.10 \times 10^{12} \ m^3 mol^{-1}$, Molar heat of fusion: $L_f = 5.95 \times 10^{16}$ with temperature range: T = 293 - 223 K. The results from these simulations can be found within Figure 4.7. EQ within this graph represents the equilibrium or absolute loss of water from a cell cooled infinitely slowly from the initial temperature T_i to final temperature T_end . Additionally, water lost from cells was transferred directly to the extracellular grid space with similar but inverse for the uptake of permeating solutes into intracellular space during cooling within our modelling. This not being present in the work of Bo Jin et al.

Overall, our simulations gave well matched results to that of Bo Jin et al's work. Producing the expected loss of water from cells at each given cooling rate with the increasing remaining intracellular water at higher cooling rates. Presenting the first successful result of introducing the standard cryopreservation modelling approaches into BioDynaMo. The only major difference in our work being a slight overestimation of water loss leading to the $0.5~{\rm ^{\circ}C}$ min^{-1} run reaching the equilibrium line slightly earlier and a slightly lower water content in the $8~{\rm ^{\circ}Cmin^{-1}}$ and $20~{\rm ^{\circ}Cmin^{-1}}$ upon reaching the final -40.3 ${\rm ^{\circ}C}$ min^{-1} hold temperature. This is not surprising however as our cells are held within a larger extracellular space with ongoing diffusion during simulation, thus producing slightly different numerical results.

Simulated fractional water loss of mouse zygotes

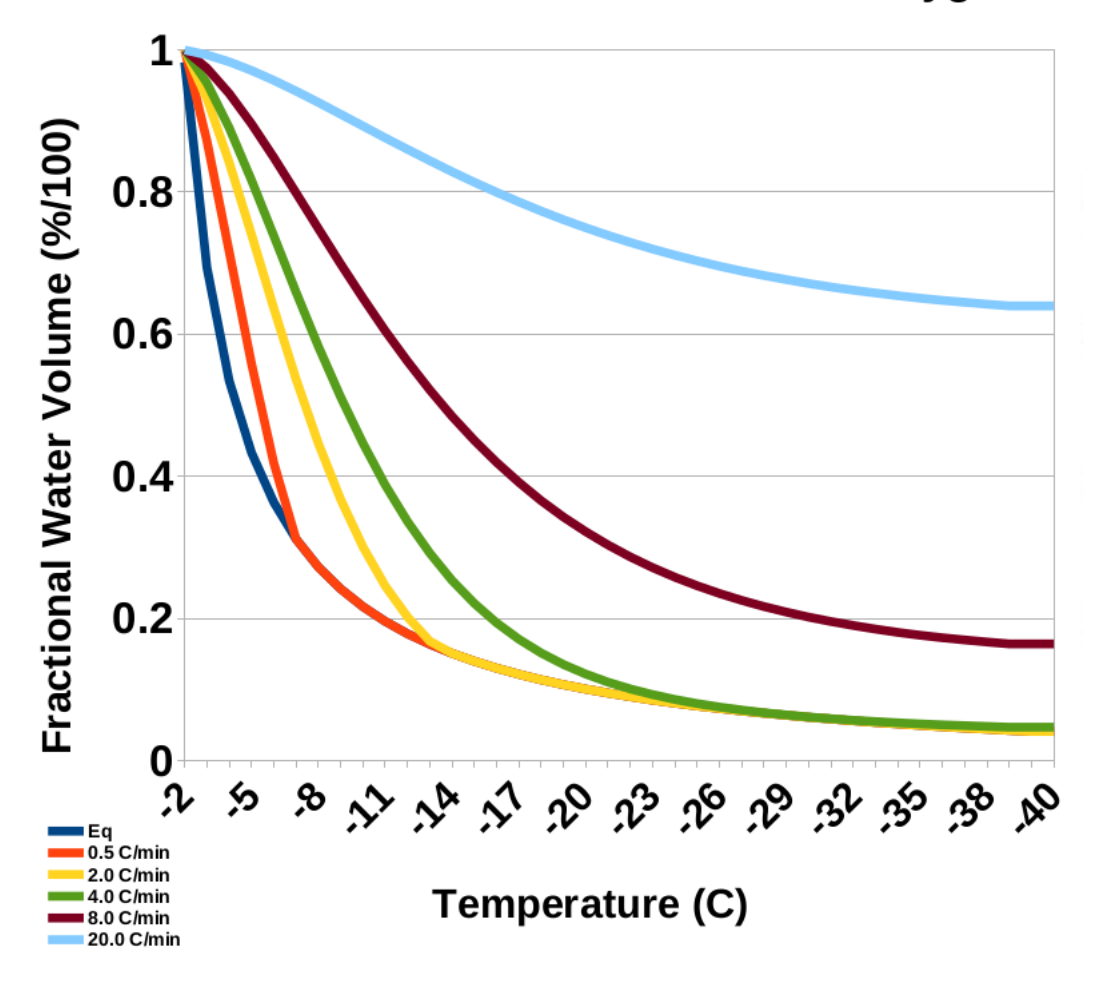


Figure 4.7: Simulated water loss from mouse zygotes undergoing cooling at 0.5 °C min^{-1} , 2.0 °C min^{-1} , 4.0 °C min^{-1} , 8.0 °C min^{-1} and 20 °C min^{-1} . Eq here represents the max water loss from mouse zygotes during cooling at the lowest possible cooling rate.

Combining our AB model of a cell with the finite difference diffusion grid allowed us to directly simulate the change in cell volume as shown in Figure 4.7 as the excretion of intracellular water into extracellular space. This was tracked through the water loss and CPA equations separately to account for each individual solute individually being transferred between extracellular and intracellular space. An example of this is shown in Figure 4.8 for a single cell undergoing cryopreservation. Cell water directly enters extracellular space (shown as the coloured area outside of the cell in this figure) and proportionally increase the extracellular concentrations based cellular water kinematics. As cells within our models are treated as "point sources", even if a cell visually overlaps into multiple regions water will only excrete into the corresponding voxel of the cell centroid. This may be a possible avenue for future work to more accurately explore cellular water loss at a finer resolution or with volume/position based diffusion. However, for current work this was not necessary.

This can then be easily applied to much larger simulations with tens of thousands of cells simultaneously interacting with their extracellular environment. As shown

in Figure 4.9. Within this example cells were randomly distributed throughout simulation space and the entire simulations space was cooled evenly at $-1^{\circ}Cmin^{-1}$ and utilised previously stated variables for mouse zygotes. Displayed in Figure 4.9 is the additional water excreted from cells into the extracellular environment which then diffuses throughout the extracellular environment. This leads to the creation of visual "hot-spots" as more water is being excreted into extracellular environments compared to other regions. This is later corrected for as excreted water will diffuse out of high concentration regions to lower concentration areas. This thus allows us to account for the transfer and diffusion of water and solutes within extracellular space leading to dynamic results based on simulation space and generated cellular positions.

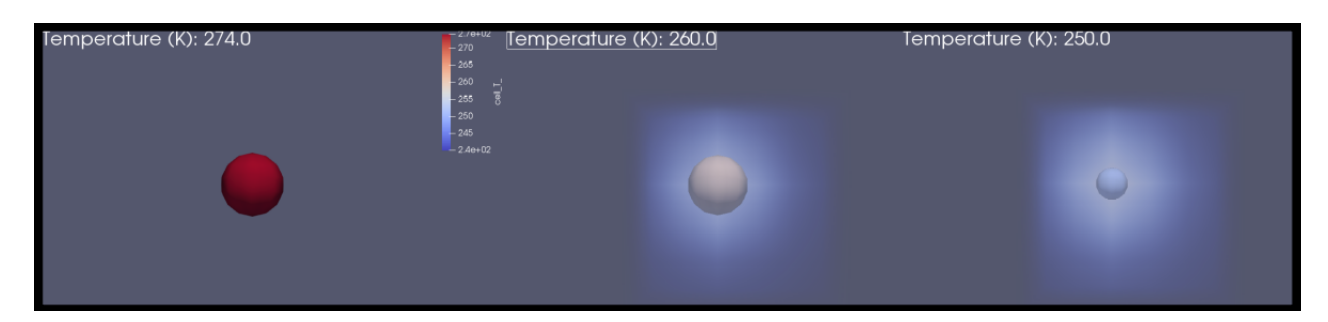


Figure 4.8: Simulated loss of intracellular water from a cooling mouse zygote into extracellular space.

In future we hope to apply this form of extracellular modelling in future with heat dynamics to investigate the observed phenomena of volume/container shape on the post-thaw survival of cryopreserved cells in suspension [162]. As it was observed that human umbilical chord blood cells post-thaw survival was dependant on container volume/shape. Thus, highly applicable to our modelling approach to investigate computationally. As cellular response will be based individually on local cell parameters compared to the larger bulk and our simulations can easily be modified to account for a change in container volume as represented by simulation space.

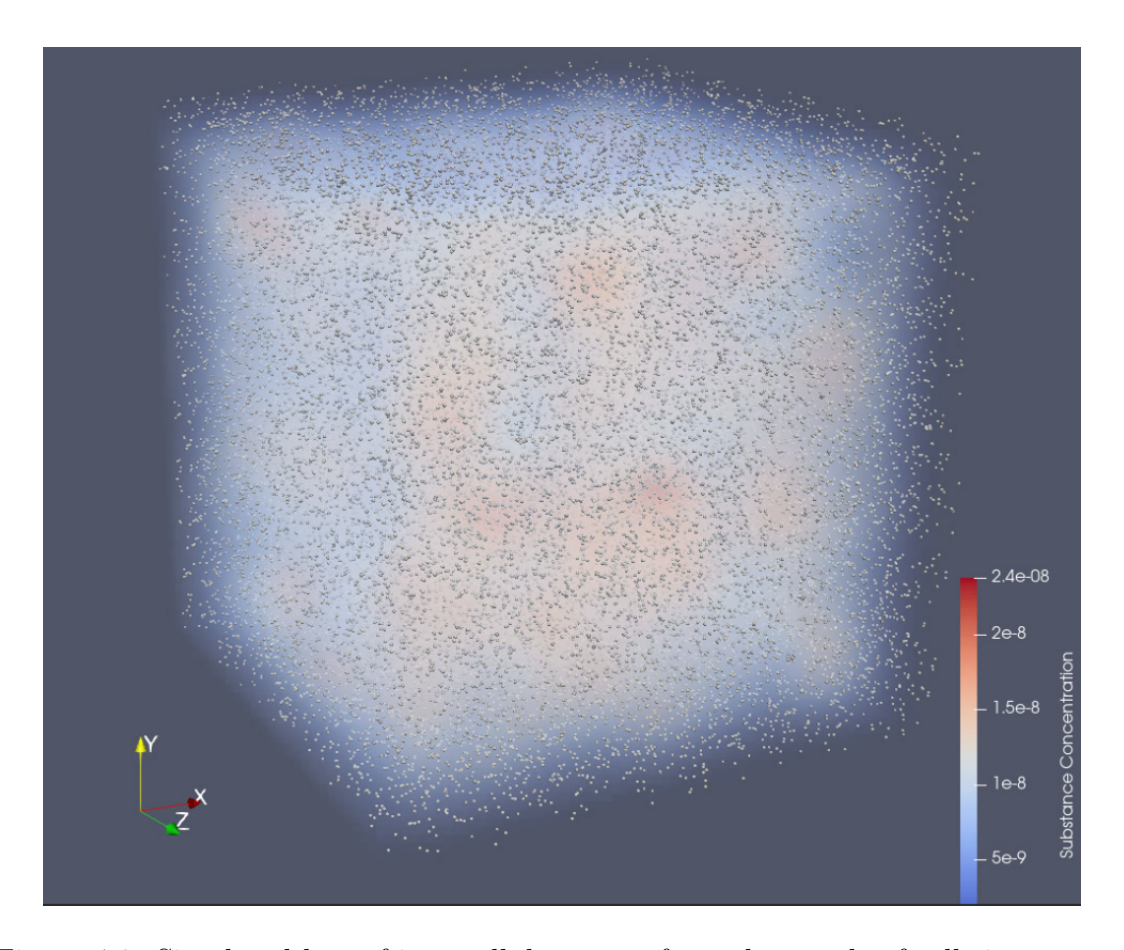


Figure 4.9: Simulated loss of intracellular water from thousands of cells into extracellular space during cooling.

4.5 Thermodynamic Simulations

Using the Runge-Kutta variant of the heat equation, as outlined in Equation 4.10 to 4.14, we have also modelled the transfer of heat within extracellular space. First focusing on modelling an insulated box undergoing controlled rate cooling. The model is based on and compared against readings from an Asymptote controlled rate freezer (Planer,141 Middlesex, UK).

The dimensions of our simulated box were matched to those of the laboratory freezer. Similarly, the freezing plate was modelled through heat sinks placed uniformally in a rectangular pattern across the base of the freezer to match the dimensions in the laboratory. Thus, causing the removal of heat only through the bottom of the box and acting as drain to account for energy removed through cooling. An example simulation of the freezing plate can be seen in Figure 4.10. The red slices represent planes in the x-y and x-z direction to act as visual indicators for temperature in those regions. This is simply a visual aid for simulations.

During simulation of cooling the "plate" uni-formally reduces its overall temperature each time step in line with expected linear cooling rate. This drives an overall cooling of the simulation space while the cooling plate is maintained at a constant temperature. This results in a heat sink effect at the base of the freezer driving heat transfer towards the plate. The system will continue to cool down until the freezing plate reaches its final temperature at which point the system will tend towards a steady state at the final temperature.

62



Figure 4.10: Simulated freezer space in CryoDynaMo with a freezing plate across the bottom of the simulation space.

To investigate our model experimentally we placed type K thermo-couples within cryovials placed at the center points on a freezing plate within an Asymptote freezer, as shown in Figure 4.11. Temperature recordings were made through a Data Logger connected to the thermo-couples externally (TC-08, DataLogger, Pico Technology). Cryovials were filled with fetal bovine serum, buffer and an equivalent of 10% DMSO. In total 4 separate temperature profiles were recorded within the freezer: -1°C min^{-1} from 0 to -20°C, -2°C min^{-1} from 0 to -20°C, -1°C min^{-1} from 0 to -40°C and -2°C min^{-1} from 0 to -40°C. Using our finite difference model we simulated the same 4 temperature profiles and compared our results against the freezer readings. These results are displayed in Figure 4.12.

As can be seen across all 4 temperature profiles, our simulated freezer is well matched to experimental readings. During cooling we see that the simulated freezer matches experimental data at freezer initialization, mid cooling and finally as the freezer ramps down towards the hold temperature. Indicating that the use of Runge-Kutta based ODE solver along with our BioDynaMo framework can accurately simulate a standard cooling procedures base temperature decrease. The only major difference between our simulation and that recorded in the laboratories freezer are the temperature spikes present across all temperature recordings. These peaks are caused by the release of latent heat during the crystallisation of water into ice. However, this heat is rapidly dissipated into the surrounding environment at a rate greater than the cooling plate rate. This is not accounted for within our simulation currently due to the difficulty in predicting and accounting for these peaks. As the nucleation of extracellular ice spontaneously is still not a well understood process for timing with a great degree of randomness due to relative availability of nucleation sites and impurities in samples. However, this is not an issue for two major reasons. Firstly, the release of latent heat during these temperature spikes is not a significantly lingering effect. As heat is rapidly drawn away during further cooling steps before returning to the homogeneous temperature of the remainder of the freezer. Overall, the simulation here is attempting to simulate the larger cooling

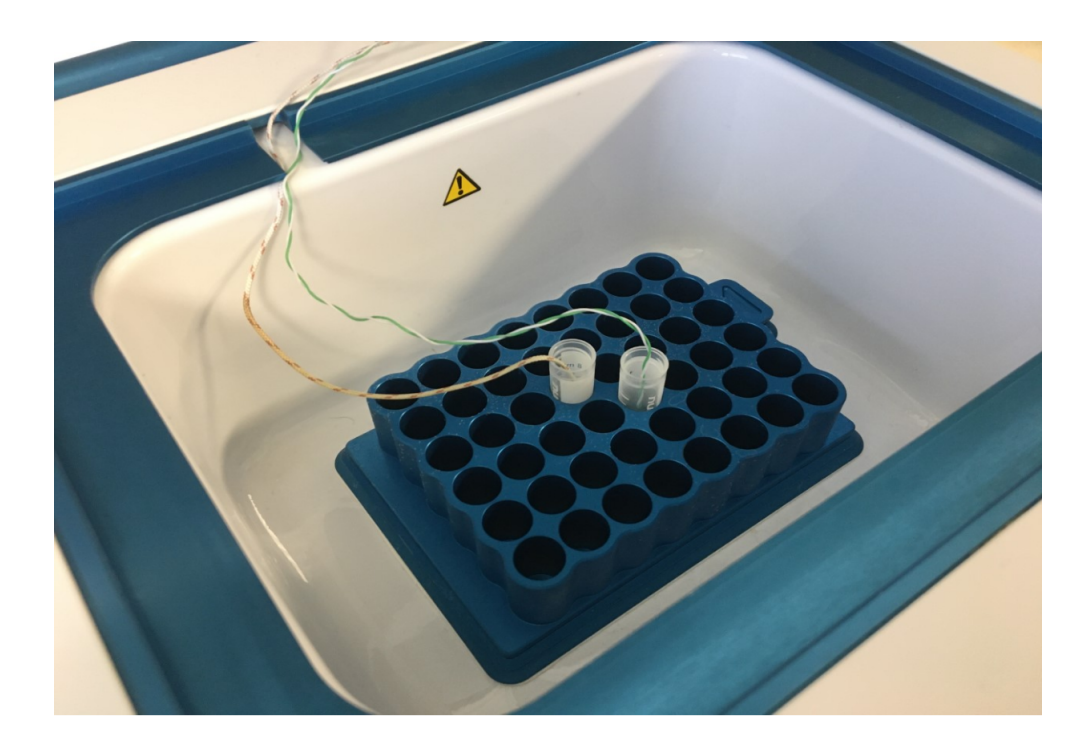


Figure 4.11: Cryovials placed in Asymptote freezers with thermocouples for data recording, the cryovials contained fetal bovine serum and 10% DMSO.

effect of the freezer in space rather than nucleation. Second, these nucleation peaks are extremely difficult to predict accurately and can occur across a great range of temperatures. This is due to multiple factors which are difficult to account for, even in simulation, leading to this real world difference in nucleation peaks. This is even clearly displayed in Figure 4.12 as we can see differing nucleation peaks between adjacent cryovials. This could represent an avenue for future possible research to introduce the formation of extracellular ice and make predictions based on relevant abundance of available nucleation sites across a range of temperatures and cooling rates. Similar to previously mentioned this would likely involve computationally investigating the phenomena of changes in bulk ice nucleation temperatures for cryopreserved cells in differing container volumes [162].

Overall, this presents that our computational framework can successfully simulate accurate cooling dynamics for the extracellular space of cells in suspensions undergoing cryopreservation. Additionally, one could see the absence of nucleation peaks in simulations essentially tracking the overall local temperature dynamics in the absence of ice nucleation.

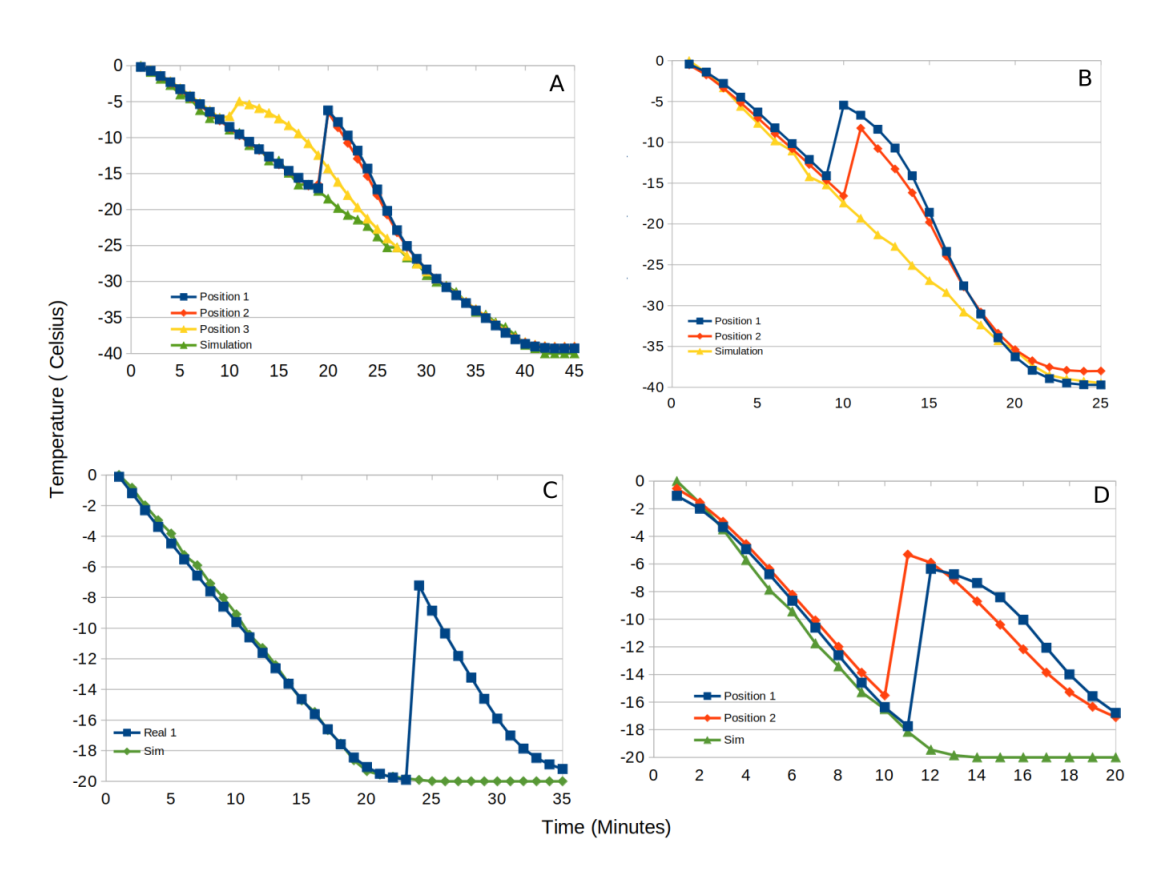


Figure 4.12: Asymptote freezer recordings and CryoDynaMo simulated freezer cooled from 0 to -40 °C at (A) -1 °C min^{-1} and (B) -2 °C min^{-1} with another two additional runs from 0 to -20 °C at (C) -1 °C min^{-1} and (D) -2 °C min^{-1}

Chapter 5

Jurkat cell cryopreservation using multi-step cooling profiles

The use of slow cooling is well explored area of research with a rich history of experimentation for defining the optimum cooling rate of various cell types experimentally. Despite this, several cell types still display relatively low cellular post-thaw survival results when utilising such regimes compared to vitrification. However, recent works have shown that utilising accelerated multi-step slow cooling profiles can lead to greater post-thaw survival results in vitro compared to standard slow cooling practices. Despite this very little work has been done in regards to further exploring the use of multi-step cooling profiles due to the difficulty of exploring cooling rates fully experimentally. Computational modelling represents a perfect solution to this problem as it can provide high-throughput data at a relatively low-cost. Here, we use our CryoDynaMo toolbox to simulate the response of Jurkat cells to multi-step cooling profiles. These profiles were compared against experimental literature in addition to our own novel experimental results. Overall, displaying the power of combining in vitro data with in silico experimentation to improve the post-thaw survival of cryorpeserved cells.

5.1 Introduction

A key use case for cryopreservation is its possible applications in the successful long term storage of reproductive tissue and cells. Representing an exciting prospect for biomedical research as a whole [18]. Spermatozoa, for example, has a great many applications. From it use cases in long range transport of livestock reproductive materials to its applications for assisting in low fertility. The banking of such cells allows for a ready supply of reproductive materials but efforts are still being made to improve post-thaw quality and quantity. However, many species such as sheep still have overall poor preservation post-thaw quality, ranging at around 50% [163, 164] leading to low fertility rates for artificial insemination.

Most studies investigating slow cooling rate cryopreservation optimisation often revolve around investigating the effects of different cryoprotective agents [165, 166, 167] or cooling rates [168, 169, 170]. However, recent studies have shown, when using slow cooling rate techniques, employing stepped accelerating cooling profiles, can achieve greater post-thaw survival results for spermatozoa than standard liquid nitrogen

plunge cooling profiles [171]. Indicating that using an initially low cooling rate into a secondary faster cooling rates could provide another avenue for avoiding intracellular ice formation in cells undergoing cryopreservation. As cells are given enough time to remove large proportions of their intracellular water content before ice nucleation, thus lethal intracellular ice formation can be avoided. This multi-step approach also allows for cells to avoid death due to high extracellular concentrations. As higher cooling rates at the later accelerating stage lead to rapid cellular cooling possibly avoiding negative effects due to large exposure time to high solute and cpa concentrations. This could be critical to improving the post-thaw survival of some cell types such as mouse spermatozoa which have previously been shown to have poor post-thaw survival results when using classical slow cooling techniques [172]. Currently however, there is very little work in regards to the testing of such multi-step cooling rates or how it may impact different cell types. This is due to the difficulty in optimising such cooling profiles experimentally, as the addition of one additional cooling rate necessitates testing across a much wider range of variables than single step. The addition of even further cooling rates further compounding this issue to the point of being un-viable to test physically.

Computational modelling of the cryopreservation process represents an excellent solution to this optimisation problem. As a computational model has the capability to simulate a vast number of cooling rate and switching temperature combinations in a relatively short time scale. In addition, the use of a computational model in this effect would allow for the investigation and interrogation of the relationship between cells and stepped cooling profiles that would be unfeasible for experimental work. Due to the necessity to run hundreds or even thousands of cooling rate relationships. For example, some cells may have greater post-thaw survival with a cooling rate that initially starts low ramping to higher rates while others may have a completely different progression in optimal rates. Previous work has already shown that computational models may be able to predict multi-step cooling profiles that lead to improved post-thaw survival of cryopreserved cells [56]. However, computationally estimated stepped cooling profiles have yet to be validated experimentally.

Therefore in this Chapter we chose to employ our computational frameworks ability to simulating multi-step cryopreservation of cells in suspension and compared these results to novel experimental work. Ultimately, we have utilised our model to investigate two major hypothesis: (1) Do multi-stepped cryopreservation cooling protocols predict for better survival results than standard single cooling rate procedures in Jurkat cells;(2) Can computationally optimised cooling profiles improve experimental post-thaw survival above that of standard experimental protocols?

5.2 Modelling and Methods

To investigate the use of two and three stepped cooling profiles for cryopreservation we expanded our model presented in Chapter 3 to allow for the use of multiple cooling rates during cryopreservation. Multi-stepped cooling simulations use the same base framework as that outlined in Chapter 3 with two notable additions. Firstly, the cooling rates experienced by cells will switch at some temperature $T_{switch(N)}$. Here, $n = 1,2,3 \dots (N-1)$ with N representing the total number of cooling steps being used.

Secondly, the simulation can use multiple cooling rates across the cooling of cells CR1, CR2....CRN.

For this work we decided to utilise two cooling profile types. First, a standard single cooling rate was used for samples being cooled from some initial temperature T_i to a final hold temperature T_f using a freezer plate which is cooled at a constant rate CR_1 . Acting not only as the traditional method but also allowing for comparison between our simulation, experimental literature and our own in vitro results. Second, stepped cooling was performed. Stepped cooling involves a sample being cooled from some initial temperature T_i down to a designated switching temperature of T_{switch} at designated cooling rate CR_1 and after which cells will then be cooled at a secondary cooling rate CR_2 . This is then conducted with N number of switches with n cooling rates to the final hold temperature of T_f .

Within our simulation, stepped cooling is handled in the following way to the n th switching temperature:

$$Cooling \ rate = \begin{cases} CR_1 & if \ T \ge T_{switch \ 1} \\ CR_2 & if \ T < T_{switch \ 1} \ and \ T \ge T_{switch \ 2} \\ ... \\ CR_N & if \ T < T_{switch \ N-1} \end{cases}$$

$$(5.1)$$

For the work in this chapter we chose to utilise a two and three stepped cooling profile. This was primarily done for comparison to later experimental work that was performed. As adding additional cooling profiles would lead to additional complexity in the experimental setup in addition to the relatively low cooling rates the available freezer could reach ($0.1\text{-}10~^{\circ}\text{C}~min^{-1}$. Thus, due to limited time remaining for experimentation we chose to investigate these profiles.

For this work simulations were performed with equivalent to 10% DMSO at cooling rates ranging between 0.1 to $10\ ^{\circ}\text{C}min^{-1}$ to match experimental literature [97]. This meant that across all cooling rates and switching temperatures, a total of 400,000 data points are referenced for a full two-stepped cooling simulation and 1.6 million for three-stepped cooling.

The greatest predicted post-survival in these ranges was then found using a grid search technique for *in vitro* parameter optimisation. This search is across all combinations of cooling rates and switching temperatures locating the highest global maxima for post-thaw survival rate.

For two-stepped cooling a unique relationship was found between CR1, CR2 and the switching temperature(s) during these searches for two-stepped cooling. Similar to standard linear cooling, we found that a maximum post-thaw survival of the cells exists at an absolute global peak. However, unlike single stepped cooling, multi-stepped cooling has multiple approaches to this peak. This data can easily be summarised within a "Survival landscape" for two-step cooling, as is shown in Figure 5.1.

For three-stepped cooling this phenomena is not as easy to visualise due to a significant increase in data dimensionality. However, we again found that there was a single global optimum for post-thaw survival across available cooling profiles. However, for three stepped cooling, unlike single and two stepped cooling, there is not necessarily a single peak; instead we observe multiple local peaks and a single global maximum post-thaw survival peak.

5.2.1 Experimental procedures

5.2.1.1 Cell cultures

For our wet-lab experiments, we used human T lymphoblasts - Jurkat cells (Clone E6-1; TIB-1522; American Type Culture Collection, Manassas, VA). Jurkat cells were cultured in a complete growth medium containing RPMI 1640 Medium (A1049101; Thermofisher Scientific, Massachusetts, US), 10% fetal bovine serum (10270106; Thermofisher Scientific, Massachusetts, US), and 1% penicillin-streptomycin (15140122; Thermofisher Scientific, Massachusetts, US) in a tissue culture incubator at 37°C with a humidified atmosphere containing 5% CO2. Cells were grown in suspension in T75 tissue culture flasks and maintained at a concentration between 1×10^5 and 1×10^6 cells mL⁻¹, as recommended by the supplier.

5.2.1.2 Freezing and thawing

For cryopreservation experiments, Jurkat cells were dispensed into cryovials at $3.0x10^6$ cells mL⁻¹, in a complete medium with the addition of 10% DMSO (102952; Merck, Darmstadt, Germany) as a cryoprotective agent. Cells were cryopreserved using a Kryo 360 controlled rate freezer (Planer, Middlesex, UK)using a three-step cooling method. The range of cooling rates used for each step lying between $1 - 10^{\circ} \text{Cmin}^{-1}$. All the experimental conditions were tested as both technical and biological triplicates. Before freezing the Kryo 360 controlled rate freezer was cooled down to $+4^{\circ}\text{C}$, which was used as a starting temperature for all experiments. After reaching -50°C, cells were kept frozen for one additional hour. Afterward, vials were quickly thawed in a 37°C water bath.

5.2.1.3 Staining and cell counting

As soon as an experimental vial content was thawed, the cell suspension was transferred to a centrifuge tube containing 9 mL complete medium and centrifuged at 1000 rpm for 5 minutes. After spinning cells down, the supernatant was removed, and the remaining cell pellet was re-suspended in the complete medium, dispensed into a 75 cm² tissue culture flask, and incubated in a tissue culture incubator at 37°C with a humidified atmosphere containing 5% CO2. The living cells were counted using a trypan blue exclusion test, 1 hour and 24 hours after thawing, with at least 200 total cells counted for each experimental condition tested.

5.2.2 Multi-step cooling profiles

5.2.3 Double cooling profiles

From our simulated two-stepped cooling of Jurkat cells we generate up to 400000 data points for post-thaw survival predictions over all possible combinations of switching temperatures and cooling rates. An easy way to visualise this data is using MatLab(R2018a; MathWorks, Natick Massachusetts) to create a 3D "survival landscape" with a heat-map colour scheme. Here, we use CR_1 and CR_2 as our x and y axis respectively with cell predicted post-thaw survival rate as our Z axis. An example of this can be seen in Figure 5.1 for Jurkat cells with a simulated switching temperature of -25°C.

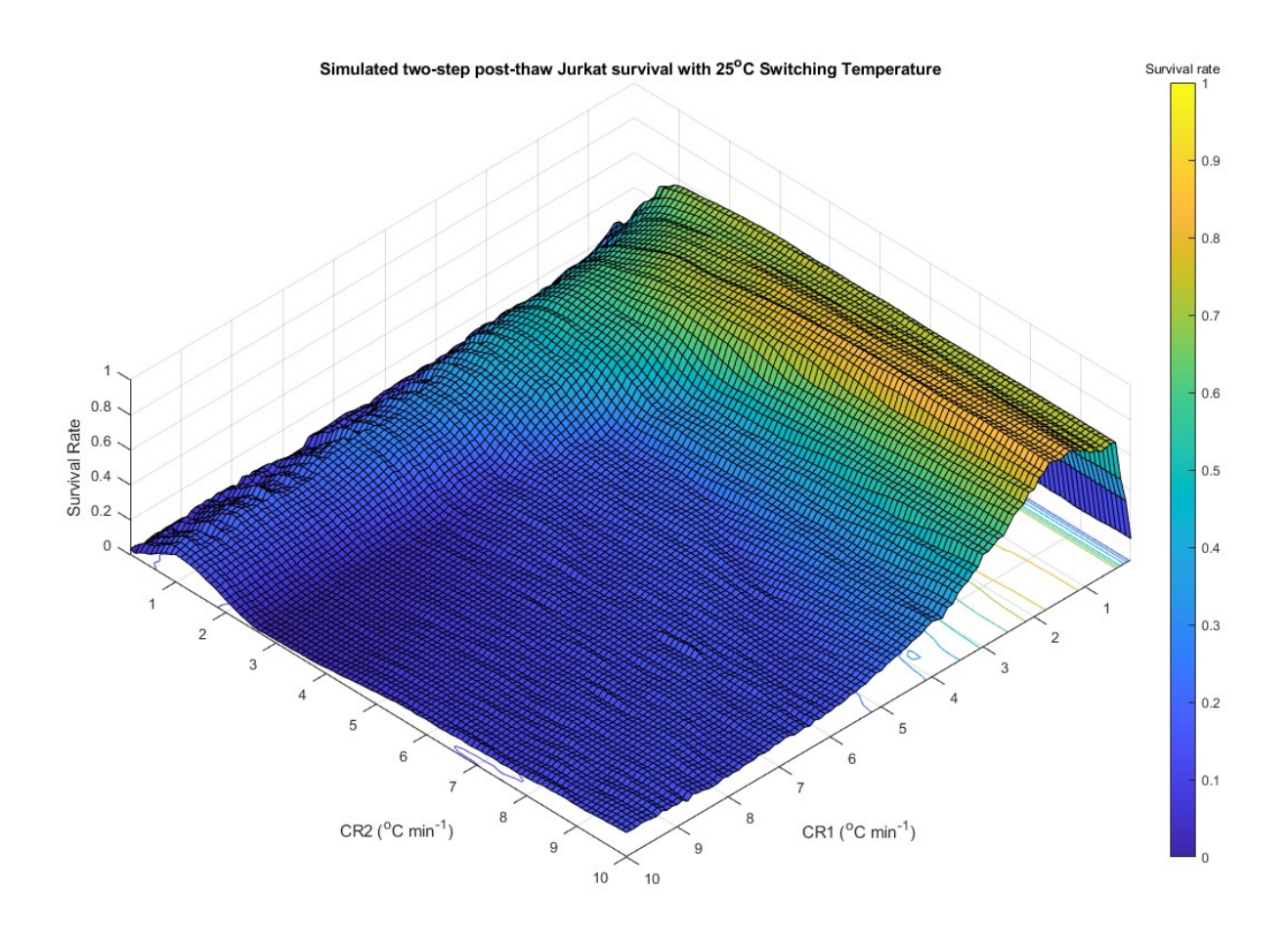


Figure 5.1: Simulated Jurkat survival chance with a -25°C switching temperature and cooling rates between 0.1 - 10°C min^{-1}

Investigating the survival landscape we begin to uncover a unique relationship between CR1, CR2 and the switching temperature for two stepped cooling profiles. Similar to standard linear cooling, we find that a maximum post-thaw survival of the cells exists at an absolute global peak in the given landscape. However, unlike single stepped cooling, multi-stepped cooling has multiple approaches to this peak. This topography can be broken down into 4 major regions:

- 1. A ridge line parallel to CR2 and perpendicular to CR1, "Ridge 1".
- 2. A ridge line parallel to CR1 and perpendicular to CR2, "Ridge 2".
- 3. The intersection between the two survival ridges.
- 4. A survival rate region outside of both ridges which has a high likely hood of death (Survival rate of < 0.1), "Flats".

These landscapes are individual to each switching temperature with a unique topography. Comparing Figure 5.1 and Figure 5.2 with switching temperatures of -25°C and -35°C respectively. The first notable difference in the survival landscape is that Ridge 1 and 2 are centered around different positions with significantly different

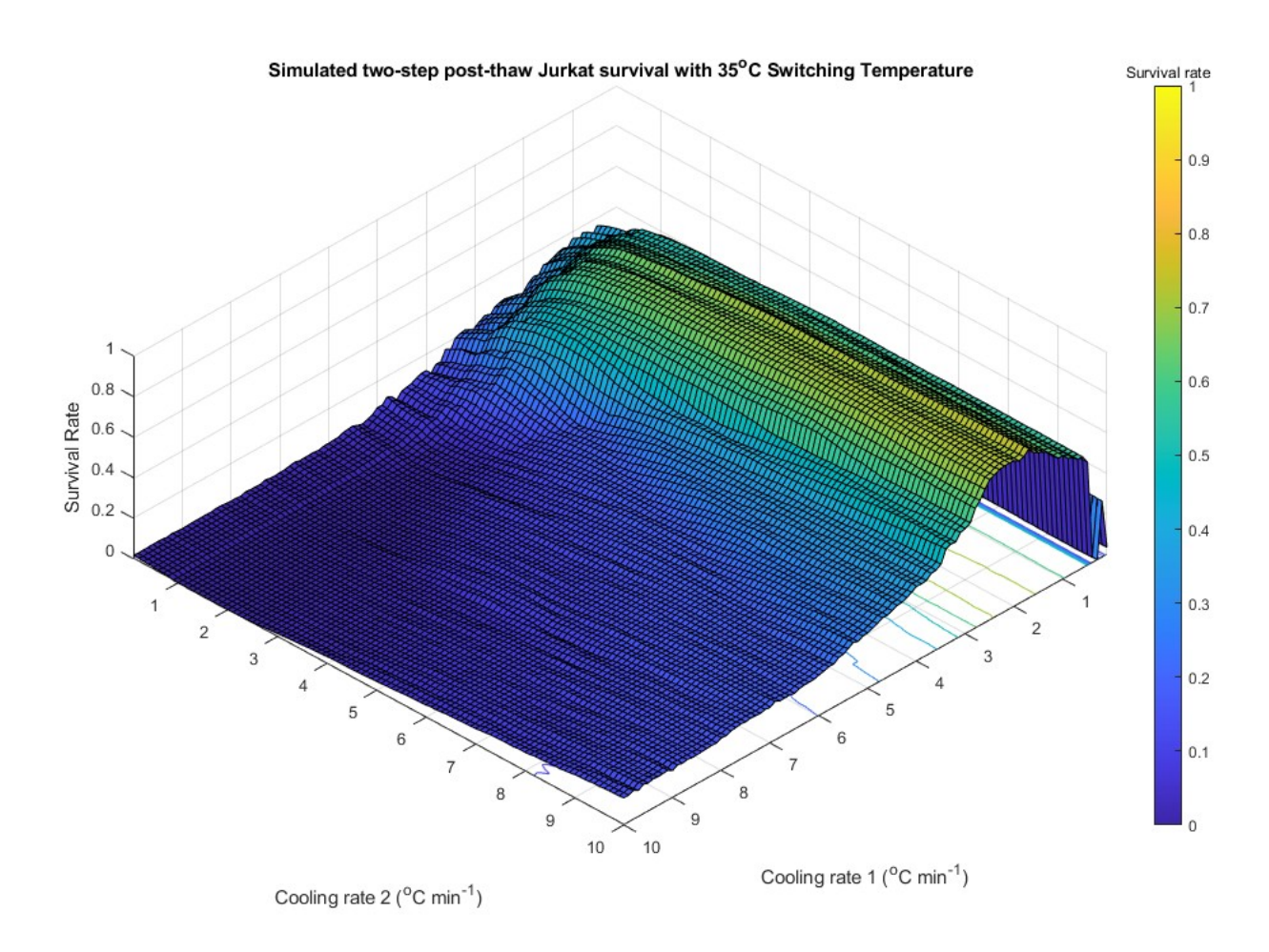


Figure 5.2: Simulated Jurkat survival chance with a -35°C switching temperature and cooling rates between 0.1 - 10°C min^{-1}

amplitudes. For the -35 °C switching temperature Ridge 1 is centered at a CR_1 of 1.7 °C min^{-1} and Ridge 2 at a CR_2 of 1.4 °C min^{-1} . In contrast, using a switching temperature of -25 °C we find Ridge 1 centered around $CR_1 = 1.2$ °C min^{-1} and Ridge 2 at a $CR_2 = 1.0$ °C min^{-1} . Second, with a higher switching temperature Ridge 2 is significantly shortened towards the intersection point and Ridge 1 has an overall lower average post-thaw survival value than in the -25 °C switch landscape. In both cases we see that the flat "death zone" is still present. Finally, there is a significant difference in maximum predicted post-thaw survival with a predicted maximum of 0.86 and 0.74 for the -25 and -35 °C switching temperatures respectively.

For further comparison across switching temperatures we have generated 2D equivalents of the survival landscapes graphs to more clearly view changes in top-down topography. These are displayed in Figure 5.3 for Jurkat cells being cryop-reserved with switching temperatures from -5 to -40°C with increments of -5°C in switching temperature.

This allows us to directly investigate the differences in topology with decreasing switching temperature. Firstly, as switching temperature decreases Ridge 1 emerges from the CR2 axis and its centering around CR1 is shifted towards higher cooling rates. Additionally, as the switching temperature increases Ridge 1 rapidly increases to its highest survival amplitude before diminishing towards lower switching tem-

peratures. Second, as switching temperature decreases, Ridge 1 decreases in both width and length until diminishing entirely. Finally, each switching temperature has a unique combination of CR1 and CR2 which predicts a maximum post-thaw survival. A simplified version of the overall topography is summarised in Figure 5.4 for two-step cooling of Jurkat cells.

Plotting the maximum predicted survival rate for each switching temperature, as shown in Figure 5.5, we see a definitive maximum in post-thaw survival. An absolute global optimum of 0.94 is predicted with an initial cooling rate of CR1 = $0.1 \, ^{\circ}$ Cmin⁻¹ switching at -9°C and using a secondary cooling rate of CR2 = $9.7 \, ^{\circ}$ Cmin⁻¹ to the final temperature. Interestingly, Unlike standard cooling, it is notable that there is not a single standard upside down "U" curve. Instead we observe a lower survival peak at a switching temperature of -25°C in addition to the global optimum at -9°C.

To approximate cooling rate fluctuations during cooling of a real freezer we have also utilised a circular stability convolution algorithm. This is done to account for minor fluctuation in freezer temperature during cooling. As due to the release of latent heat during ice formation, cells can experience a difference in temperature profile based on their position in space above the cooling plate. Thus, applying a specific convolution to the data can account for minor differences that could be experienced in cooling rate for cells undergoing cryopreservation. This allows for an error corrected version of survival landscapes to generated based on these minor fluctuations. This produces an overall smoother survival landscapes and reduces the impact of outliers on the overall shape of the landscape.

Finally, we investigated three stepped cooling. Achieving a maximum post-thaw survival of 0.98 ± 0.01 with a cooling profile of $CR1 = 1^{\circ}Cmin^{-1}$, Switch1 = -13°, $CR2 = 2^{\circ}Cmin^{-1}$, Switch2 = -26°, $CR3 = 10^{\circ}Cmin^{-1}$. This computational protocol greatly outperforms the linear cooling simulation's maximum predicted survival of 0.72 ± 0.02 . In addition, three stepped cooling also outperformed the maximum experimental result of 0.8 ± 0.04 from other experimental literature [97].

To experimentally validate our results we utilised the predicted optimum three stepped cooling profile along with standard cooling in vitro. Standard cooling rates included Jurkat cells being cooled at 0.5, 3 and 10° Cmin⁻¹. Survival estimates for Jurkat cells were made 1 hour and 24 hours post-thaw, as shown in Figure 5.6A and B respectively.

A comparison between our standard linear model, multi-stepped model and state of the art storage for Jurkat cells can be found in Figure 5.6.

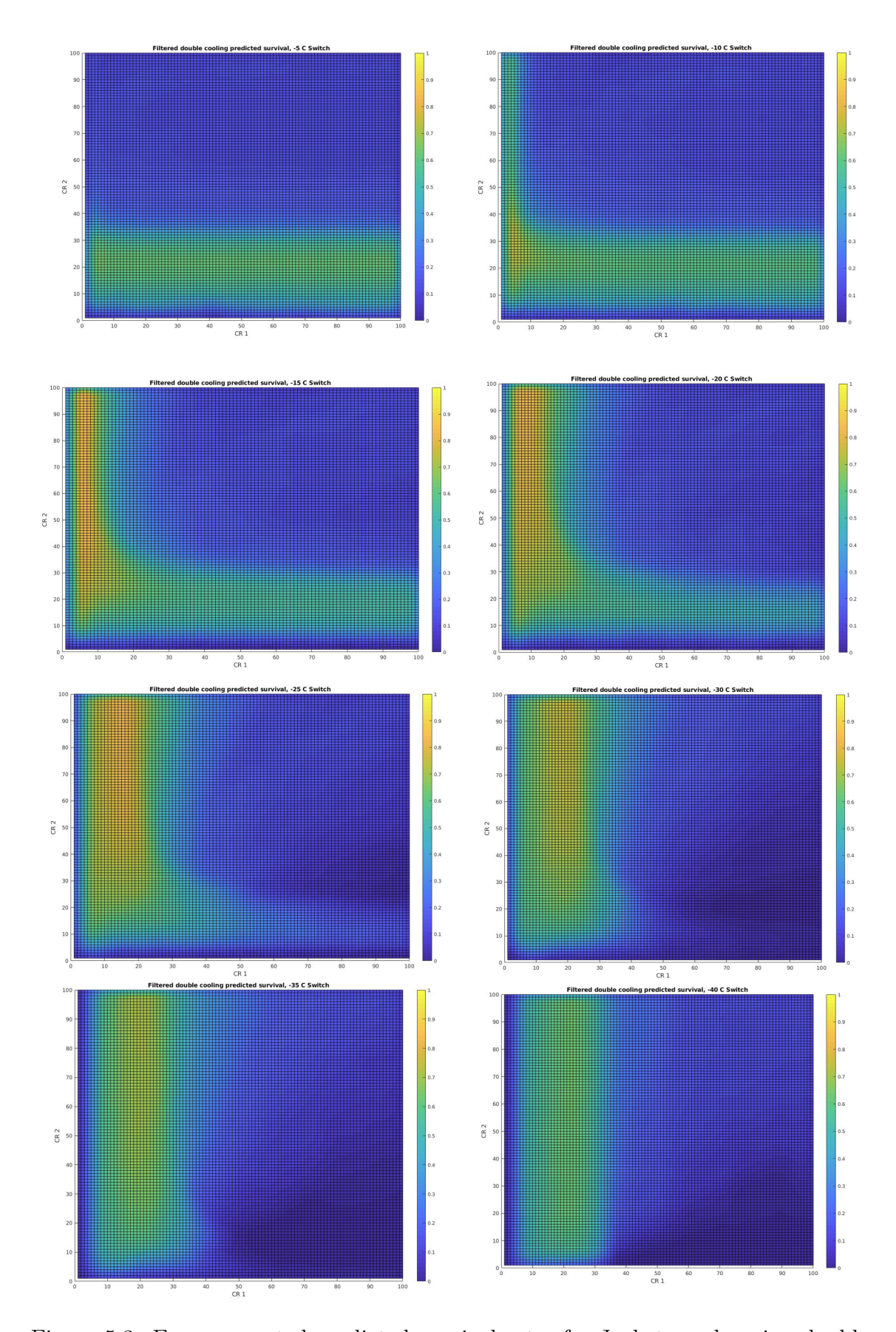


Figure 5.3: Error corrected predicted survival rates for Jurkats undergoing double cooling all switching temperatures between -5 to -40 $^{\circ}\mathrm{C}$

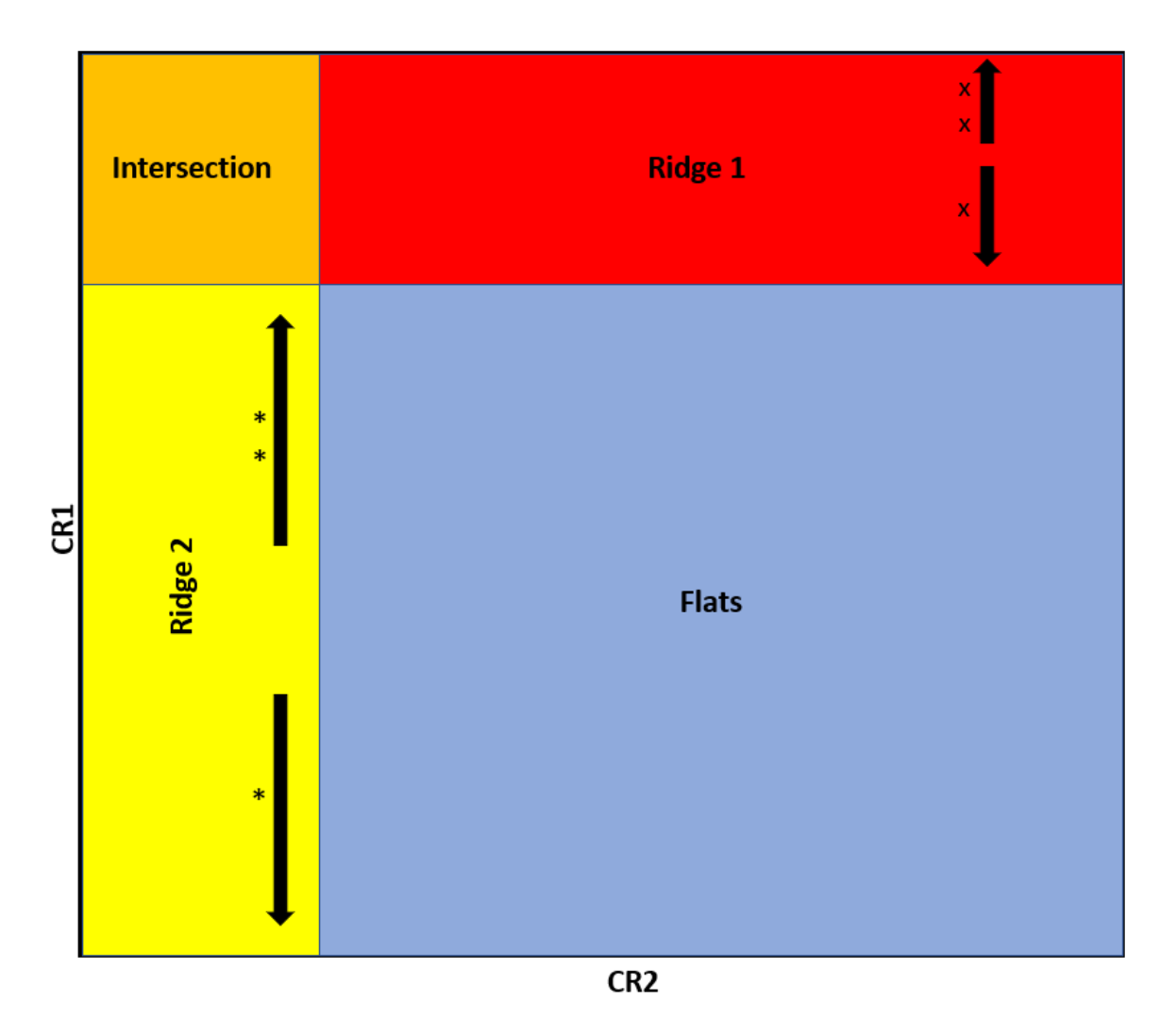


Figure 5.4: General 2D layout of two-stepped cooling survival landscape for Jurkat cells. * Ridge length increases at higher switching temperatures. ** Ridge length decrease at lower switching temperatures. x Ridge centre moves up in relative to CR1 as switching temperature decreases. xx Ridge centre moves down relative to CR1 as switching temperature increases.

Max predicted survival rate against switching temperature

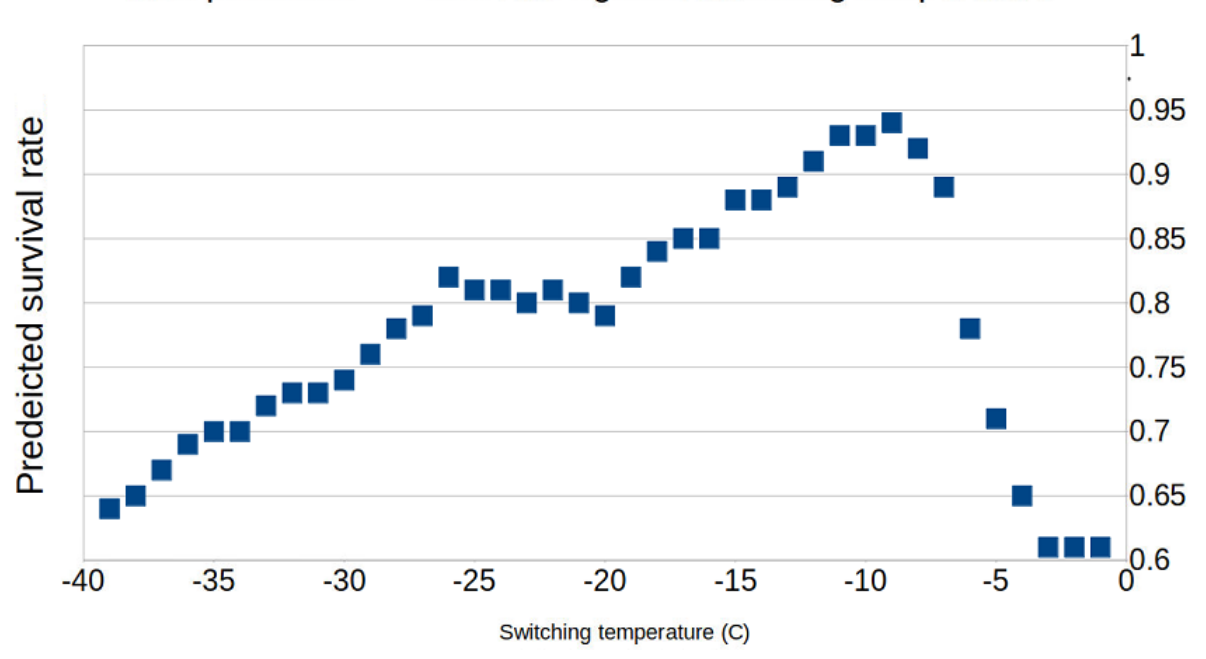


Figure 5.5: Maximum predicted survival rates for Jurkats undergoing two-step cooling. Utilising the optimum predicted cooling trajectory for each switching temperatures between 0 to -40 °C and cooling rates between 0.1 to 10° C min^{-1} . A maximum predicted post-thaw survival of 0.94 being achieved using a cooling profile of CR1 = 0.1° C min^{-1} , CR2 = 9.70° C min^{-1} and Switch = -9°C. Unlike the single peak of standard cooling, we can see a second local optimum at a switching temperature of -25°C.

75

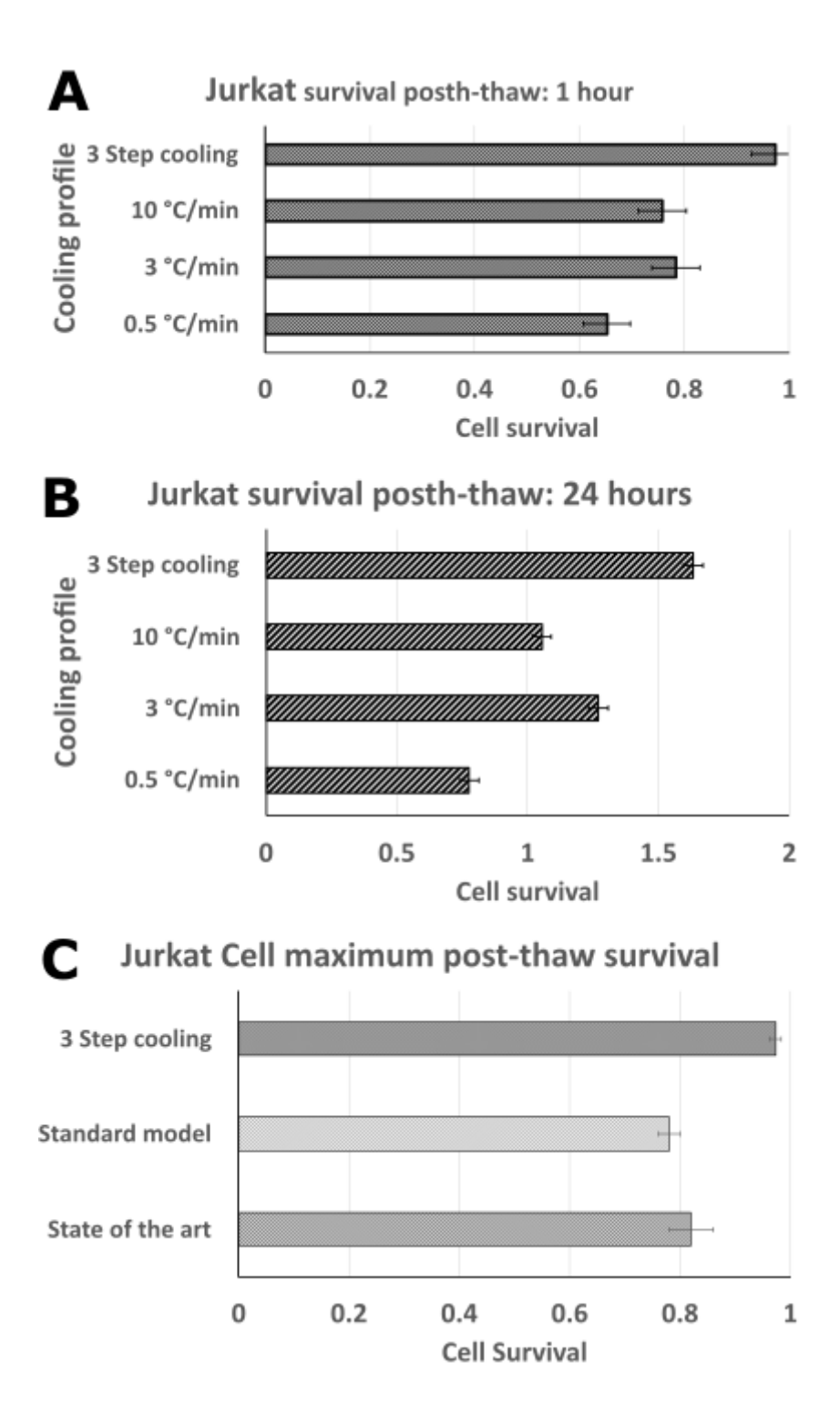


Figure 5.6: Post-thaw survival of Jurkat cells utilising a 0.5, 3, $10 \, {}^{\circ}\text{C}min^{-1}$ and 3 step cooling profile Jurkat cell survival (A) 1 hour after thawing (B) 24 hours after thawing and (C) a comparison between our experimental results for 3-step cooling, standard cooling against and state of the art Jurkat storage.

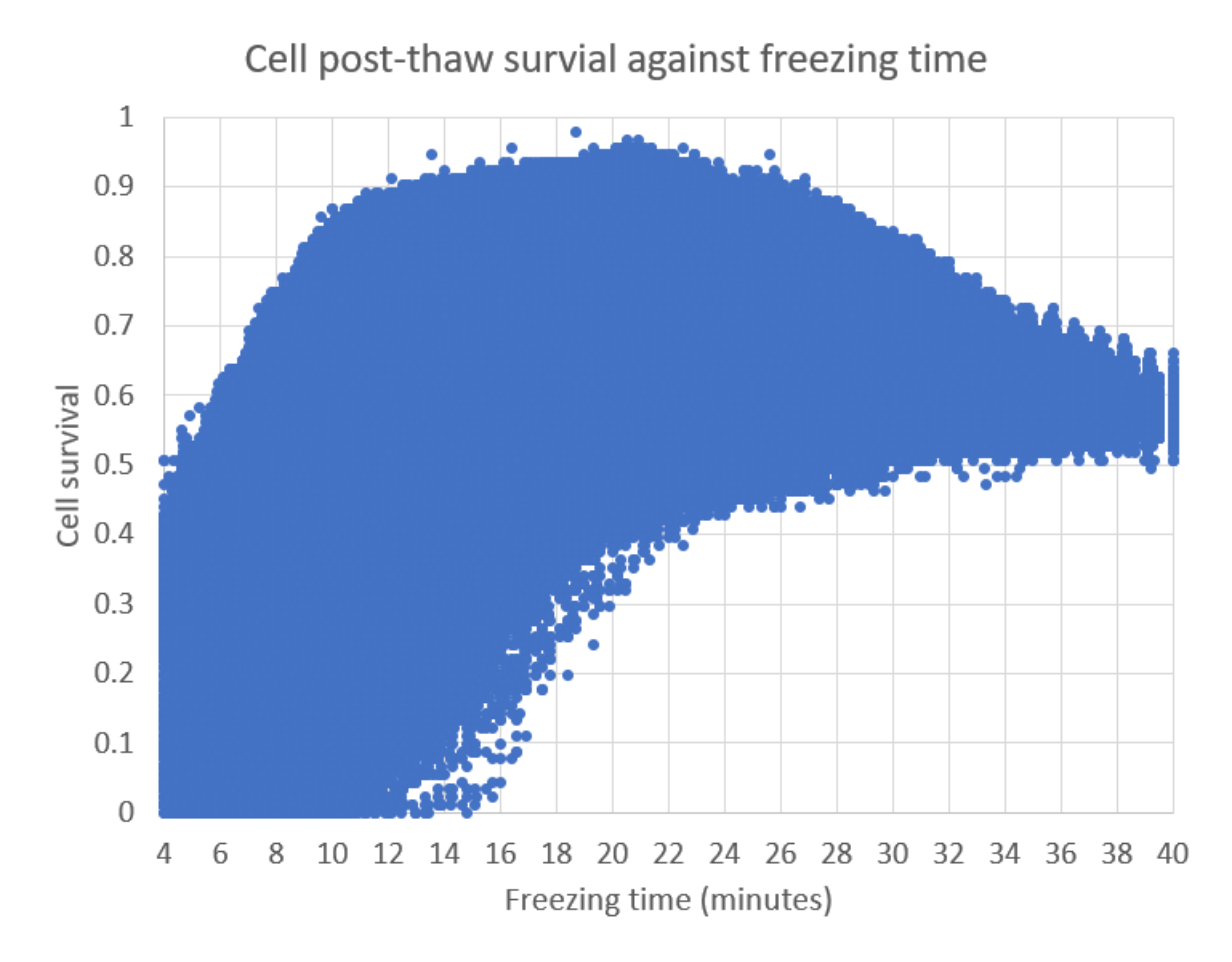


Figure 5.7: Simulated post-thaw survival of Jurkat cells cryopreserved using three-stepped cooling profiles and against freezing time. Data displayed includes surival predictions using multiple siwtching temperature combinations. Notably, there is still a clear structure to the overall survival curve and still presents an overall "inverted-U" curve".

5.3 Discussion

5.3.1 Simulate multi-step cooling profiles of Jurkat cells

Using standard and multi-stepped cooling procedures, we have investigated our computational frameworks capability to predict the post-thaw survival of Jurkat cells undergoing cryopreservation. From our simulations we observed that Jurkat cells cooled slower than the optimum experienced a greater risk of cell death due to an excessive efflux of water during cooling. This is accounted for within our framework by an increase in P_{SOL}^{Lethal} . Secondly, cells cooled at rates higher than the optimum experienced a decrease in post thaw survival due the increasing likelihood of IIF. Indicated in our modelling by an increasing probability of P_{IIF}^{Lethal} . Overall, our results are well matched to the "Inverted-U" survival curve defined by the two-factor hypothesis proposed by Mazur et al and others [103, 8, 96].

Another major part of our work was investigating the difference in simulated post-thaw survival of cells when using multi-step cooling profiles. To do this we have investigated three profiles types: standard single, two-stepped and three-stepped cooling profiles. Jurkat cells are consistently used in many areas of biomedical and pharmaceutical research. This includes cell toxicity tests [173, 174] often used in pharmaceutical research and immune cell signal processing [175, 176] for cancer research. Thus, due to their significant use across many research disciplines in addition to within industry, we have chosen Jurkat cells as our target of investigation.

For two-stepped cooling we performed a total of 400000 simulations. Achieving a maximum predicted post-thaw survival of 0.94 ± 0.03 using a cooling profile of CR1 = 0.1° C min^{-1} , CR2 = 9.70° C min^{-1} and a switching temperature of -9°C. Thus, two-step cooling is predicted to significantly outperform standard cooling procedures. Notably, the maximum post-thaw survival achieved by 27 of the possible 40 switching temperature cooling profiles outperformed simulated single step cooling. Of those 27 cooling profiles, 13 outperformed the experimentally observed maximum in G Yu et al's work of 0.8 ± 0.03 . The maximum post-thaw survival achieved for cooling profiles using each switching temperature can be found in Figure 5.5.

Finally, 1.6 million simulations were performed using three-step cooling profiles. A maximum post-thaw survival of 0.98 ± 0.03 was predicted for Jurkat cells using a cooling profile of CR1 = 1°C min^{-1} , $T_{Switch1} = -13$ °C, CR2 = 2°C min^{-1} , $T_{Switch2} = -26$ °C, CR3 = 10°C min^{-1} . Thus, three-stepped cooling profiles predicted significantly higher post-thaw survival rates than single or two-stepped cooling profiles.

5.3.2 Experimental validation of multi-stepped cooling predictions

To validate the capability of our three-step cooling protocol, we performed several experiments for Jurkat cells using standard single step cooling at 0.5, 3 and $10^{\circ}\text{C}\ min^{-1}$ in addition to using the computationally derived optimum 3-step cooling profile. Cellular post-thaw survival was calculated 1 and 24 hours post-thaw. Experimental results for standard linear cooling of Jurkat cells achieved similar post-thaw retrieval as those in literature, as shown in Figure 5.6C, with an maximum post-thaw survival of 0.78 ± 0.02 being achieved at a cooling rate of 3°C min^{-1} . In addition, we observed the expected reduction in post-thaw survival either side

of the optimum for the 0.5and 10° C min^{-1} cooling rate experiments. Using our computationally generated three-step cooling profile, Jurkat post-thaw cell survival was observed to significantly exceed single step cooling results. Achieving an overall post-thaw survival of 0.98 ± 0.03 . These results are displayed in supplementary Figure 5.6A.

In addition to calculating cellular post-thaw survival 1-hour after freeze we have also assessed each cell population 24-hours after thawing. As this can display the ability of cellular populations to proliferate after being frozen. Here we compare the number of cells in thawed populations to pre-freeze. As shown in Figure 5.6B, the three-stepped cooling profile had significantly more cells 24-hours after freeze than pre-thaw. The 3 and 10° C min^{-1} populations having more cells than pre-freeze. However, the 0.5 °C min^{-1} had still not reached pre-freeze numbers. This likely indicates significant amounts of apoptosis as numbers had not significantly increased above those 1-hour post-thaw.

The increase in overall post-thaw survival achieved by our multi-step cooling profiless is greater than results found in other optimisation work. For instance, in their 2017 work K Pollock et~al~[138] utilised a convergence algorithm to optimise the freeze/thaw of Jurkat cells. In this work they achieved a maximum post-thaw survival of 0.90 ± 0.02 for Jurkat cells via optimisation of cryopreservation solutions and cooling rates. An overall reduction in maximum post-thaw survival of 8% compared to our own. Pollock's work has several major differences to our own. Firstly, unlike our own work Pollock controlled for two variables during cryopreservation. As in addition to cooling rate, CPA concentrations were also optimised over iterative simulations. The requirement of utilising multiple variables inherently leads to greater variability within results due to requiring a greater range of local-global searches to find a true optimum. Additionally, unlike our own work Pollock et~al's required continual iterative feedback from experimental work until an optimum is found. The requirement of repeat experimental verification and updating of results means a much more time consuming process.

In addition to computational optimisation approach's, other works have also attempted to optimise cryopreservation procedures in vitro. For example, liquidus tracking (LT) has been used in the works of A Kayet al and E Puschmann et al to optimise CPA concentrations and cooling rates experimentally. This is done through the addition of external CPA pumps to the freezer, combining incremental changes to CPA during cooling and rate controlled freezing to keep the extracellular medium above the homogeneous freezing temperature of the medium. Unlike Pollocket al's work, this methodology relies on the real time alteration of CPA concentrations via external pumps. Using this method Puschman managed to increase the post-thaw survival of cryopreserved alginate encapsulated liver cells (AELCs) from 60% to 90%. This increase in survival is comparable to that achieved by our own work when utilising multi-step cooling profiles for Jurkat cells. One major thing of note with the LT method is its need for suitable CPA mixtures to first be tested for and optimised before the LT process itself is employed. This requires significant trial and error wet lab work before LT optimisation is even employed.

A major benefit of our own work is its ability to be improved and adapted modularly. This means that in future it will be possible to adapt the computational framework we have created already to include aspects from methods such as those presented in Puschman, Pollock and Kay's work. For example, the introduction of multi-variate optimisation such as CPA concentrations/composition and cooling profiles. In addition, for LT CPA optimisation our framework could be used as a complimentary technique in the initial optimisation of cooling rate and CPA compositions. Thus, reducing a significant portion of the required trial and error wet-lab work.

The work of Y Hayashi et al is likely the most direct comparison to our own computational approach [56]. Utilising a mathematical modelling approach derived from first principles, Hayashi also made predictions for cells cryopreserved using multi-step cooling profiles. Hayashi made several observations that differ with the findings of our own work.

Firstly, within their work Hayashi predicted that a considerable number of cooling profiles can achieve the same maximum post-thaw survival results, as displayed by the total time to freeze. This is in contrary to our results, as shown in Figure 5.7 which indicate that there is still an overall increase to an optimum value. This is somewhat reminiscent of the "inverted-U" shape with an overall decrease in post-thaw survival either side of the optimum. These discrepancies could be due to one of several differences presented between us and Hayashi et al. First of all, Hayashi's work performs CPA free cryopreservation simulations. The lack of CPA being used in Hayashi's work may generate a completely different dynamic for cooling profiles due to a different extracellular medium makeup. However, for slow cooling we believe that the inclusion of CPA's is paramount due to their prevalence in the industry and the significant impact they have on cellular post-thaw survival. Additionally, the inclusion of CPAs within such simulations is of high importance for large volume cell suspensions or tissues.

Second, the optimum cooling rates presented by Hayashi utilise a single cooling rate from 0 to -40/50 °C at which point they switch to a slower cooling rate until reaching -60°C. This is significantly different from our work, as we found that utilizing multiple stepped cooling rates before reaching -40°C predicted for the greatest post-thaw survival. In addition to this, Hayashi's top profiles often followed a pattern of C2 < C1 > C1 and C3 > C1. This is contrary to our own findings for Jurkat cells. As an optimum cooling profiles for any giving switching temperature always followed the form of C1 < C2 < C3. This could be due to differing responses between Jurkat and HiPSCs cells to cryopreservation. However, this cannot be confirmed due to Hayashi's findings on multi-step cooling profiles, as of yet not being experimentally validated. In addition, as discussed previously our work indicates that for both two-step and three-step profiles an overall increase in cooling rate predicts for greater post-thaw survival which is in agreement with other works [171].

Overall, we believe our computational framework and its approach to modelling the response of cells in suspension to cryopreservation is extremely powerful for predicting the optimal cooling profiles for cells. In addition, our approach achieves experimentally validated results which outperform current gold standards and other more complex optimisation techniques.

5.4 Limitations

Our work here is limited by its reliance on exact experimental protocols, the same as in Chapter 4. Only predicting the response of the specified cell type for exact experimental protocols. Thus, any changes made to these initial experimental variables requires simulations to be ran again.

In addition, our computational approach uses a relatively simplistic grid search method for optimising these multi-stepped profiles. In future, we intend to improve our computational frameworks by using more complex optimisation techniques. For example, the use of a closed loop variable optimisation algorithm would likely significantly reduce both the time to optimise cooling profile variables and the number of simulations which need to be ran.

Jurkat cells were chosen for the multi-stepped cooling investigation over other cell types due to experimental availability and cooling rate limitations of available freezers. In future we hope to extend our work by testing multiple cell types across a greater range of cooling rates. In addition, in future we hope to explore the effect

As we only utilised a maximum of three cooling rates in our multi-stepped cooling protocol, further work is required to investigate more complex cooling profiles. In addition, within our model we did not explore the cooling rates which predicted the greatest post-thaw survival below -50 $^{\circ}$ C. Ultimately, we hypothesise that an accelerating cooling rate may prove optimum for cellular post-thaw survival. Finally, we have not tested the efficiency of our model for large-scale cryo-banking (Volume > 200 mL).

5.5 Conclusions

In this chapter, we have presented the ability of multi step cooling profiles to outperform standard cooling protocols. Through simulation we predicted that the use of a multi-stepped cooling profile could achieve greater post-thaw survival than standard single rate cooling. Notably, a three stepped cooling profile was predicted to outperform standard and two-stepped cooling. This finding was validated experimentally, our optimum cooling profile results in an order of magnitude reduction in cell death compared to standard single rate cooling. Additionally, it was found that multi-step cooling profiles could have more than one peak in terms of post-thaw survival locally. However, overall a single optimum was still found globally.

Overall, within this chapter we present the assistive power computational modelling of cryopreservation procedures can have in optimisation of $in\ vitro$ experimental work .

Chapter 6

Conclusions and Future Work

In this thesis we tackled two major hypothesis for cryopreservation:

- 1. An agent based modelling approach for cells undergoing cryopreservation can be used to encapsulate and predict the response of cells to various cryopreservation procedures. Including different cell types, multiple cooling regimes, in the presence and absence of CPA.
- 2. A computational model of cryopreservation will be able to optimise and improve experimental procedures for the cryopreservation of cells in suspension. Through the prediction of optimal cooling rate for a given cryopreservation protocol or by offering new insights into changes that could be made to protocols to improve post thaw survival.

Our first hypothesis has been addressed in Chapter 2 and 5 using the background information and modelling approach presented in Chapters 2 and 3. The work in this chapter displayed that a computational framework with a hybrid modelling approach can be used to simulate cells in suspension undergoing cryopreservation. Including the modelling of cellular water kinematics, intracellular ice formation predictions and cellular post-thaw survival rates across multiple cooling regimes. Most importantly we displayed that our model could give comparable post-thaw survival prediction for three distinct cells types (Jurkat, HiPSc's and HeLa cells) when compared against experimental literature. To our knowledge this is the first example of a hybrid computational framework predicting the response of multiple cell types to cryopreservation. Overall, this displays the power of computational modelling when compared with experimental data for the prediction of cells to cryopreservation and its adaptability across multiple different cell types. Ultimately, pairing of such in silico modelling and experimental data could significantly reduce the need for repeat trial and error wetlab work. Significantly reducing the cost and time associated with standard experimental optimisation. A major limitation of this work is its reliance on exact experimental protocols. For example, highly cell specific variables such as membrane pereability to water and CPAs and ice formation parameters. Future work will likely involve expanding the model to be more flexible with predictions making from some critical initial conditions.

Chapter 5 utilised the same modelling approaches outlined for Chapter 2 to investigate the ability of our computational framework to improve experimental post-thaw survival of Jurkat cells. In this section we showed a computationally derived multi-step cooling protocol predicted for significantly reduced cell death compared

to standard methodologies. Notably, it was found that a three-step cooling protocol predicted for the greatest post-thaw survival compared against single and two-step profiles. These findings were also experimentally validated. Overall, this displayed the ability of computational modeling in cryopreservation to optimise experimental cryopreservation procedures. It should also be noted that such a multi-step cooling approach would likely be infeasible to through experimental work alone. This is due to the time and expense required that would be required to identify optimal parameters without computational assistance. This section has three possible avenues for future work. Firstly, our work used a relatively simplistic grid search method for locating optimum protocols. Utilising more advanced methods such as closed loop variable optimisation could significantly reduce the number of simulations required before reaching an optimum. This would not only save time needed for running computational simulations but would also lead to an overall reduction in computational power required for optimisation. Second, due to both time constraints, relative availability of cells and experimental hardware limitations we could only investigate the Jurkat cell type. Future work into identifying the response of other cells types to multi-stepped cooling profiles is of key importance. This is due to the need to identify the individual response of multiple cell types to multi-stepped cooling procedures. Finally, within our work we only investigated up to three cooling rates being employed during the cryopreservation process of cells. Thus, it is hypothesised that the use of further stepped cooling may results in greater post-thaw survival results.

Future work for the computational framework presented in this thesis has at least three immediate possible avenues for expansions. First, work could explore the expansion of our computational framework to also make predictions for tissue and whole organs. As to date the ability to cryopreserve larger biological samples is incredibly difficult. The modularity of our framework makes it excellently suited for such expansion and could further provide insight into cryopreservation techniques that may yield greater post-thaw viability of larger samples. However this is not trivial work and will require a significant amount of expansion and improvement. As the cryopreservation of tissues includes multiple new issues such as cell type heterogeneity, cell and extracellular matrix interaction and the reaction of tissue super structures to stresses and strain generated during cryopreservation. Second, we wish to further explore the use of our computational framework utilising more complex changes in cryopreservation protocols. As our current iteration purely optimised the cooling rate of cells undergoing cryoprervation. Thus, one could also explore the use of multiple independent or mixed CPA types, cooling rates and warming rates.

In summary, we believe our computational framework has successfully addressed the major hypothesis set out at the start of this work with ample room for future expansion. Presenting the significant benefit of utilising hybrid computational modelling to assist in and improve the post-thaw survival of cryopreserved cells in suspension.

Finally I present a brief summary of each chapter presented throughout this thesis:

Chapter 2: Here, we outlined the background of cryopreservation research. From initial discoveries and early issues to modern cryobiology research. Additionally, here we also outlined the various risk factors that effect cells during cryopreser-

vation such as the solution effect and damage due to intracellular ice formation. Including background on the discovery and development of CPAs to combat many of the issues faced due to intracellular ice formation. Finally, the difference in issues faced by single cell to tissue based cryopreservation was also discussed with a insite into possible future avenues for cryobiology research.

Chapter 3: Within this section we outline the background behind cryobiology mathematical modelling research. Beginning with initial approaches to modeling by Peter Mazur and how this has been adapted in modern cryobiology research. Additionally, we also outline how we utilise variations of existing models in our computational framework to make predictions for multiple aspects of cells in suspension undergoing cryopreservation. This includes: water kinematics, prediction of intracellular ice formation and estimating cell survival chance. Here, we also used our computational framework to model the cooling dynamics in slow-cooling for several cell types and compare our results against experimental literature for optimal cooling. Providing the output computational predictions for several cell types. Moreover, we assess the predictions with data obtained from the literature, as well as novel experimental results. Overall, providing the first major use case for our computational approach to generate predictions for slow-cooling profiles for the cryopreservation of cells in suspension

Chapter 4: Here, we presented the role of BioDynaMo as the basis for our computational modelling framework. Allowing us to include extracellular concentrations and heat transfer in 3D space within our computational simulations. In addition we also present some relevant demons developed within the BioDynaMo modelling framework in addition to the ability of our computational framework to estimate the osmotic response of cells to various cooling temperatures.

Chapter 5: In this chapter we proposed a mathematical method to optimise the cooling dynamics in slow-cooling, to reduce the risk of injury and cell death. Our framework first independently predicted that using multi-stepped cooling profiles could produce post-thaw survival rates significantly above that of standard methodologies. These predictions were further assessed with data obtained from literature as well as novel experimental results. It was found that our computationally derived three-stepped cooling profile could achieve post-thaw survival results experimentally significantly above that of single-step cooling. In addition, it was also found that multi-stepped cooling profiles produced unique "survival landscapes" that could have multiple local survival peaks but still generated an overall global maximum. Future work for this chapter involves utilising our framework to make multi-step cooling predictions for other cell types. Ultimately, aiming to asses if multi stepped accelerating cooling rates may produce higher post-thaw cell viability than traditional slow cooling methods.

Bibliography

- [1] S. Michel, G. La Muraglia II, M. Madariaga, and L. Anderson, "Innovative cold storage of donor organs using the paragonix sherpa pak [™] devices," *Heart, lung and vessels*, vol. 7, pp. 246–55, 10 2015.
- [2] J. Neuberger, P. Trotter, and R. Stratton, "Organ transplantation rates in the uk," *BMJ*, vol. 359, p. j5218, 11 2017.
- [3] K. G. Wong, S. D. Ryan, K. Ramnarine, S. A. Rosen, S. E. Mann, A. Kulick, E. De Stanchina, F.-J. Müller, T. J. Kacmarczyk, C. Zhang, et al., "Cryopause: a new method to immediately initiate experiments after cryopreservation of pluripotent stem cells," Stem cell reports, vol. 9, no. 1, pp. 355–365, 2017.
- [4] M. G. Meneghel J, Kilbride P, "Cryopreservation as a key element in the successful delivery of cell-based therapies-a review," *Front Med*, vol. 9, p. 7, 2020.
- [5] T. E. Luz AL, "Pluripotent stem cells in developmental toxicity testing: A review of methodological advances," *Toxicol Sci.*, p. 8, 2018.
- [6] H. P. Bosch E, De Vos M, "The future of cryopreservation in assisted reproductive technologies," *Front Endocrinol*, p. 11, 2020.
- [7] J. Edesi, J. Tolonen, A. Ruotsalainen, J. Aspi, and H. Häggman, "Cryopreservation enables long-term conservation of critically endangered species rubus humulifolius," *Biodiversity and Conservation*, vol. 29, 01 2020.
- [8] P. Mazur, "Physical factors implicated in the death of microorganisms at subzero temperatures*," *Annals of the New York Academy of Sciences*, vol. 85, no. 2, pp. 610–629, 1960.
- [9] A.-S. MJ, "Preservation of mouse bone marrow at -79 degrees c," *Nature*, vol. 190, 1961.
- [10] L. JE, "The denaturation of lipid-protein complexes as a cause of damage by freezing," *Proc R Soc Lond B Biol Sci*, p. 6, 1957.
- [11] G. DC and J. Critser, "Gao d, critser jk.mechanisms of cryoinjury in living cells. ilar j 41:187-196," *ILAR journal / National Research Council, Institute of Laboratory Animal Resources*, vol. 41, pp. 187–96, 02 2000.
- [12] J. Levitt, "A sulfhydryl-disulfide hypothesis of frost injury and resistance in plants," *Journal of Theoretical Biology*, vol. 3, no. 3, pp. 355–391, 1962.

- [13] E. Cabrita, C. Sarasquete, S. Martínez-Páramo, V. Robles, J. Beirão, S. Pérez-Cerezales, and M. Herráez, "Cryopreservation of fish sperm: applications and perspectives," *Journal of Applied Ichthyology*, vol. 26, no. 5, pp. 623–635, 2010.
- [14] C. Seawright, A., "Modulation of cell-matrix interaction for cryopreservation of engineered tissue," *Purdue University.*, 2013.
- [15] L. Breitwieser, R. Bauer, A. Di Meglio, L. Johard, M. Kaiser, M. Manca, M. Mazzara, F. Rademakers, and M. Talanov, "The biodynamo project: Creating a platform for large-scale reproducible biological simulations," arXiv preprint arXiv:1608.04967, 2016.
- [16] P. G. de Aledo, A. Vladimirov, M. Manca, J. Baugh, R. Asai, M. Kaiser, and R. Bauer, "An optimization approach for agent-based computational models of biological development," *Advances in Engineering Software*, vol. 121, pp. 262– 275, 2018.
- [17] "New experiments and observations touching cold." http://name.umdl.umich.edu/A29001.0001.001. Accessed: 2022-08-18.
- [18] S. Bojic, A. Murray, B. L. Bentley, R. Spindler, P. Pawlik, J. L. Cordeiro, R. Bauer, and J. P. de Magalhães, "Winter is coming: the future of cryopreservation," BMC biology, vol. 19, no. 1, pp. 1–20, 2021.
- [19] L. Spallanzani, "Opuscoli di fisica animale e vegetabile dell'abate spallanzani," Spallanzani L. Edizione nazionale delle opere di Lazzaro Spallanzani. Parte quarta, volume terzo. Modena: Mucchi, pp. 15–109, 1776.
- [20] D. Whaley, K. Damyar, R. P. Witek, A. Mendoza, M. Alexander, and J. R. Lakey, "Cryopreservation: An overview of principles and cell-specific considerations," *Cell Transplantation*, vol. 30, p. 0963689721999617, 2021.
- [21] H. Herman, *Improving Cattle by the Millions*. MO: University of Missouri Press, 1981.
- [22] W. E. C. J. Walters EM, Benson JD, "The history of sperm cryopreservation," Sperm Banking: Theory and Practice, pp. 1–17, 2009.
- [23] E. J. C. Polge and A. S. Parkes, "Low-temperature storage of mammalian spermatozoa," *Proceedings of the Royal Society of London. Series B Biological Sciences*, vol. 147, no. 929, pp. 498–508, 1957.
- [24] A. U. Smith, "Prevention of haemolysis during freezing and thawing of red blood-cells," *The Lancet*, vol. 256, no. 6644, pp. 910–911, 1950.
- [25] C. Polge, A. U. Smith, and A. S. Parkes, "Revival of spermatozoa after vitrification and dehydration at low temperatures," *Nature*, vol. 164, no. 4172, pp. 666–666, 1949.
- [26] C. Polge and L. Rowson, "Fertilizing capacity of bull spermatozoa after freezing at-79° c.," *Nature*, vol. 169, no. 4302, pp. 626–627, 1952.

- [27] R. Bunge and J. Sherman, "Fertilizing capacity of frozen human spermatozoa," *Nature*, vol. 172, no. 4382, pp. 767–768, 1953.
- [28] J. Lovelock, "The haemolysis of human red blood-cells by freezing and thawing," *Biochimica et biophysica acta*, vol. 10, pp. 414–426, 1953.
- [29] J. Lovelock, "The protective action of neutral solutes against haemolysis by freezing and thawing," *Biochemical Journal*, vol. 56, no. 2, p. 265, 1954.
- [30] B. M. LOVELOCK, J., "Prevention of freezing damage to living cells by dimethyl sulphoxide," *Nature*, vol. 183, p. 1394–1395, 1959.
- [31] F. Mueller, T. Casey, and P. Trevor-Roper, "Use of deep-frozen human cornea in full-thickness grafts," *British Medical Journal*, vol. 2, no. 5407, p. 473, 1964.
- [32] L. HB, B. RB, L. PA, and C. LL, "Permanent survival of preserved skin autografts.," Surgery, vol. 56, pp. 742–746, 1964.
- [33] G. M. Fahy, "The relevance of cryoprotectant "toxicity" to cryobiology," Cryobiology, vol. 23, no. 1, pp. 1–13, 1986.
- [34] D. E. Pegg, "Banking of cells, tissues, and organs at low temperatures," in *Current Trends in Cryobiology*, pp. 153–180, Springer, 1970.
- [35] L. M. S. Y. C. O. N. R. B. S. T. B. S. N. S. R. G. H. G. S. G. J. H. R. K. J. C. F. Verheijen, M., "Dmso induces drastic changes in human cellular processes and epigenetic landscape in vitro.," *Scientific reports*, vol. 9, no. 1, p. 8, 2019.
- [36] H. C. J., "Cryopreservation of human stem cells for clinical application: A review.," Transfusion medicine and hemotherapy: offizielles Organ der Deutschen Gesellschaft fur Transfusionsmedizin und Immunhamatologie, vol. 38, no. 2, pp. 107–123, 2011.
- [37] M. T. Li Y, "Bioprocessing of cryopreservation for large-scale banking of human pluripotent stem cells.," Biores Open Access., vol. 1, no. 5, pp. 205–214, 2012.
- [38] H. C. J., "Technical considerations in the freezing, low-temperature storage and thawing of stem cells for cellular therapies.," *Transfus Med Hemother.*, vol. 46, no. 3, pp. 134–150, 2016.
- [39] M. G. Meneghel J, Kilbride P, "Cryopreservation as a key element in the successful delivery of cell-based therapies-a review.," Front Med (Lausanne)., vol. 26, no. 7, 2020.
- [40] M. R. Ugur, A. Saber Abdelrahman, H. C. Evans, A. A. Gilmore, M. Hitit, R. I. Arifiantini, B. Purwantara, A. Kaya, and E. Memili, "Advances in cryopreservation of bull sperm," Frontiers in veterinary science, vol. 6, p. 268, 2019.
- [41] F. Migishima, R. Suzuki-Migishima, S.-Y. Song, T. Kuramochi, S. Azuma, M. Nishijima, and M. Yokoyama, "Successful cryopreservation of mouse ovaries by vitrification," *Biology of reproduction*, vol. 68, no. 3, pp. 881–887, 2003.

- [42] M. Di Santo, N. Tarozzi, M. Nadalini, and A. Borini, "Human sperm cryop-reservation: update on techniques, effect on dna integrity, and implications for art," *Advances in urology*, vol. 2012, 2011.
- [43] S. E. Lanzendorf, J. F. Mayer, J. Toner, S. Oehninger, D. S. Saffan, and S. Muasher, "Pregnancy following transfer of ooplasm from cryopreserved-thawed donor oocytes into recipient oocytes," *Fertility and sterility*, vol. 71, no. 3, pp. 575–577, 1999.
- [44] E. P. de Fried, J. Notrica, M. Rubinstein, A. Marazzi, and M. G. Gonzalez, "Pregnancy after human donor oocyte cryopreservation and thawing in association with intracytoplasmic sperm injection in a patient with ovarian failure," Fertility and Sterility, vol. 69, no. 3, pp. 555–557, 1998.
- [45] A. M. K. jun. and D. E. Pegg., "Organ preservation for transplantation.," British Journal of Surgery, vol. 69, p. 705, 2005.
- [46] W. R. M. A. A. M. L. J. Whaley D, Damyar K, "Cryopreservation: An overview of principles and cell-specific considerations.," *Cell Transplant*, vol. 30, 2021.
- [47] C. A. K. Mandumpal, Jestin B. and R. L. Mancera., "A molecular mechanism of solvent cryoprotection in aqueous dmso solutions.," *Physical Chemistry Chemical Physics*, vol. 13, pp. 3839–3842, 2011.
- [48] W. MacGregor, "The chemical and physical properties of dmso.," Annals of the New York Academy of Sciences, vol. 141, pp. 3–12, 1967.
- [49] E. A., "Cryopreservation of mammalian oocytes by using sugars: Intraand extracellular raffinose with small amounts of dimethylsulfoxide yields high cryosurvival, fertilization, and development rates.," *Cryobiology*, vol. 60, p. Supplement 3, 2010.
- [50] F. BJ., "Cryoprotectants: the essential antifreezes to protect life in the frozen state.," *Cryo Letters*, vol. 6, pp. 375–3888, 2004.
- [51] H. C.J, "Cryopreservation: vitrification and controlled rate cooling," Stem cell banking: concepts and protocols, pp. 41–77, 2017.
- [52] L. Mouttham and P. Comizzoli, "The preservation of vital functions in cat ovarian tissues during vitrification depends more on the temperature of the cryoprotectant exposure than on the sucrose supplementation.," *Cryobiology*, vol. 73, no. 2, pp. 187–195, 2016.
- [53] E. J. J. N. Yong KW, Laouar L, "Review of non-permeating cryoprotectants as supplements for vitrification of mammalian tissues.," *Cryobiology*, pp. 1–11, 2020.
- [54] K. E. Loutradi, E. M. Kolibianakis, C. A. Venetis, E. G. Papanikolaou, G. Pados, I. Bontis, and B. C. Tarlatzis, "Cryopreservation of human embryos by vitrification or slow freezing: a systematic review and meta-analysis," Fertility and sterility, vol. 90, no. 1, pp. 186–193, 2008.

- [55] K. Amps, M. Jones, D. Baker, and H. Moore, "In situ cryopreservation of human embryonic stem cells in gas-permeable membrane culture cassettes for high post-thaw yield and good manufacturing practice," *Cryobiology*, vol. 60, no. 3, pp. 344–350, 2010.
- [56] Y. Hayashi, I. Horiguchi, M. Kino-oka, and H. Sugiyama, "Slow freezing process design for human induced pluripotent stem cells by modeling intracontainer variation," Computers Chemical Engineering, vol. 132, p. 106597, 2020.
- [57] G. Vajta and Z. P. Nagy, "Are programmable freezers still needed in the embryo laboratory? review on vitrification," Reproductive biomedicine online, vol. 12, no. 6, pp. 779–796, 2006.
- [58] C. Consuegra, F. Crespo, J. Dorado, M. Diaz-Jimenez, B. Pereira, I. Ortiz, R. Arenas, J. M. Morrell, and M. Hidalgo, "Vitrification of large volumes of stallion sperm in comparison with spheres and conventional freezing: effect of warming procedures and sperm selection," *Journal of equine veterinary science*, vol. 83, p. 102680, 2019.
- [59] S. Lee, K.-J. Ryu, B. Kim, D. Kang, Y. Y. Kim, and T. Kim, "Comparison between slow freezing and vitrification for human ovarian tissue cryopreservation and xenotransplantation," *International journal of molecular sciences*, vol. 20, no. 13, p. 3346, 2019.
- [60] B. Kulikova, M. Kovac, M. Bauer, M. Tomkova, L. Olexikova, J. Vasicek, A. Balazi, A. V. Makarevich, and P. Chrenek, "Survivability of rabbit amniotic fluid-derived mesenchymal stem cells post slow-freezing or vitrification," *Acta Histochemica*, vol. 121, no. 4, pp. 491–499, 2019.
- [61] H. Mikus, A. Miller, G. Nastase, A. Serban, M. Shapira, and B. Rubinsky, "The nematode caenorhabditis elegans survives subfreezing temperatures in an isochoric system," *Biochemical and biophysical research communications*, vol. 477, no. 3, pp. 401–405, 2016.
- [62] C. Lyu, G. Nastase, G. Ukpai, A. Serban, and B. Rubinsky, "A comparison of freezing-damage during isochoric and isobaric freezing of the potato," *PeerJ*, vol. 5, p. e3322, 2017.
- [63] G. Năstase, C. Lyu, G. Ukpai, A. Şerban, and B. Rubinsky, "Isochoric and isobaric freezing of fish muscle," *Biochemical and Biophysical Research Com*munications, vol. 485, no. 2, pp. 279–283, 2017.
- [64] M. J. Powell-Palm, Y. Zhang, J. Aruda, and B. Rubinsky, "Isochoric conditions enable high subfreezing temperature pancreatic islet preservation without osmotic cryoprotective agents," Cryobiology, vol. 86, pp. 130–133, 2019.
- [65] T. Takahashi, A. Kakita, Y. Takahashi, I. Sakamoto, K. Yokoyama, and T. Fujiu, "Functional integrity of the rat liver after subzero preservation under high pressure," in *Transplantation proceedings*, vol. 32, pp. 1634–1636, 2000.
- [66] G. J. Suppes, S. Egan, A. J. Casillan, K. W. Chan, and B. Seckar, "Impact of high pressure freezing on dh5α escherichia coli and red blood cells," *Cryobiol*ogy, vol. 47, no. 2, pp. 93–101, 2003.

- [67] B. Rubinsky, P. A. Perez, and M. E. Carlson, "The thermodynamic principles of isochoric cryopreservation," *Cryobiology*, vol. 50, no. 2, pp. 121–138, 2005.
- [68] P. Mazur, S. Leibo, and E. Chu, "A two-factor hypothesis of freezing injury: evidence from chinese hamster tissue-culture cells," *Experimental cell research*, vol. 71, no. 2, pp. 345–355, 1972.
- [69] J. P. Acker, J. A. Elliott, and L. E. McGann, "Intercellular ice propagation: Experimental evidence for ice growth through membrane pores," *Biophysical Journal*, vol. 81, no. 3, pp. 1389–1397, 2001.
- [70] J. A. E. Ken Muldrew, Jason P. Acker and L. E. McGann., *The Water to Ice Transition: Implications for Living Cells. In Life in the Frozen State*. Boca Raton: CRC Press, 2004.
- [71] L. S. Hochi S, Semple E, "Effect of cooling and warming rates during cryop-reservation on survival of in vitro-produced bovine embryos," *Theriogenology*, vol. 46, no. 5, pp. 837–847, 1996.
- [72] K. F. Seki, S. and P. Mazur, "Intracellular ice formation in yeast cells vs. cooling rate: predictions from modeling vs. experimental observations by differential scanning calorimetry.," *Cryobiology*, vol. 58, no. 2, pp. 157–165, 2009.
- [73] K. P. D. M. Baboo, J., "The impact of varying cooling and thawing rates on the quality of cryopreserved human peripheral blood t cells," *Sci Rep*, vol. 9, 2019.
- [74] X. H. Y. T. S. Zhang, W. Liu, "Incorporate delivery, warming and washing methods into efficient cryopreservation," Frontiers in Bioengineering and Biotechnology, vol. 11, 2023.
- [75] B. G. C. J. R. L. B. S. M. M. Mfarrej, B., "Pre-clinical assessment of the lovo device for dimethyl sulfoxide removal and cell concentration in thawed hematopoietic progenitor cell grafts," *Cytotherapy*, vol. 19, no. 12, pp. 1501– 1508, 2017.
- [76] L. C. Y. N. B. E. H. Z. T. D. R. J. S. Sharma, A., "Cryopreservation of whole rat livers by vitrification and nanowarming," *Ann. Biomed*, vol. 51, no. 3, pp. 566–577, 2023.
- [77] R. J. S. H. Z. G. L. N. B. G. Z. Sharma, A., "Vitrification and nanowarming of kidneys," Adv. Sci, vol. 8, no. 19, 2021.
- [78] B. M. S. D. P. K. C. T. Syme, R. and S. Gluck, "The role of depletion of dimethyl sulfoxide before autografting: On hematologic recovery, side effects, and toxicity.," *Biol. Blood Marrow Transpl*, vol. 10, no. 2, pp. 135–141, 2004.
- [79] E. A. G. J. M. M. A. G. N. W. C. Cazares-Cortes, E., "Doxorubicin intracellular remote release from biocompatible oligo(ethylene glycol) methyl ether methacrylate-based magnetic nanogels triggered by magnetic hyperthermia.," ACS Appl. Mater Interfaces, vol. 9, no. 31, p. 25775–25788, 2017.

- [80] M. P. Seki S, "Ultra-rapid warming yields high survival of mouse oocytes cooled to -196°c in dilutions of a standard vitrification solution.," *PLoS One*, vol. 7, no. 4, 2012.
- [81] E. L. E. G. Z. B. J. C. Joshi, P., "Thermal analyses of nanowarming-assisted recovery of the heart from cryopreservation by vitrification.," *J. Heat. Transf*, vol. 144, no. 3, 2022.
- [82] L. J. P. A. SMITH, A., "Resuscitation of hamsters after supercooling or partial crystallization at body temperatures below 0° c.," *Nature*, vol. 173, pp. 1136–1137.
- [83] J. D. Benson, "Modeling and optimization of cryopreservation," *Cryopreservation and Freeze-Drying Protocols*, pp. 83–120, 2015.
- [84] H. Y. C. X. T. S. Chen J, Liu X, "Cryopreservation of tissues and organs: present, bottlenecks, and future.," *Front Vet Sci.*, vol. 25, no. 10, 2023.
- [85] P. F. Liu D, "Advances in cryopreservation of organs.," *Huazhong Univ Sci Technolog Med Sci.*, vol. 36, no. 2, pp. 153–161, 2016.
- [86] F. PJ., "Strategies in organ preservation-a new golden age.," *Transplantation.*, vol. 104, no. 9, pp. 1753–1755, 2020.
- [87] R. J. G. L. Han, Z., "Vitrification and nanowarming enable long-term organ cryopreservation and life-sustaining kidney transplantation in a rat model.," *Nat Commun*, 2023.
- [88] H. Z. J. P. R. J. R. V. Gao Z, Namsrai B, "Vitrification and rewarming of magnetic nanoparticle-loaded rat hearts.," *Adv Mater Technol*, 2022.
- [89] D. M. Hossay C, Donnez J, "Whole ovary cryopreservation and transplantation: a systematic review of challenges and research developments in animal experiments and humans.," J Clin Med, 2020.
- [90] M. Awan, I. Buriak, R. Fleck, B. Fuller, A. Goltsev, J. Kerby, M. Lowdell, P. Mericka, A. Petrenko, Y. Petrenko, O. Rogulska, A. Stolzing, and G. N. Stacey, "Dimethyl sulfoxide: a central player since the dawn of cryobiology, is efficacy balanced by toxicity?," Regenerative Medicine, vol. 15, no. 3, pp. 1463–1491, 2020. PMID: 32342730.
- [91] M. Turing, A, "The chemical basis of morphogenesis," *Phil. Trans*, vol. 237, 1952.
- [92] M. P, "Kinetics of water loss from cells at subzero temperatures and the likelihood of intracellular freezing," *Gen Physiol*, vol. 47, no. 2, 1963.
- [93] P. W. Anne E. Duncan, "Predictive water loss curves for ram spermatozoa during cryopreservation: Comparison with experimental observations," Cryobiology, vol. 29, no. 1, pp. 95–105, 1992.
- [94] W. P. Curry MR, Millar JD, "Calculated optimal cooling rates for ram and human sperm cryopreservation fail to conform with empirical observations.," *Biol Reprod*, vol. 51, no. 5, pp. 1014–1021, 1996.

- [95] K.-o. M. Hayashi, Y. and H. Sugiyama, "Hybrid-model-based design of fill-freeze-thaw processes for human induced pluripotent stem cells considering productivity and quality," Computers Chemical Engineering, vol. 156, p. p107566, 2022.
- [96] P. Mazur, "Freezing of living cells: mechanisms and implications," *American journal of physiology-cell physiology*, vol. 247, no. 3, pp. C125–C142, 1984.
- [97] J. Yi, X. M. Liang, G. Zhao, and X. He, "An improved model for nucleation-limited ice formation in living cells during freezing," *PLOS ONE*, vol. 9, pp. 1–9, 05 2014.
- [98] J. Yi, X. M. Liang, G. Zhao, and X. He, "An improved model for nucleation-limited ice formation in living cells during freezing," *PloS one*, vol. 9, no. 5, p. e98132, 2014.
- [99] F. T. J. H. J. B. Willem F. Wolkers, Harriëtte Oldenhof and H. Sieme, "Factors affecting the membrane permeability barrier function of cells during preservation technologies," *Langmuir*, vol. 35, no. 23, pp. 7520–7528, 2019.
- [100] E. K., "Permeability of the plasma membrane to water and cryoprotectants in mammalian oocytes and embryos: Its relevance to vitrification.," *Reproductive medicine and biology*, vol. 16, no. 1, pp. 36–39, 2016.
- [101] C. S. H. S. W. F. W. Maryam Akhoondi, Harriëtte Oldenhof, "Membrane hydraulic permeability changes during cooling of mammalian cells.," *Biochimica et Biophysica Acta (BBA) Biomembranes*, vol. 1808, no. 3, pp. 642–648, 2011.
- [102] G. M. Fahy, "Simplified calculation of cell water content during freezing and thawing in nonideal solutions of cryoprotective agents and its possible application to the study of "solution effects" injury," *Cryobiology*, vol. 18, no. 5, pp. 473–482, 1981.
- [103] D. G. Whittingham, S. P. Leibo, and P. Mazur, "Survival of mouse embryos frozen to -196° and -269°c," *Science*, vol. 178, no. 4059, pp. 411–414, 1972.
- [104] K. II, "Challenge from the simple: some caveats in linearization of the boyle-van't hoff and arrhenius plots," *Cryobiology*, vol. 57, pp. 142–149, 2008.
- [105] J. Benson, Mathematical Modeling and Optimization of Cryopreservation in Single Cells. In: Wolkers, W.F., Oldenhof, H. 2021.
- [106] . A.-S. R. B. Dhaliwal, L. K., "Cell membrane features as potential breeding targets to improve cold germination ability of seeds.," *Basel*, vol. 11, p. 3400, 2022.
- [107] R. Pitt and P. Steponkus, "Quantitative analysis of the probability of intracellular ice formation during freezing of isolated protoplasts," *Cryobiology*, vol. 26, no. 1, pp. 44–63, 1989.

92

- [108] M. Toner, E. G. Cravalho, and M. Karel, "Thermodynamics and kinetics of intracellular ice formation during freezing of biological cells," *Journal of Applied Physics*, vol. 67, no. 3, pp. 1582–1593, 1990.
- [109] J. Karlsson, E. Cravalho, and M. Toner, "A model of diffusion-limited ice growth inside biological cells during freezing," *Journal of Applied Physics*, vol. 75, no. 9, pp. 4442–4455, 1994.
- [110] I. B. R. R. T. M. Y. M. T. J.O.M. Karlsson, E.G. Cravalho, "Nucleation and growth of ice crystals inside cultured hepatocytes during freezing in the presence of dimethyl sulfoxide biophys," *Biophys. J.*, vol. 65, pp. 2524–2536, 1993.
- [111] E. H. W. D. B. J. R. B. H. Y. T. M. Lee, H.J. and T. Toth, "Ultra-rapid vitrification of mouse oocytes in low cryoprotectant concentrations.," *Reproductive biomedicine online*, vol. 20, no. 2, pp. 201–208, 2010.
- [112] H. I. K.-o. M. Hayashi, Y., "Model-based assessment of temperature profiles in slow freezing for human induced pluripotent stem cells," *Computers Chemical Engineering*, vol. 144, p. p107150, 2021.
- [113] C. E. S.-O. Toscano, W.M. and C. Huggins, "The thermodynamics of intracellular ice nucleation in the freezing of erythrocytes.," *J. Heat Transfer*, vol. 97, no. 3, pp. 326–332, 1975.
- [114] Z. A. X.-L. Yang, G. and X. He, "Modeling the cell-type dependence of diffusion-limited intracellular ice nucleation and growth during both vitrification and slow freezing.," *Journal of Applied Physics*, vol. 105, p. 11, 2009.
- [115] J. P. R.E. Pitt, M. Chandrasekaran, "Performance of a kinetic model for intracellular ice formation based on the extent of supercooling," *Cryobiology*, vol. 29, no. 3, pp. 359–373, 1992.
- [116] M. S. L. T. Pitt, R.E. and P. Steponkus, "Subfreezing volumetric behavior and stochastic modeling of intracellular ice formation in drosophila melanogaster embryos," *Cryobiology*, vol. 28, no. 1, pp. 72–86, 1991.
- [117] A. Z. L. X. W. Li, G. Yang, "Numerical study of cell cryo-preservation: a network model of intracellular ice formation," *PLoS One.*, vol. 8, p. e58343, 2013.
- [118] J. A. E. L. E. M. Richelle C. Prickett, Leah A. Marquez-Curtis, "Effect of supercooling and cell volume on intracellular ice formation," *Cryobiology*, vol. 70, no. 2, pp. 156–163, 2015.
- [119] D. Irimia and J. Karlsson, "Kinetics of intracellular ice formation in one-dimensional arrays of interacting biological cells.," *Biophysical Journal*, vol. 88, no. 1, pp. 647–660, 2005.
- [120] F. Amiri and J. Benson, "An agent based model of intracellular ice formation and propagation in small tissues.," bioRxiv, 2022-3.

- [121] J. Benson, "Mathematical problems from cryobiology," Doctoral dissertation, University of Missouri-Columbia, 2009.
- [122] K. A. Benson, J.D. and A. Higgins, "Mathematical optimization of procedures for cryoprotectant equilibration using a toxicity cost function.," *Cryobiology*, vol. 64, no. 3, pp. 144–151, 2012.
- [123] B. J. Anderson, D.M. and A. Kearsley, "Numerical solution of inward solidification of a dilute ternary solution towards a semi-permeable spherical cell.," *Mathematical Biosciences*, vol. 316, 2019.
- [124] E. E. B. "Barry J. Fuller, Nick Lane, "Life in the Frozen State". "Boca Raton": "CRC Press", 2004.
- [125] E. E. B. "Barry J. Fuller, Nick Lane, "Life in the Frozen State". "Boca Raton": "CRC Press", 2004.
- [126] P. Van Liedekerke, M. Palm, N. Jagiella, and D. Drasdo, "Simulating tissue mechanics with agent-based models: concepts, perspectives and some novel results," *Computational particle mechanics*, vol. 2, pp. 401–444, 2015.
- [127] Z. Wang, J. D. Butner, R. Kerketta, V. Cristini, and T. S. Deisboeck, "Simulating cancer growth with multiscale agent-based modeling," in *Seminars in cancer biology*, vol. 30, pp. 70–78, Elsevier, 2015.
- [128] B. C. Thorne, A. M. Bailey, and S. M. Peirce, "Combining experiments with multi-cell agent-based modeling to study biological tissue patterning," *Briefings in bioinformatics*, vol. 8, no. 4, pp. 245–257, 2007.
- [129] H. Zahedmanesh and C. Lally, "A multiscale mechanobiological modelling framework using agent-based models and finite element analysis: application to vascular tissue engineering," *Biomechanics and modeling in mechanobiology*, vol. 11, pp. 363–377, 2012.
- [130] D. Nolan and C. Lally, "Coupled finite element–agent-based models for the simulation of vascular growth and remodeling," in *Numerical methods and advanced simulation in biomechanics and biological processes*, pp. 283–300, Elsevier, 2018.
- [131] A. M. Bailey, B. C. Thorne, and S. M. Peirce, "Multi-cell agent-based simulation of the microvasculature to study the dynamics of circulating inflammatory cell trafficking," *Annals of biomedical engineering*, vol. 35, pp. 916–936, 2007.
- [132] N. Seekhao, C. Shung, J. JaJa, L. Mongeau, and N. Y. Li-Jessen, "Real-time agent-based modeling simulation with in-situ visualization of complex biological systems: A case study on vocal fold inflammation and healing," in 2016 IEEE International Parallel and Distributed Processing Symposium Workshops (IPDPSW), pp. 463–472, IEEE, 2016.
- [133] S. M. Rikard, T. L. Athey, A. R. Nelson, S. L. Christiansen, J.-J. Lee, J. W. Holmes, S. M. Peirce, and J. J. Saucerman, "Multiscale coupling of an agent-based model of tissue fibrosis and a logic-based model of intracellular signaling," *Frontiers in physiology*, vol. 10, p. 1481, 2019.

- [134] E. Lejeune and C. Linder, "Understanding the relationship between cell death and tissue shrinkage via a stochastic agent-based model," *Journal of biomechanics*, vol. 73, pp. 9–17, 2018.
- [135] Q. Peng and F. Vermolen, "Agent-based modelling and parameter sensitivity analysis with a finite-element method for skin contraction," *Biomechanics and Modeling in Mechanobiology*, vol. 19, pp. 2525–2551, 2020.
- [136] R. Storn and K. Price, "Differential evolution—a simple and efficient heuristic for global optimization over continuous spaces," *Journal of global optimization*, vol. 11, no. 4, pp. 341–359, 1997.
- [137] H. Tsutsui, B. Valamehr, A. Hindoyan, R. Qiao, X. Ding, S. Guo, O. N. Witte, X. Liu, C.-M. Ho, and H. Wu, "An optimized small molecule inhibitor cocktail supports long-term maintenance of human embryonic stem cells," *Nature communications*, vol. 2, no. 1, pp. 1–8, 2011.
- [138] K. Pollock, J. W. Budenske, D. H. McKenna, P. I. Dosa, and A. Hubel, "Algorithm-driven optimization of cryopreservation protocols for transfusion model cell types including jurkat cells and mesenchymal stem cells," *Journal* of tissue engineering and regenerative medicine, vol. 11, no. 10, pp. 2806–2815, 2017.
- [139] G. Yu, Y. R. Yap, K. Pollock, and A. Hubel, "Characterizing intracellular ice formation of lymphoblasts using low-temperature raman spectroscopy," *Biophysical Journal*, vol. 112, no. 12, pp. 2653–2663, 2017.
- [140] T. Yang, J. Peng, Z. Shu, P. K. Sekar, S. Li, and D. Gao, "Determination of the membrane transport properties of jurkat cells with a microfluidic device," *Micromachines*, vol. 10, no. 12, p. 832, 2019.
- [141] A. Skorupa and A. Piasecka-Belkhayat, "Numerical modeling of heat and mass transfer during cryopreservation using interval analysis," *Applied Sciences*, vol. 11, no. 1, p. 302, 2020.
- [142] A. Cincotti and S. Fadda, "Modelling the cryopreservation process of a suspension of cells: The effect of a size-distributed cell population," in *Computational Modeling in Tissue Engineering*, pp. 145–181, Springer, 2012.
- [143] Y. Hayashi, B. X. Scholz, and H. Sugiyama, "A cfd-model-based approach to continuous freezing process design for human induced pluripotent stem cells," in *Computer Aided Chemical Engineering*, vol. 52, pp. 65–70, Elsevier, 2023.
- [144] J. McGrath, E. Cravalho, and C. Huggins, "An experimental comparison of intracellular ice formation and freeze-thaw survival of hela s-3 cells," *Cryobiology*, vol. 12, no. 6, pp. 540–550, 1975.
- [145] C. J. Hunt, "Cryopreservation of human stem cells for clinical application: a review," *Transfusion Medicine and Hemotherapy*, vol. 38, no. 2, pp. 107–123, 2011.
- [146] P. Mazur, "The role of intracellular freezing in the death of cells cooled at supraoptimal rates," *Cryobiology*, vol. 14, no. 3, pp. 251–272, 1977.

- [147] L. Breitwieser, A. Hesam, J. de Montigny, V. Vavourakis, A. Iosif, J. Jennings, M. Kaiser, M. Manca, A. Di Meglio, Z. Al-Ars, et al., "Biodynamo: a modular platform for high-performance agent-based simulation," *Bioinformatics*, vol. 38, no. 2, pp. 453–460, 2022.
- [148] N. Cogno, R. Bauer, and M. Durante, "An agent-based model of radiation-induced lung fibrosis," *International Journal of Molecular Sciences*, vol. 23, no. 22, p. 13920, 2022.
- [149] J. de Montigny, A. Iosif, L. Breitwieser, M. Manca, R. Bauer, and V. Vavourakis, "An in silico hybrid continuum-/agent-based procedure to modelling cancer development: Interrogating the interplay amongst glioma invasion, vascularity and necrosis," Methods, vol. 185, pp. 94–104, 2021.
- [150] S. H. Friedman, A. R. Anderson, D. M. Bortz, A. G. Fletcher, H. B. Frieboes, A. Ghaffarizadeh, D. R. Grimes, A. Hawkins-Daarud, S. Hoehme, E. F. Juarez, et al., "Multicellds: a community-developed standard for curating microenvironment-dependent multicellular data," bioRxiv, p. 090456, 2016.
- [151] A. Csikasz-Nagy, "Computational systems biology of the cell cycle," *Briefings* in bioinformatics, vol. 10, no. 4, pp. 424–434, 2009.
- [152] N. T. Ingolia and A. W. Murray, "The ups and downs of modeling the cell cycle," *Current Biology*, vol. 14, no. 18, pp. R771–R777, 2004.
- [153] A. Kriete, E. Noguchi, and C. Sell, "Introductory review of computational cell cycle modeling," *Cell Cycle Control*, pp. 267–275, 2014.
- [154] V. Noel, D. Grigoriev, S. Vakulenko, and O. Radulescu, "Tropical geometries and dynamics of biochemical networks application to hybrid cell cycle models," *Electronic Notes in Theoretical Computer Science*, vol. 284, pp. 75–91, 2012.
- [155] A. Brú, J. M. Pastor, I. Fernaud, I. Brú, S. Melle, and C. Berenguer, "Superrough dynamics on tumor growth," *Physical Review Letters*, vol. 81, no. 18, p. 4008, 1998.
- [156] P. Järvinen, A. Bonabi, V. Jokinen, and T. Sikanen, "Simultaneous culturing of cell monolayers and spheroids on a single microfluidic device for bridging the gap between 2d and 3d cell assays in drug research," *Advanced Functional Materials*, vol. 30, no. 19, p. 2000479, 2020.
- [157] K. Duval, H. Grover, L.-H. Han, Y. Mou, A. F. Pegoraro, J. Fredberg, and Z. Chen, "Modeling physiological events in 2d vs. 3d cell culture," *Physiology*, vol. 32, no. 4, pp. 266–277, 2017.
- [158] D. Dell'Arciprete, M. Blow, A. Brown, F. Farrell, J. S. Lintuvuori, A. McVey, D. Marenduzzo, and W. C. Poon, "A growing bacterial colony in two dimensions as an active nematic," *Nature communications*, vol. 9, no. 1, pp. 1–9, 2018.
- [159] T. Yoda, H. Miyaki, and T. Saito, "Effect of container shape on freeze concentration of apple juice," *Plos one*, vol. 16, no. 1, p. e0245606, 2021.

- [160] P. Kilbride, S. Lamb, S. Milne, S. Gibbons, E. Erro, J. Bundy, C. Selden, B. Fuller, and J. Morris, "Spatial considerations during cryopreservation of a large volume sample," *Cryobiology*, vol. 73, no. 1, pp. 47–54, 2016.
- [161] B. Jin, S. Seki, E. Paredes, J. Qiu, Y. Shi, Z. Zhang, C. Ma, S. Jiang, J. Li, F. Yuan, *et al.*, "Intracellular ice formation in mouse zygotes and early morulae vs. cooling rate and temperature-experimental vs. theory," *Cryobiology*, vol. 73, no. 2, pp. 181–186, 2016.
- [162] P. Kilbride, J. Meneghel, S. Lamb, J. Morris, J. Pouzet, M. Jurgielewicz, C. Leonforte, D. Gibson, and A. Madrigal, "Recovery and post-thaw assessment of human umbilical cord blood cryopreserved as quality control segments and bulk samples," *Biology of Blood and Marrow Transplantation*, vol. 25, no. 12, pp. 2447–2453, 2019.
- [163] P. F. Watson, "The causes of reduced fertility with cryopreserved semen," *Animal reproduction science*, vol. 60, pp. 481–492, 2000.
- [164] P. Watson, "Recent developments and concepts in the cryopreservation of spermatozoa and the assessment of their post-thawing function," Reproduction, Fertility and Development, vol. 7, no. 4, pp. 871–891, 1995.
- [165] W. V. Holt, A. Medrano, L. M. Thurston, and P. F. Watson, "The significance of cooling rates and animal variability for boar sperm cryopreservation: insights from the cryomicroscope," *Theriogenology*, vol. 63, no. 2, pp. 370–382, 2005.
- [166] L. Johnson, K. Weitze, P. Fiser, and W. Maxwell, "Storage of boar semen," *Animal reproduction science*, vol. 62, no. 1-3, pp. 143–172, 2000.
- [167] S. Salamon and W. M. C. Maxwell, "Storage of ram semen," *Animal reproduction science*, vol. 62, no. 1-3, pp. 77–111, 2000.
- [168] I. Ashrafi, H. Kohram, H. Naijian, M. Bahreini, and H. Mirzakhani, "Effect of controlled and uncontrolled cooling rate on motility parameters of cryopreserved ram spermatozoa," *BMC Research Notes*, vol. 4, pp. 1–6, 2011.
- [169] J. Dalal, A. Kumar, M. Honparkhe, S. Singhal, and N. Singh, "Comparison of three programmable freezing protocols for the cryopreservation of buffalo bull semen," *The Indian Journal of Animal Reproduction*, vol. 37, no. 2, pp. 54–55, 2016.
- [170] S. Kumar, J. Millar, and P. Watson, "The effect of cooling rate on the survival of cryopreserved bull, ram, and boar spermatozoa: a comparison of two controlled-rate cooling machines," *Cryobiology*, vol. 46, no. 3, pp. 246–253, 2003.
- [171] D. A. Galarza, A. López-Sebastián, H. Woelders, E. Blesbois, and J. Santiago-Moreno, "Two-step accelerating freezing protocol yields a better motility, membranes and dna integrities of thawed ram sperm than three-steps freezing protocols," *Cryobiology*, vol. 91, pp. 84–89, 2019.

- [172] C. Koshimoto and P. Mazur, "Effects of cooling and warming rate to and from- 70° c, and effect of further cooling from- 70 to- 196° c on the motility of mouse spermatozoa," *Biology of reproduction*, vol. 66, no. 5, pp. 1477–1484, 2002.
- [173] E. Buenz, J. Weaver, B. Bauer, S. Chalpin, and A. Badley, "Cordyceps sinensis extracts do not prevent fas-receptor and hydrogen peroxide-induced t-cell apoptosis," *Journal of Ethnopharmacology*, vol. 90, no. 1, pp. 57–62, 2004.
- [174] M. Werner, K. Biss, V. Jérôme, F. Hilbrig, R. Freitag, K. Zambrano, H. Hübner, R. Buchholz, R. Mahou, and C. Wandrey, "Use of the mitochondria toxicity assay for quantifying the viable cell density of microencapsulated jurkat cells," *Biotechnology Progress*, vol. 29, no. 4, pp. 986–993, 2013.
- [175] R. T. Abraham and A. Weiss, "Jurkat t cells and development of the t-cell receptor signalling paradigm," *Nature reviews immunology*, vol. 4, no. 4, pp. 301–308, 2004.
- [176] G. Gaud, R. Lesourne, and P. E. Love, "Regulatory mechanisms in t cell receptor signalling," *Nature Reviews Immunology*, vol. 18, no. 8, pp. 485–497, 2018.